MODELLING PHOTOSYNTHETIC CO_2 FIXATION IN *RADIATA PINE* CLONES WITH CONTRASTING CROWN CHARACTERISTICS AT AGE FIVE AT DALETHORPE, CANTERBURY, NEW ZEALAND

A thesis
submitted in partial fulfilment
of the requirements for the Degree
of
Doctor of Philosophy in Forestry
in the
University of Canterbury

by
Hongyuan Xu

University of Canterbury
2000

CONTENTS

LIST OF FIGURES

LIST OF TABLES

List of symbols

Symbol	Unit	Description
A	$\mu mol\ m^{-2}s^{-1}$	net photosynthesis rate
Amax	$\mu mol\ m^{-2}s^{-1}$	photosynthesis rate at saturating irradiance
DBOB	cm	diameter at breast height out of bark
GLD	cm	ground level diameter
H	cm	tree height
k	~	light extinction coefficient value
LAI	~	leaf area index
A, B, C, D, K	~	parameters in an equation
NSA	m^2	needle surface area
NSAD	m^{-1}	needle surface area density
PAR	$\mu mol\ m^{-2}s^{-1}$	photosynthetic active radiation
Qc	$\mu mol\ m^{-2}s^{-1}$	light compensation point
Qs	$\mu mol\ m^{-2}s^{-1}$	light saturation point
Rd	$\mu mol\ m^{-2}s^{-1}$	respiration
STEMB	kg	total stem biomass for an individual tree
TBB	kg	total branch biomass for an individual tree
TBIO	kg	total biomass for an individual tree
TNB	kg	total needle biomass for an individual tree
TNS	m2	total needle surface area for an individual tree
V	m^3	crown volume
VPD	kPa	vapor pressure deficit
$\angle\beta$	~	elevation angle
$\angle\theta$	~	azimuth angle
$\angle\varphi$	~	zenith angle

ACKNOWLEDGMENTS

I am extremely grateful to my supervisors, Dr. Euan G. Mason, Professor Roger Sands (SOF School of Forestry), and Dr. Osbert Sun (FRI Forestry Research Institute), for spending a great deal of their time on guidance, and contributing very helpful recommendations throughout the research described in this thesis. I especially thank Dr. Euan G. Mason for his encouragement and patience, supporting me throughout the long journey that this thesis represents.

It is a pleasure to acknowledge the help of the staff and my fellow postgraduates of SOF, who have generously given their time and expertise to help me in field and lab. I especially thank to Bob Bullsmith for his patient and skillful in helping me using equipment.

The University of Canterbury Research Awards (Doctoral level) during 1998 and 1999 are gratefully acknowledged. They gave very helpful financial support to the author of this thesis.

The experiment at Dalethorpe was made possible by a University of Canterbury research grant, by a donation of clones from the Fletcher Challenge Centre for Advanced Biotechnology and the Selwyn Plantation Board LTD, by an initial small grant from the Foundation for Research Science and Technology, and by subsequent research grants from the University of Canterbury.

I am also grateful to Daphne Hazelgrove for her proof reading Chapter 3, 4 and 5 of this thesis.

Finally, I thank my wife, Ru, and my daughter, Rui for providing spiritual and emotional support and love during the research of this thesis. Thanks to my parents also for their continuous support and encouragement throughout my education.

ABSTRACT

A program was developed to simulate the individual tree photosynthesis of ten *Pinus radiata* D. Don clones at age 5, and a comparison was made between the clones at a given condition to estimate photosynthesis from leaf level to tree level. The model linked the sub-models of leaf level photosynthesis, crown shape, foliage area, foliage area density distribution, and light penetration probability within tree crowns together to estimate total net photosynthesis on individual tree level. This study was carried out at a radiata pine clonal experiment at the same site with the same treatment located at Dalethorpe, Canterbury, New Zealand.

At leaf level, seasonal photosynthetic responses to light and temperature curves of 1-, 2- and 3-year-old needles were measured under controlled environmental conditions in the field. Needle net photosynthetic rates did not show statistically significant differences between clones. Net photosynthesis decreased with leaf age but increased with temperature (5°C - 20°C). Comparing the maximum photosynthetic rates under the same measurement conditions, there were no statistically significant differences among the ten clones or according to crown position (crown level and aspect i.e. north-, south-, east-, and west-facing).

In describing crown shape, a simple crown shape was developed. The model can be used to calculate crown radii, the maximum crown radius, the crown base radius, crown volume and vertical volume distribution of different needle age classes.

Above-ground biomass and needle surface area were estimated. The total above-ground biomass and its allocation showed significantly difference among growth difference clones. Tree height was poorly correlated with total biomass production, but DBH was strong correlated with needle, branch and total biomass. The vertical distributions of needle biomass, needle surface area, and needle surface area density were studied according to age class.

In estimating light penetration within tree crowns, a simple light penetration program was developed. The program was based on data from crown architecture analysis, geometrical analysis of the light penetration distance within crowns and models of crown shapes. The program can be used to estimate the probability of direct light penetration at any given sun zenith angle and diffuse light penetration at any given direction with azimuth angle $\angle\theta$ and elevation angle $\angle\beta$.

With the developed individual tree net photosynthesis process model, the influence of foliage mass, crown shape, light penetration probability, incoming sun zenith angle, crown light extinction coefficient k-value and needle photosynthetic capacity on total tree net photosynthesis was studied. Simulation results indicated that foliage mass was an important factor influencing total tree photosynthetic rate. However, other factors, such as crown shape and needle photosynthetic capacity, all influenced the variation of total tree photosynthetic rates in various environment conditions.

CHAPTER 1

INTRODUCTION

Pinus radiata D. Don grows naturally in California. Since it was first introduced into New Zealand, as an exotic species, it has been outstandingly successful. New Zealand's exotic forest consists of approximately 1.7 million hectares, with around 90% being *Pinus radiata* (New Zealand Forest Owners Assoc. Inc. 1998). *P. radiata* grows fast in New Zealand; its rotation age is 25-30 years (Maclaren, 1993). Its timber is regarded as excellent for general construction purposes, joinery, furniture, panelling, flooring and formwork (Cown, 1992).

It has been known for over 60 years that cuttings can be grown from young radiata pine trees (Field 1934) and clonal forestry has many advantages (Libby 1983; McKeand 1981). Carson (1986) discussed the advantages of *P. radiata* clonal forestry in New Zealand, for example, shorter plant production times, control of pedigree, flexibility of deployment, multiplication of valuable crosses, and efficient capture of additive genetic gains. In addition, clonal forestry may have advantages in increasing uniformity, allowing of clones to sites, and controlling growth habit. Nevertheless, whatever the advantages are, clonal testing is necessary for selecting good clones. Clonal testing could have different aims: for example, growth and form, disease or insect resistance, high wood density, or long internodes. Normally, growth rate and tree forms are the most important for production forestry.

For greater economic gains, higher growth rates with quality wood or biomass production are important aims. In field clonal growth tests, different clones may show great differences in growth rate on different sites, even under the same environmental conditions. The variation in growth rate could result from a variety of causes, such as differences in foliage photosynthetic rates, crown shape, foliage surface areas and light interception. For selecting better clones in the future, it is necessary to not only just select better clones, but also try to understand the reasons why some selected clones grow better than others do.

1.1 Questions addressed

In the same field treatment (soil preparation, chemical weed control, planting spacing (2 x 4 m), and no pruning) and environmental conditions, tree height and diameter growths were very different among different radiata pine clones. The questions addressed in this study were:

- Were there differences in foliage photosynthetic capacity among radiata pine clones? Were there any significant differences in foliage photosynthetic capacity with changing foliage age or season among the clones?

- Were there differences in crown shape and volume, foliage area and foliage area density for different clones?

- Were there differences between clones in above ground biomass production and its allocation to tree components?

- What were the effects of crown shape and foliage area density on light penetration?

- Were there differences in total tree photosynthetic CO_2 fixation for the different clones?

- What were the major factors that affected observed growth rate differences for radiata pine clones?

1.2 Research Objectives

- To determine physiological and morphological attributes affecting growth differences among radiata pine clones observed in an experiment in Dalethorpe, Canterbury.

- To develop a simple process-based growth model incorporating photosynthesis and crown characteristics as functions of clonal variation and environmental conditions.

1.3 Framework of the study in this thesis

To achieve the above research objectives and address the listed questions, this thesis includes 9 Chapters (Figure 1.1).

Chapter one introduces the objectives and framework of the study in this thesis.

Chapter two reviews the literature related to the research project.

Chapter three examines differences in growth between radiata pine clones under the same experimental treatment and environmental conditions.

In Chapter four, needle net photosynthetic rates were compared by foliage ages in all four seasons among the clones. A simple model of needle photosynthesis was developed, and it

was used further (in Chapter 8) to simulate whole tree photosynthetic CO_2 fixation when combined with studies of the crown shape (Chapter 5), needle surface area (Chapter 6), and light interception (Chapter 7).

In Chapter five, two measurement methods were used to collect crown shape data. One method was image analysis of crown shape, and another detailed direct measurement of crown architectures. A model to describe crown shape was developed. The model can be used to calculate crown radii, the maximum crown radius, the crown base radius, crown volume and vertical volume distribution of different needle age classes. The results were used in a later (Chapter 6) study of needle surface area density and distribution.

Chapter six presents the results of the study on above ground biomass production and biomass allocation into different crown components. In addition, needle surface area and its vertical distribution were studied. Combining this result with crown shape (Chapter 5), the vertical distributions of needle surface area were described according to clones. The results were useful for predicting light penetration in the crown (Chapter 7).

In Chapter seven, a simulation combining the results of crown shape (Chapter 5) with needle surface area density (Chapter 6), light penetration in the crown is presented. These results were useful for simulating whole tree photosynthesis.

In Chapter eight, whole tree photosynthesis was described by using the needle photosynthesis model (Chapter 4), and was combined with needle surface area (Chapter 6) and with light penetration in crowns (Chapter 7).

Finally, Chapter nine is a general discussion and it is followed by the overall conclusions. All references in this thesis are listed together following Chapter 9.

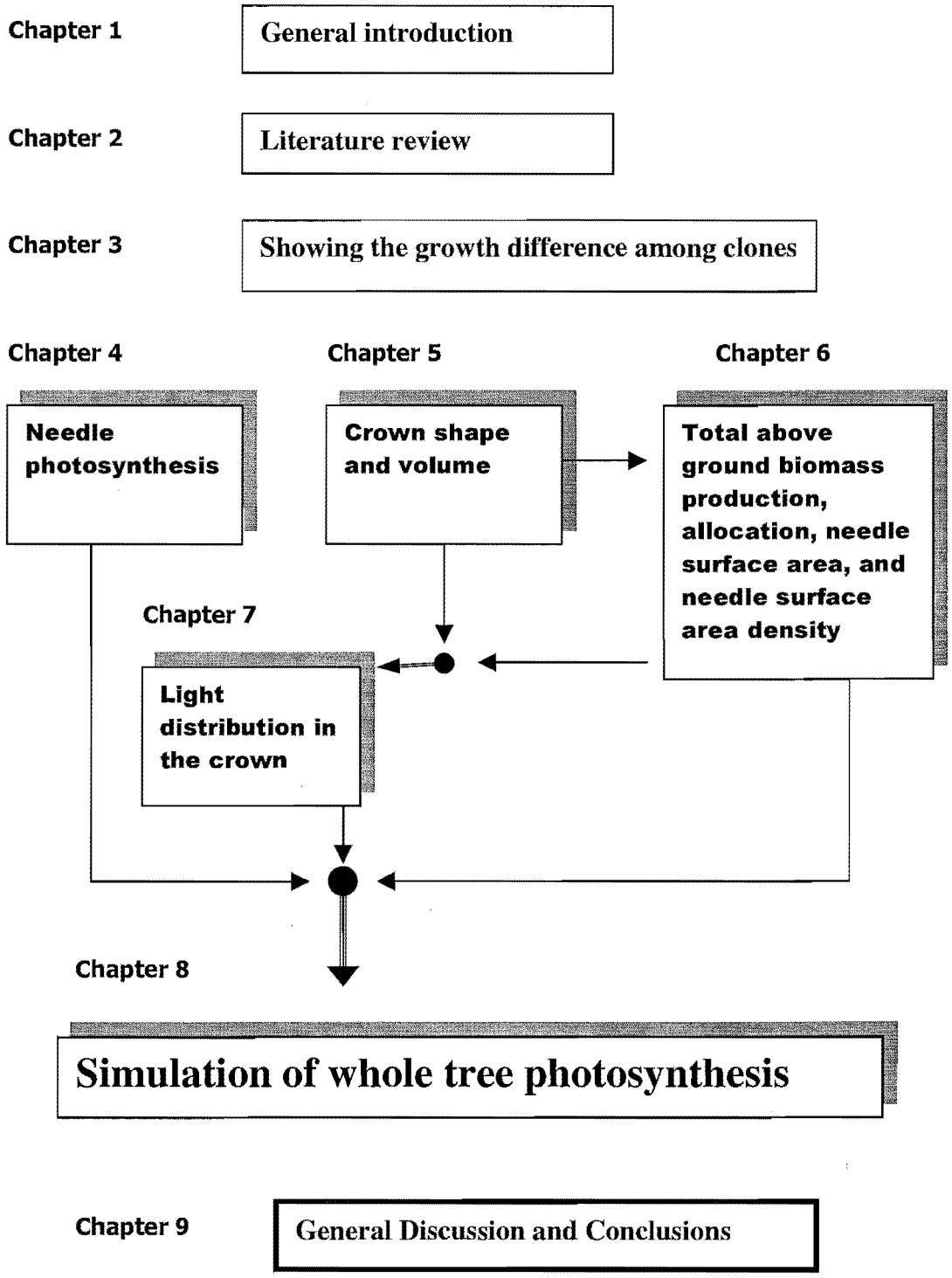

Fig. 1.1 Diagrammatic framework of the study in this thesis.

CHAPTER 2

LITERATURE REVIEW

2.1 Introduction

All tree growth relies on tree photosynthetic production. A number of factors (e.g., physiological, morphological and phenological factors) influence tree growth rates. Variation of a tree species' physiological and morphological characteristics is thought to result from its evolutionary adaptation to environmental conditions during the long geological past. It is known that the physiological characteristics (e.g., foliage photosynthetic capacity, respiration and the ability to survive under different environmental stress) are important for tree growth; nevertheless, other characteristics such as morphological and phenological ones play an important role too in tree growth and competition. Morphological features as characterized by the architecture of plant canopies or tree crowns have a great influence upon the processes of light interception and hence affect total CO_2 fixation.

In this study, different clones grew with different growth rates at the same site in the same field treatment (Chapter 3). These differences may have resulted from the different physiological or morphological characteristics among the clones. Understanding the relationship between photosynthetic activity and the structure of clonal tree crowns may allow breeders to select and obtain clones with high yield biomass or high quality wood production.

In the following sections, each aspect will be reviewed, such as foliage photosynthetic capacity, crown shape and structure, light penetration within the crown and total crown photosynthesis, which relate the study reported in this thesis

2.2 Foliage photosynthetic capacity

Foliage photosynthetic capacity is influenced by many environmental factors. As a photochemical process, photosynthesis is directly dependent upon the availability of radiation, and limited especially by temperature, water, the supply of CO_2, and foliage ages.

2.2.1 The influence of light on foliage net photosynthesis

Foliage net photosynthesis varies greatly with changed light intensity. Light response curve represents the relationship between foliage net photosynthesis and radiation. If leaves are exposed to increasing intensities of illumination, the CO_2 fixation increases at first in proportion to light intensity and then gradually approaches a maximum values. This is called light response curve. In dim light, the light curve reflects a net release of CO_2, because more CO_2 is given off by respiration than is fixed by photosynthesis. At somewhat greater light intensities the light compensation point is reached. At the light compensation point, photosynthesis fixes CO_2 equaling to the CO_2 released by respiration. Once the compensation point has been passed, CO_2 uptake increases rapidly. When light intensity increases to a very high level, photosynthesis continues to increase only slightly or not at all; and the rate of CO_2 uptake is now limited not by photochemical but rather by enzymatic processes, and by the supply of CO_2 (Larcher 1980).

The maximum rate of net photosynthesis by a plant at a given state of development and activity, under natural conditions of atmospheric CO_2 content and optimal conditions with respect to all other external factors, is called photosynthetic capacity (Larcher 1980).

Different plant species have different light response curves, and even within the same tree different foliage ages have different photosynthetic capacities (Kitajima, 1997; Oleksyn, 1997; Schoettle, 1999).

Scaling leaf-level light curve measurements to estimate carbon gain of entire leaf crowns or canopies requires an understanding of the distribution of photosynthetic capacity of different leaf age classes and corresponding light microenvironments within a crown.

2.2.2 The influence of temperature on foliage net photosynthesis

Photosynthesis of plants occurs over a wide temperature range from near 0 to over 40 °C, and the specific range depends on species and genotype, plant age, plant origin and season. As temperature increases, plant activities increase up to an optimum temperature and then decrease until, at very high temperatures, death occurs. Barnes *et al.* (1998) concluded that the processes influenced by temperature are (i) the activity of enzymes that catalyze biochemical reactions, especially photosynthesis and respiration; (ii) the solubility of carbon dioxide and oxygen in plant cells; (iii) transpiration; (iv) the ability of roots to absorb water and minerals from the soil; and (v) membrane permeability. Different growth processes may require different optimum temperatures. Wood and Brittain (1973) reported that the maximum photosynthetic capacity was influenced by increasing temperature between 11 °C and 23 °C for radiata pine seedlings. This was possibly due to temperature effects on the enzymatic reactions, and a depression at elevated temperatures that was attributed to disruption of the photochemical systems of the chloroplasts. Bassow and Bazzaz (1998) concluded that large differences in temperature and vapour pressure deficit (VPD) throughout the growing season partly led to the seasonal differences observed in photosynthesis rates. Walcroft *et al.* (1997) measured the responses of photosynthesis (A) to intercellular CO_2 concentration (ci) in 2-year-old *Pinus radiata* seedlings at a range of temperatures in order to parameterize a biophysical model of leaf photosynthesis. They found that increasing leaf temperature from 8 to 30°C caused a 4-fold increase in Vcmax, the maximum rate of carboxylation (10.7-43.3 μmol m-2 s-1) and a 3-fold increase in Jmax, the maximum electron transport rate (20.5-60.2 μmol m-2 s-1). The temperature

optimum for Jmax was lower than that for Vcmax, causing a decline in the ratio Jmax:Vcmax from 2.0 to 1.4 as leaf temperature increased from 8 to 30°C.

Soil temperature as well as air temperature affects photosynthesis. Schwarz *et al.* (1997) measured gas exchange and daily minimum and maximum soil and air temperatures in ten red spruce (*Picea rubens*) saplings, growing near Ithaca, New York, throughout the early spring and late-autumn growing periods. The rates of net photosynthesis were positively correlated with both minimum daily soil and air temperatures but minimum soil temperature was a better predictor of net photosynthesis. Moreover, net photosynthesis was more sensitive to changes in soil temperature than to changes in air temperature, and photosynthesis was approximately twice as sensitive to temperature changes during the autumn than during the spring.

2.2.3 The influence of water on foliage net photosynthesis

The influences of water deficit on CO_2 fixation have been widely studied (Whitehead, 1985; Clinton and Mead, 1990; Yunusa *et al.*, 1995b). It is known that water stress reduces the net photosynthetic rate (Thompson and Wheeler, 1992) and hence tree growth rate. Benecke (1980) measured gas-exchange of *Pinus radiata* foliage with climatised cuvettes under natural light in the sun-crown of 8 m tall trees in a forest stand. Measurement was made at different levels of soil moisture. He found that soil and air moisture deficits severely restricted gas exchange, and watering resulted in an immediate decline in stomatal resistance (rs) and an increase in net photosynthesis of 13%. Radiata pine needles responded directly to changes in atmospheric humidity by adjusting their stomatal diffusive resistance. Rook *et al.* (1977) used two large artificially-lit controlled-environment rooms to test the influence of water stress on 5 radiata pine trees. They found that greater stress caused rates of transpiration and photosynthesis and root growth to decrease to near zero and the older foliage began to be shed. Throughout the drought cycle, foliage carbohydrate levels decreased. On rewatering, partial recovery of drought stress occurred overnight and stem diameter increased dramatically. Rates of transpiration and photosynthesis slowly recovered.

2.2.4 The influence of leaf ages on foliage net photosynthesis

Leaf age influenced the shape of the photosynthetic response curve during studies conducted by Kitajima (1997) and Oleksyn (1997). Troeng and Linder 1982 reported that photosynthetic capacity declined with leaf ages within a tree, and Teskey *et al.* (1984) found the same trends. This decline was related to increased by new leaf cohorts (Schoettle and Smith, 1991; Schoettle and Fahey, 1994) and re-translocation of nutrients from aging needles (Son and Gower, 1991).

Vandana and Bhatt (1996) reported that the rate of photosynthesis, stomatal conductance, carboxylation efficiency and water use efficiency were higher in fully expanded mature leaves compared with young and old leaves for *Sesbania sesban* and *S. grandiflora.* Oleksyn *et al.* (1997) reported that the physiological characteristics were evaluated for eight needle-age classes of *P. heldreichii* grown at the Arboretum of the Institute of Dendrology in Kornik, Poland. Current-year foliage had the highest rates of mass-based light-saturated net photosynthesis (Asat) of 33.5 μmol CO_2 g-1 s-1. Asat decreased with needle age, but older needle classes retained approximately 62 to 26% of the current needles' rate. The relationship between leaf N and chlorophyll a concentration among all needle-age classes was highly significant ($r = 0.96$, $P = 0.0006$). The variation in Asat of 1- to 7-year-old needles was linearly related to needle N concentration ($r = 0.98$, $P = 0.0001$). Needle dark respiration rates among these needle age classes ranged from 0.8 to 2.2 μmol g-1 s-1 and decreased with needle age and nitrogen concentration. Total phenols and glucose concentrations increased linearly with needle age.

Radoglou and Teskey (1997) measured the net photosynthetic rates of developing foliage and one-year-old foliage of loblolly pine (*Pinus taeda*) under field conditions in the Whitehall Forest, near Athens, Georgia. Loblolly pine foliage grows slowly, reaching its final size 3.5 to 4 months after bud burst. Positive rates of net photosynthesis were recorded when the foliage was 13 and 18% of final length, under controlled-environmental and field conditions, respectively. However, because of high rates of dark respiration during the initial growth period, a positive diurnal carbon balance did not occur until foliage was about a third of final length (40 days after bud burst). Two months after bud

burst, when foliage was about 55% of final length, its photosynthetic capacity exceeded that of one-year-old foliage. The highest rates of net photosynthesis were achieved when foliage was more than 90% fully expanded.

2.2.5 Leaf photosynthesis models

Photosynthesis has been studied at scales ranging from the leaf level (Farquhar and von Caemmerer ,1982; Field, 1983; Harley *et al.*, 1985; Leuning 1990) to the canopy level (Jarvis *et al.*, 1989; McMurtrie *et al.*, 1992; Harley and Baldocchi, 1995). At the leaf level, the biochemical model (or called mechanistic model) developed by Farquhar and Caemmerer (1982), has been used to characterize leaf photosynthesis by many researchers (Leuning, 1990, 1995; McMurtrie *et al.*, 1992a; McMurtrie and Wang, 1993; Wullschleger, 1993; Wang and Polglase, 1995). The model estimates the net rate of leaf photosynthesis as:

$$A = Vc\ (1- \Gamma /ci\ )-Rd$$

Where A is the net rate of leaf photosynthesis ($\mu mol\ m^{-2}\ s^{-1}$), Γ is the CO_2 compensation point in the absence of day respiration, ci is the intercellular concentration of CO_2, and Rd is the rate of day respiration. Vc is given by

$$Vc = \min (Wj, Wc, Wp)$$

where Wj, Wc, and Wp are the rates of carboxylation limited by RuBP regeneration, by Rubisco activity, and by triose phosphate utilization, respectively. Wullschleger (1993) believed Wp could be ignored.

$$Wj = J / (4 + 8\ \Gamma /ci)$$

where J is the potential electron transport rate ($\mu mol\ m^{-2}\ s^{-1}$).

The Rubisco-limited rate is

$$Wc = Vcmax\ ci / (ci + Kc\ (1 + Oi / Ko))$$

Where Kc and Ko are Michaelis coefficients for CO_2 and O_2, respectively, and Oi is intercellular O_2 concentration. Wullschleger (1993) found that Vcmax and Jmax are strongly related.

Even though a mechanistic model has many advantages for many purposes, it is still more convenient to use empirical equations, rather than the mechanistic equations of Farquhar and von Caemmerer (1982), to model leaf photosynthesis and scale to canopy photosynthesis (Samson *et al.*, 1997; Pearcy *et al.*, 1998, 1996; Grace *et al.*, 1987). Landsberg (1997) provided disillusion to support this conclusion.

2.3 Canopy architecture

All physiological processes are strongly influenced by the interaction between environmental factors such as solar radiation, air temperature, air humidity, nutrient availability, and biological factors, such as canopy architecture, leaf longevity and foliage's physiological characteristics. In order to understand how these processes impact on tree growth it is necessary to have a detailed knowledge of canopy architecture. Canopies of plants consist of individual trees with crowns, leaves, branches and stems. Canopy architecture is described by the vertical and horizontal distributions and arrangement of foliage through the canopy space. At the stand level, canopy architecture is determined by stand structure such as the number, spacing, height and size distributions of trees. At the tree level, genetic and environmental factors affect canopy architecture. Crown shape of individual tree species is strongly influenced by genetic factors. Different tree species, even different clones could have different canopy architecture (Karnosky *et al.*, 1993). Growing trees in open or closed stand also affect canopy structures.

2.3.1 Crown shape and volume

The shape and volume of a tree crown are two most important characteristics. All physiological processes take place in the crown. Crown shape and foliage density (foliage mass or foliage area / crown volume) distribution influence light interception within the crown (Norman and Jarvis, 1975; Grace *et al.* 1987). Qualitative descriptions of crown shape include terms such as parabolic, conic, oval, flat-topped, and spire-like, which have been used to describe the profile shapes of many crowns. However, quantitative descriptions are not so common.

Many researchers have used diameter at breast height (dbhob) to estimate crown width (Krajicek *et al.*,1961; Vezina, 1962; Smith and Bailey, 1964). Morris (1955) assessed the crown shape of 78 balsam fir (*Abies balsamea* (L.) Mill.) and concluded that the form of the crown was not that of a cone. Stiell (1962) reported that red pine (*Pinus resinosa* Ait) could be described as a triangular shape for the portions above the plane of maximum width and a rectangular shape for the portion below it. Dirr (1990) reported that loblolly pine crowns are loosely pyramidal when young, losing their lower branches with age and forming an open, oval-rounded crown at maturity. Baldwin and Peterson (1997) reported a crown shape model that could estimate maximum crown radius and its height, crown volume, and crown surface area. The model considered the inner defoliated region and could estimate the crown volume that the foliage occupied. Matsue et al. (1999) reported differences in crown shapes due to tree age, silvicultural treatment and stand structure. Ceulemans *et al.* (1990) reported that genotype had a major influence on crown architecture in *Populus*. Clonal differences in branch characteristics and branching patterns were found that resulted in striking differences in crown form and architecture. Branch angle and curvature differed significantly among clones, and among height growth increments within clones. Branch length and diameter were significantly correlated in all clones. Sylleptic branches and the considerable leaf area they carry had important implications for whole tree light interception, and thus, played a critical role in the superior growth and productivity of certain hybrid poplar clones.

2.3.2 Biomass and foliage area

2.3.2.1 Biomass and its allocation

Biomass and its allocation is of ecological interest because it is related to carbon allocated to the component parts of trees, which influences their growth patterns and capacity to compete with other plants. The ratios of biomass allocation within trees are affected by many environmental factors, such as soil fertility and water availability. Nitrogen fertilization trends to increase the allocation of carbon to foliage (Grier *et al.*, 1985; Gower *et al.*, 1993a). The increasing nutrient availability trends to increase the ratio of new to total foliage mass (Brix and Mitchell, 1983). Water availability has similar effect on the allometric relations for foliage (Brix and Mitchell, 1983; Raison *et al.*, 1992).

To study biomass allocation, many models have been developed (Thorley, 1972; Givnish, 1986; Dewar 1993; Luo *et al.*, 1994). The models could be classified into four groups (Wilson 1988): (a) allometric model; (b) functional equilibra model; (c) Thornley-type model; and (d) hormone models. Allometric models fit equations to data sets, and can describe the data well. However, it is an empirical model and does not provide the explanation of the biomass allocation mechanisms. Functional equilibra models emphasize the importance of the differential functioning of shoots and roots (Givnish, 1986; Dewar 1993). Although functional equilibra models are a significant development over allometric models, these models still provide no information about the mechanisms of biomass allocation. Thornley developed mechanistic models based on carbon and nitrogen uptake and transport. Hormone models suggest the roots produce a hormone that controls the biomass allocation (Wilson 1988).

From the study of biomass allocation, it seems likely that changes in allocation of biomass, resulting from CO_2 enrichment influence water use, nutrient and light capture, and nutrient use efficiency. However, the mechanisms of controlling biomass allocation are still not well understood (Landsberg and Gower, 1997).

2.3.2.2 Foliage area

Foliage area is an important parameter that is used in forest ecology and tree physiology in calculations of photosynthesis and productivity. A number of techniques have been developed to measure leaf surface area. Kvet and Marshall (1971) identified two major approaches: (i) estimation methods using a mathematical relationship between some leaf characteristics and leaf area; and (ii) planimetric methods including photo-electric techniques. Thompson and Leyton (1971) described a third approach to surface area estimation. All the three approaches have been employed to estimate surface area of conifer needles. Beets (1977) and Wood (1971), Kerner *et al.* (1977), Madgwick (1964), and Rutter (1957) used various estimation methods for radiata pine (*Pinus radiata*), Norway spruce (*Picia abies*), red pine (*Pinus resinosa*), and Scotch pine (*Pinus sylvestris*), respectively.

Foliage area can be calculated with foliage mass if specific leaf area is known. Specific leaf area is the ratio of fresh foliage surface area to unit dry foliage mass. It is a very important parameter to convert foliage mass to leaf area. Johnson (1984) reported a rapid technique for estimating total surface area of pine needles. Johnson's method only required three variables for calculating surface area: (1) displaced volume of the needle sample; (2) cumulative needle length of the sample; and (3) the number of needles per fascicle. The form of surface area equation:

$$Area = 2l\left[1+\frac{\pi}{n}\right]\sqrt{\frac{Vn}{\pi l}}$$

Where *Area* is the total surface area (cm^2), *V* is the displaced volume of the needle sample (cm^3), n is the number of needles per fascicle, and l is the cumulative needle lengh of the nedles in the sample (cm). Using Johnson's method, the total sampled fresh foliage surface area and specific leaf area can be easily estimated.

2.3.3 Crown structure models

Modelling light transfer in plant canopies requires description of the spatial arrangement of crown elements (leaves, branches and stems, etc.; Ross, 1981). The ideal crown model should be simple enough to describe crown geometry in experimental plots and to simulate light transfer, but also flexible to enough to represent irregular crown shapes (Cescatti, 1997). There are mainly two kinds of crown models: one is geometrical description of crown shape, and the other is analytical description of crown architecture. For the geometrical description approach, generally crown shape is represented by shapes such as cones, ellipsoids, cylinders or combination of these (Koop and Sterck, 1994; Wang and Javis, 1990a; Grace *et al.*, 1987). Crown architecture is usually defined by statistical distributions of crown elements within crowns (Campbell and Norman, 1989). The limits of this approach are the approximate description of crown asymmetry and the assumption of infinite dimension of crown elements. For the analytical description approach, crown architecture is described in terms of branching pattern, leaf size, position and orientation, on the basis of empirical observation of the branching habit and of the spatial arrangement of leaves (Kurth, 1994; Aries *et al.*, 1993; Stenberg *et al.*, 1998). This approach requires a high number of species specific parameters for the numerical description of crown elements, and, as a result, the simulation of radiative transfer is a complex and computationally demanding procedure (Andrieu *et al.*, 1995; Chen *et al.*, 1994). Recently, Cescatti (1997 a and b) presented a versatile model for mechanistic simulation of the radiative transfer in discontinuous canopies. Canopy structure is described with arrays of asymmetric crown envelopes, adaptable to various tree geometries and based on the following parameters: total tree height, height at crown insertion and at the greatest width of the crown, crown radii in four orthogonal directions, and shape coefficients of vertical crown profiles. Unlike previous models, this canopy model simulates the high level of asymmetry in crown shape and displacement typical of natural and semi-natural forests.

2.4 Solar radiation

Tree crown light interception is dependent on the light coming from the sun, the crown structure and the distribution of the density of foliage area. The photosynthetic active radiant (PAR) energy is necessary for plant photosynthesis, and the light (PAR) distributed

outside and inside tree crown mainly consists of direct and diffuse radiation. Many radiative transfer models have been developed to estimating light interception within canopy (Norman and Jarvis 1975, Kellomaki *et al.* 1985, Kuuluvainen and Pukkala 1987, McKelvey 1990). The following section will review each aspect of global light, direct and diffuse light (PAR) and light penetration within canopies or tree crowns.

2.4.1 Total solar radiation

Solar radiation is the source of energy for the photosynthetic processes of plants. Radiant energy is converted into chemical energy by the leaves of plants for growth. However, not all incoming radiant energy is absorbed by plants even though most of it absorbed and transmitted in canopy. Generally, the solar radiation is divided into two fractions (Pereira, *et al.*, 1982). One fraction is the waveband between 400 and 700 nm referred to as photosynthetic active radiant (PAR), which most plants used for photosynthesis. The other fraction above 700 nm is known as near-infrared radiant (NIR). Many researchers have reported how to measure the two fractions (Gates, 1965; Allen *et al.*,1964; Szeicz, 1968; Monteith, 1973; Newton and Blackman, 1970). Pereira (1982) reported that the photosynthetic active radiation (PAR) and near infrared radiation (NIR) were, respectively, 0.46 and 0.54 of the incoming solar radiation for solar elevation greater than 20° and clear sky conditions.

2.4.2 Direct beam and diffuse radiation

To study the utilization of solar energy requires splitting the direct beam and diffuse radiation from total solar irradiance (Erbs *et al.*, 1982). It is necessary to split the light (PAR) into direct beam and diffuse radiation, because the penetration of direct beam and diffuse radiation into the canopy is very different. For example, a canopy with leaf area index of two might typically have a diffuse transmittance of 25%, while the direct beam transmittance may vary from near zero to 40% or more, depending on solar zenith angle. Failure to distinguish the direct beam and diffuse radiation within the canopy can lead to erroneous calculations of photosynthesis (Norman, 1980), because diffuse radiation is used

much more efficiently than direct radiation by photosynthetic leaves in the canopy. Many researchers have reported how to estimate direct beam and diffuse radiation (Weiss and Norman, 1985; Flint and Caldwell, 1998). Smith (1993) described a computer-based system to estimate photosynthetically active solar radiation (direct and diffuse radiation PAR) received on a horizontal surface from hemispherical photographs. It was developed to analyze the effect of PAR and its spatial distribution on annual growth of the crown and bole of loblolly pine (*Pinus taeda*). This system reduces cost and time required for manual analysis to estimate radiation from hemispherical photographs, and requires a camera with a 180° fisheye lens, computer and scanner. The system is designed to produce data applicable to a broad range of research projects studying light-plant interactions.

2.5 Light penetration

Light penetration within canopies and tree crowns play a very important role in photosynthetic production. At the stand level, there is a common belief that there is a linear relationship between absorbed light (PAR) and dry matter production (Landsberg *et al.*, 1997; Haxeltine and Prentice, 1996; Stenberg *et al.*,1994; McMurtrie et al., 1994; Azam-Ali *et al.*, 1994; West and Wells, 1992; Wang *et al.*,1991; Oker-Blom *et al.*,1991a; Jarvis and Leverenz, 1983; Sievanen *et al.*,1988; Cannell *et al.*, 1987; Grace *et al.*, 1987a; Linder, 1985; Linder *et al.*, 1984; McMurtrie and Wolf, 1983; Monteith, 1977), although others question it (Monteith, 1994; Kiniry, 1994; Arkebauer *et al.*, 1994 Demetriades-Shah *et al.*, 1994; Russell, 1993). At the tree level, the growth of an individual tree depends on a complex of factors, and it is not known if this type of relationship applies. However, light is a dominating factor in ecosystems. Many individual tree growth models include the light values as parameters (Golser and Hasenauer, 1996, 1997; Biging and Dobbertin, 1992). Light penetration can be approached by experimental measurement or light transfer models.

2.5.1 Experimental approaches

Most understanding of the light (PAR) penetration within tree crown or canopies comes from direct field measurements. Approaches to the measurement of light activity have been reviewed by Chazdon (1986) and Pear (1989). Recently, some new methods were reported for direct measurement light within tree crown or canopies. Ammer (1997) described a method for measuring light in forests. It utilizes amorphous silicon cells, and is based on the principle that light in amorphous semiconductors (such as hydrogenated amorphous silicon) produces electrically active defects within the mobility gap, which can be used to measure photoconductivity. The method was tested in the field in summer. Results were compared with conventional data for relative light levels, and were reasonably accurate. The advantages of the method are that it requires no external energy source, and is low-cost. Brown (1994) described a method of estimating solar radiant energy incident (irradiance) in the shade of deciduous (landscape) trees using photographs, and was tested against measured values. Photographs of trees were computer digitized to determine optical porosity of crowns. Wilkinson (1991) compared the photographic and photometric measurements of light attenuation under crowns in full leaf in late June to early September 1989 in the UK, and no significant difference was found between the two methods for the 5 species tested.

2.5.2 *Light transfer model approaches*

Light (PAR) penetration within a forest canopy depends on crown shape, foliage area distribution, and the amount of incoming solar radiation. The development of realistic and simple light interception models for forest stands is a very complex task, still lacking satisfactory solutions (Oker-Blom *et al.*, 1991). When modelling light penetration, not only the canopy structure and the interaction between the light and canopy structure are important as well as light transmission. However, to describe canopy structure requires knowledge of internal structures such as leaf orientation, crown shape and spatial pattern of trees, which are difficult to measure and express with simple equations; and the interaction is more complex with the changed incoming light, and canopy structure according to seasons, ages and species. Many light penetration models have been developed with

varying levels of complexity (see reviews by Norman, 1975; Ross, 1981; Menyni *et al.*, 1989). The main difference between those models is how to treat the canopy structure.

2.5.2.1 Light models with one dimensional approach

In light models with a one-dimensional approach, the canopies are assumed to be continuous on the horizontal plane with foliage randomly distributed (Monsi and Saeki 1953, De Wit 1965, Lemeur, 1973). Bouguer's law (also called Beer-Lambert law or Beer's law, see Iqbal, 1983) describing the exponential attenuation of monochromatic radiation in a turbid medium has often used to model the light regime. Many researchers have reported radiative transfer theory for plant stands with horizontally homogeneous canopies (Nilson, 1971; Norman and Jarvis, 1975; Ross, 1981; Myneni *et al* 1989; Thornley and Johnson, 1990). These kinds of model are easy to describe mathematically. If the model was used in closed canopy with dense foliage distribution and with one species, the assumption of one-dimensional random foliage distribution does not produce excessive errors (Norman and Jarvis, 1975). However, in the case of horizontal heterogeneous or discontinuous canopies such as row crops with wide spacing and most plants in their earlier growth stages, the one-dimensional models are inapplicable (Jarvis and Leverenz 1983).

2.5.2.2 Light models for discontinuous canopies

For discontinuous canopies, some other efforts have considered the non-random distribution of foliage over the vertical or horizontal direction with simple equations that are still fundamentally one-dimensional. In this situation, a discontinuous canopy is assumed to be made up of a group of foliage of a given shape. For plants with closed space within rows, but widely spaced between rows, an appropriate model would be one that assumes each row is a group of foliage, and in each group it is assumed that the foliage is distributed continuously (Allen 1974; Brrown and Pandolfo, 1969; Jackson and Palmer, 1972, 1979; Goudriaan, 1977; Palmer, 1977; Mann *et al.*, 1980). If plants grow with wide spaces both within and between rows, each isolated tree could be treated as a foliage group (Norman and Welles 1983;). For individual trees, it can be treated as a geometrical object,

with the tree crown made up of foliage groups in a certain arrangement, such as foliage ages and levels (Jack and Long, 1992; Grace, 1990; Wang and Javis, 1990a,b; Grace *et al.*, 1987a,b; Nunez, 1985; Stamper and Allen 1979). Still, the foliage is assumed to be randomly distributed within each small group.

2.5.2.3 Light models with more detailed crown architecture for individual tree

These are models where the individual tree crown is assumed to be made up of small cells. The leaf area density within each small cell is assumed to be uniformly distributed, but the cells can be reduced to a suitable size that depends on the foliage distribution specified (Myneni, 1991, Chen *et al.*, 1994; Cescatti, 1997, Castro and Fetcher, 1998). These kind of models need more detailed crown architectural information or require techniques of botanical morphological analysis (Fournier *et al.*, 1996; Kellomaki and Strandman, 1995; Fournier *et al.*, 1995; De Reffye *et al.*,1995; Kurth, 1994; Jaeger and De Reffye, 1992).

2.6 Modelling canopy photosynthesis

The relationship between canopy photosynthesis and canopy structure is one of the important subjects in plant ecology (Monsi 1973). For given solar radiation, canopy photosynthesis results from the interaction between the photosynthetic response of foliage elements and the distribution of radiation on the elements within the canopy. Many researchers have reported results on various aspects of canopy photosynthesis (Kull and Kruijt, 1999, Grace 1987, Myneni 1991, Hollinger 1992, De Pury and Farquhar 1997). The main difference between the developed canopy photosynthesis models is that the various approaching light interception models were applied and connected with different level foliage photosynthesis models.

Recently, some stand level models have used the relationship between leaf photosynthesis and nitrogen concentration to scale carbon assimilation from the leaf level to canopy level (e.g., Running and Gower, 1991; Aber and Federer, 1992; Schulze *et al.*, 1994).

2.6.1 Experimental approaches to modelling canopy photosynthesis

Canopy photosynthesis can be approached with experimental methods. For different canopies, with various species at different sites, the different characteristics of canopy architecture and light penetration within canopies are not easy to model with simple functions. So, for many purposes, it is still convenient to use experimental approaches to estimate canopy photosynthesis. There have been numerous attempts to measure or model canopy structure and light interception, using a range of equipment to measure light distribution within canopies (Gendron, 1998). Henson (1998) reported a simple empirical canopy photosynthesis model which was based on relationships between CO_2 flux and radiation, and CO_2 flux and atmospheric vapor pressure deficit. The model satisfactorily predicted above-canopy flux from measurements of these variables using site-specific regression constants. The limitations and practical implications of the model are discussed.

2.6.2 Theoretical approaches to canopy photosynthesis

Canopy photosynthesis can be theoretically approached with two methods. One, the most used, is based upon light interception theory, and the other is based on the relationship between leaf photosynthesis and leaf nitrogen concentration (Farquhar 1989; Sellers *et al.* 1992).

2.6.2.1 Canopy photosynthesis models based on light interception theory

Many models to predict canopy photosynthesis use the light interception theory of Monsi and Saeki (1953) to estimate light distribution within canopies. With the light interception theory, canopy photosynthesis can be approached from leaf photosynthesis models scaling to canopy. At the leaf level of the photosynthetic model, light (PPFD) is an essential variable to estimate leaf photosynthesis. At the canopy level, canopy photosynthesis depends not only on leaf photosynthetic capacity, but also on light distribution outside and inside the canopies. Canopy photosynthesis can be approached according to various light interception models (Ross, 1981; Myneni *et al* 1989; Thornley and Johnson, 1990; Jack

and Long, 1992; Grace, 1990; Wang and Javis, 1990a,b; Grace *et al.*, 1987a,b). They divided the canopy into multiple layers with many different leaf angle classes, for which absorbed irradiance was used to determine leaf photosynthesis. Numerical integration of photosynthesis from each leaf class yields canopy photosynthesis (Norman 1979).

2.6.2.2 Scaling leaf photosynthesis to canopy photosynthesis model using N distribution

A big-leaf model was first demonstrated by Farquhar (1989) and has been used by many researchers (Sellers *et al.* 1992; Amthor 1994; Lloyd *et al.* 1995; De Pury and Farquhar 1997). It based on the theory that the equation describing whole-leaf photosynthesis would have the same form as for individual chloroplasts across a leaf, provided the distribution of chloroplasts photosynthetic capacity is in proportion to the profile of absorbed irradiance and that the shape of the response to irradiance is identical in all layers. This can be extended to canopies if the distributions of leaf photosynthesic capacity, which is linearly related to leaf nitrogen concentration, and absorbed irradiance are the same throughout the canopy. Under these conditions, equations describing leaf photosynthesis will also represent canopy photosynthesis (Sellers *et al.* 1992). De Pury and Farquhar (1997) presented a theoretical framework of the Big-leaf model. The model is more suitable at large-scale (stand or globe level) and long-period (month, season or year) to approach canopy photosynthesis.

Raulier *et al.* (1999) made a comparison between a big-leaf model (without details of the canopy profile) and two multilayer models (with details of the canopy profile) to estimate daily canopy photosynthesis of a sugar maple stand, using data from 2 stands of contrasting vertical structure in S. Quebec, Canada. The big-leaf model underestimated daily canopy photosynthesis by 26% because of an assumed proportionality between photosynthetic capacity and relative irradiance that was inconsistent with the data used. However, the residual bias was almost eliminated when the big-leaf model was run using a weekly averaged irradiance. Samson *et al.* (1997) concluded that the big-leaf model could be constructed which simulated the net canopy photosynthesis as well as did the multi-layer model. However a multi-layer model for simulating the net canopy photosynthesis is preferable as it allows simpler incorporation or adaptation of parameters. Kull (1998) used

the mechanistic model of leaf photosynthesis and scaled this to canopy photosynthesis using the big-leaf model. Big-leaf models can estimate canopy photosynthesis based on the relationship between the profiles of absorbed irradiance and leaf nitrogen. Leuning *et al.* (1995) used simple mathematical theory linking leaf photosynthesis, nitrogen concentration, and radiation regime to predict vertical distribution of nitrogen (which was needed to maximize canopy photosynthesis) in the canopy.

2.6.3 Process-based ecosystem models

Tree growth is determined by a lot of environmental factors. Recently, a number of process-based ecosystem models were developed, such as MAESTRO, BIOMASS, FOREST-BGC, CENTURY, BEX, PnET AND LINKAGES. These models include not only canopy photosynthesis, but also various detailed environment parameters which are related to carbon balance.

MAESTRO was developed by Wang and Jarvis (1990 a,b). It is considered as a research tool with very detailed descriptions of canopy structure, and it deals with each individual tree in considerable detail and calculates net photosynthesis and transpiration rates in canopies. MAESTRO requires a great deal of data input, including soil surface temperature, crown structure, leaf transmittance and reflectance values for PAR, leaf age class and its density distributions, and a range of physiological parameters for each leaf age. At the leaf level, photosynthesis is calculated using the Farquhar and von Caemmereer (1982) model.

BIOMASS, developed by McMurtrie *et al.*(1990), is a stand-level model consisting of a number of submodels that calculate the carbon balance of the canopy from a radiation interception model that uses information about the canopy structure and foliage photosynthetic characteristics. Tree crown is represented by geometrical constructions (ellipsoids, cones, etc). The foliage is divided into three horizontal layers and different photosynthetic parameters can be specified for the foliage of each layer. BIOMASS has far less detailed radiation interception and photosynthesis routines but includes respiration, the

allocation of carbon to tree components, and a water balance module, none of which are in MAESTRO.

FOREST-BGC (BioGeoChemical), developed by Running and Coughlan (1988), is an ecosystem model designed primarily to provide estimates of carbon, nitrogen, and water cycling across forested landscapes. FOREST-BGC requies no information about canopy properties such as stand density or canopy architecture. Requiring only LAI (leaf area index), which can be estimated by remote sensing. FOREST-BGC simulates the carbon cycle by calculating photosynthesis, respiration, above- and below-ground net primary production, litter-fall, and decomposition.

BEX, developed by Gordon Bonan (1990a, 1991b), was constructed to simulate energy, water and carbon fluxes in boreal forests. The model considered the incorporation of permafrost and the explicit modeling of energy, water, and carbon budgets of the moss layer. No other ecosystem model attempts to model the two important components of boreal forests. The forest energy budget is computed for a multi-layered forest canopy. Daily estimates of ground surface temperature, evapotranspiration, and snowmelt are used to determine soil moisture and soil temperature. Environmental constraints on tree photosynthesis are mediated through mesophyll resistance, thereby including rate limitations imposed by CO_2 diffusion within the plant cells and biochemical processes of CO_2 fixation.

PnET, developed by Aber and Federer (1992), is a simple model that simulates carbon and water circulation. PnET consists of four computational components: climate, canopy photosynthesis, water balance, and carbon allocation. PnET, like FOREST-BGC, uses canopy architecture and Beer's law to calculate light absorption by the canopy. Leaf CO_2 and water fluxes are based on two ecophysiological relationships: (1) maximum net photosynthesis calculated as a linear function of foliar N concentration; and (2) dry mass produced per unit of water transpired, known as the water use efficiency, which provides a link between carbon gain and transpiration.

LINKAGES, developed by Pastor and Post (1986), is a forest stand growth model. It belongs to the forest stand model FOREST family (Shugart, 1984). LINKAGES is unique among those FOREST models because it links carbon and nitrogen cycles with the population dynamics of overstory tree species. The model uses subroutines called BIRTH, GROW, and KILL to simulate the birth, growth, and death, respectively, of trees in stands that contain a number of species.

CENTURY, developed by Parton *et al.* (1987,1988,1993), is an ecosystem model that simulates the water, carbon, and nutrient budgets of grasslands and forests. CENTURY uses different plant production submodels for each of the major vegetation types and a common soil organic matter (SOM) submodel (Sanford *et al.*, 1991). The SOM submodel of CENTURY has been widely used to simulate soil organic matter. Burke *et al.* (1989) reported the grassland version of CENTURY has been coupled to geographical information systems and used to simulate regional grassland dynamics.

Consequently, a number of ecosystem models have been developed, and they all have advantages at different particular levels. However, no model is perfect for all scales. For focusing different problems or requirements, it is still essential to use models at particular level to analyze and view the various aspects of tree and forest growth.

CHAPTER 3

DIFFERENCES IN GROWTH OF RADIATA PINE CLONES

3.1 Abstract

Growth rates of mean tree height (H), diameter at breast height (DBHOB, 1.4m), and groundline diameter (GLD) were analyzed for ten clones of *Pinus radiata* D. Don at the same site with the same treatment at Dalethorpe, Canterbury, in New Zealand. The ten clones could be separated into four significantly different growth groups according to the growth rate of H and DBHOB. A simple model was developed for estimating initial growth of the four groups of radiata pine clones. Comparing the four groups, the mean tree height ranged from 3.5 to 4.8 m, and the mean DBHOB ranged from 7.3 to 10.4 cm at age 5. The results showed that different clones could grow with greatly different rates in H and DBHOB at the same site.

3.2 Introduction

The growth of trees, as measured by changes in height and diameter, has been studied by many researchers (e.g.: Madgwick 1983, Mason 1997, and Murphy 1983). The growth rate can be differing between species (West 1981) and between clones of the same species (Madgwick 1983) growing in the same environmental conditions. For different species of

trees, it is known that their genotypes can be greatly different, and phenotypes are very different too, hence, there are great differences in physiological and morphological characteristics among different species. However, for different clones of the same species, the reasons for the growth differences among clones are often unknown.

The differences in growth of clones could result from a variety of causes, such as variations in foliage photosynthetic efficiency, crown shape and crown volume, foliage surface area and its density distribution, light penetration, biomass allocation, respiration, nutrient, water use efficiency, and litter fall and root turnover.

The objectives of this study were (a) to compare variation of growth of ten radiata pine clones which grew at the same site with the same field treatments; and (b) to develop a simple growth model to predict the initial growth of H, DBHOB, and GLD for the different clones. The results will be used in following chapters for detailed studies aimed at understanding what were the most important factors, such as foliage photosynthetic rates, crown shape, foliage mass and light penetration, which affected growth differences among the clones.

3.3 Materials and methods

3.3.1 Materials

An experiment containing ten clones of radiata pine was established on a site at Dalethorpe, Canterbury, New Zealand in September 1993. The soil was well-developed silt-loam. Mean annual precipitation is 1447 mm. Distribution of precipitation is fairly even throughout the year although a marked dry period can occur during February and March (McCracken 1980).

The clones came from controlled pollinated seed. They were propagated by organogenesis following cryogenic storage of the embryos to retard maturation. After propagation they were hardened off in a nursery, conditioned with an undercutting and wrenching regime, and then sent to the planting site as bare-root plants.

Three complete blocks of ten different clone treatments were established on the site. Each plot contained 5 x 8 trees of the same clone, and avoiding the buffer lines a total of 18 trees was measured. Planting spacing was 2 x 4 m. Planting rows were ripped to a depth of 30 cm prior for planting. Height and groundline diameters (GLD) of all individuals of each clone were measured immediately after planting. Height was remeasured annually from planting. GLD was measured from year 0 to 3 years, and after 3 years when the trees had grown higher than 1.4 m, the diameters at breast height outside of bark (DBHOB, 1.4 m) were measured. No pruning or thinning treatments was applied to the experiment from 0-6 years.

3.3.2 Methods

The annual data measured as H (height), DBHOB (diameter at breast height), and GLD (groundline diameter) were analyzed with SAS (SAS Institute Inc., 1996). The analytical procedures used were GLM for linear regression models, NLIN for non-linear regression models and PLOT for graphical analysis.

Firstly, growth in height and DBHOB were subjected to analysis of variance by using GLM, and the ten clones were separated to significant different groups according to the variation in H and DBHOB.

Secondly, different growth group data were used to fit height and diameter functions with procedure NLIN in SAS. The mean height function (Mason 1997) used was as follows:

$$Ht = H_0 + a * T^b \qquad (3.1)$$

Where H_0 = mean height after planting, T = stand age, Ht = mean height at stand age T, and a and b were estimated coefficients.

The mean DBHOB equation 3.2 was as follows:

$$DBHOBt = a * \exp(-T) * T^b \qquad (3.2)$$

Where DBHOBt = mean diameter at breast height at stand age T, T = stand age, and a and b were estimated coefficients.

The mean GLD function was as follows:

$$GLDt = GLD_0 + a * T^{b} \qquad (3.3)$$

Where GLDt = mean groundline diameter at stand age T, GLD_0 = mean groundline diameter after planting, T = stand age, and a and b were estimated coefficients.

Next, the means of the residuals were presented by using PLOT procedure to show the function's predicting biases. Finally, the results of predicting H, DBHOB, and GLD were reported for the different growth groups of radiata pine clones.

3.4 Results

All data measured in height and DBHOB were analyzed by using the GLM procedure and the TUKEY option in SAS. There were significant differences in growth among clones. Combining the results of the analysis of variance and the TUKEY analysis of H and DBHOB, the ten clones could be separated to four different growth groups. For example, the first group A included clone 9 only, which had the highest stem growth rate among the ten clones; the second group B included clones 4, 5, and 2; the next group C contained clones 6, 7, 8, and 1; and the last group D included clones 10 and 3. In the following sections, the results of analysis for each variable (H, DBHOB, and GLD) are presented for the four different growth groups.

3.4.1 Height

Results in table 3.1 show the parameters from fitting mean height function (3.1) for each different group of clones. Figure 3.1 shows the distribution of residuals about the mean height models for the four different growth groups of clones. Most of the residuals were within ± 50 cm of the predictions, and all were within ± 70 cm.

Table 3.1 : The results of fitting height function $Ht = H_0 + a * T^b$ with four groups of different clones.

Clone group	H_0 (cm)	Parameter	Parameter estimate	Asymptotic	95 % Confidence Interval	
				Std. Error	Lower	Upper
Group A	27.6	a	33.57986	4.106332	24.70868	42.45105
		b	1.619034	0.082828	1.440095	1.797973
Group B	26.6	a	21.04799	2.145699	16.72079	25.37519
		b	1.840442	0.068241	1.702822	1.978062
Group C	28.3	a	20.74858	1.568146	17.60959	23.88756
		b	1.776948	0.050751	1.675358	1.878538
Group D	29.9	a	17.58308	1.871301	13.74992	21.41624
		b	1.804784	0.071366	1.658599	1.950969

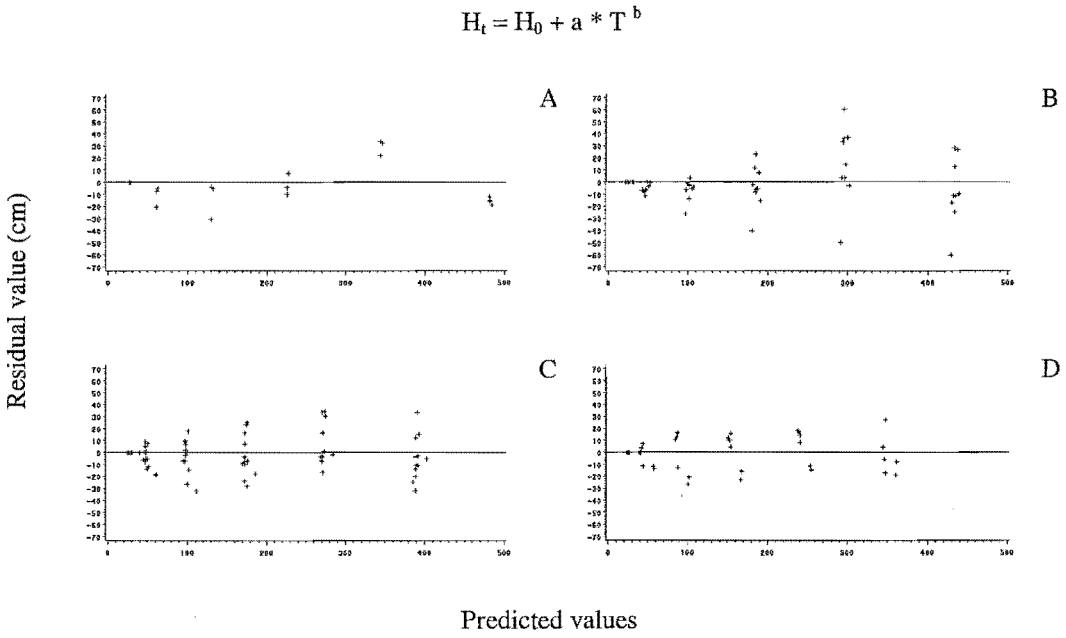

Figure 3.1. Residual (cm) vs predicted values for mean height model estimated from four group data of growth different clones. A = clone 9. B = clone 4, 5 and 2. C = clone 6, 7, 8 and 1. D = clone 10 and 3.

With the function 3.1 was fitted to predict mean height growth, when different clonal groups showed significantly differences. Figure 3.2 clearly shows that mean height ranged

from 3.5 to 4.8 m at age 5. Group A had the highest growth rate in mean height, followed by group B group C, and group D.

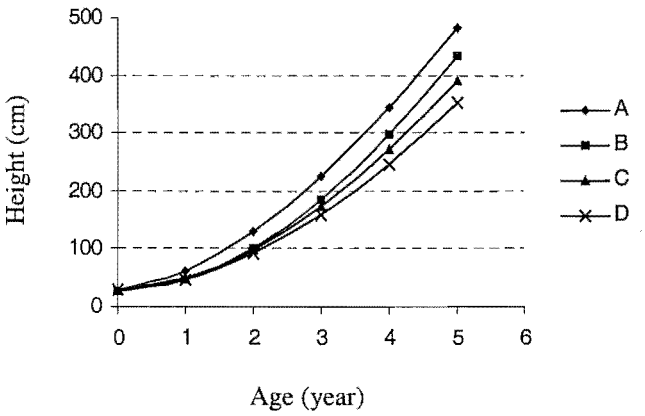

Figure 3.2. Using developed height function $H_t = H_0 + a * T^b$ to predict heights according to ages for four growth difference groups of radiata pine clones. A = clone 9. B = clone 4, 5 and 2. C = clone 6, 7, 8 and 1. D = clone 10 and 3.

3.4.2 Diameters at breast height (DBHOB)

The best fit for mean DBHOB equation was equation 3.2 for the DBHOB data of the four different growth groups. Table 3.2 shows the estimated parameters of the four different

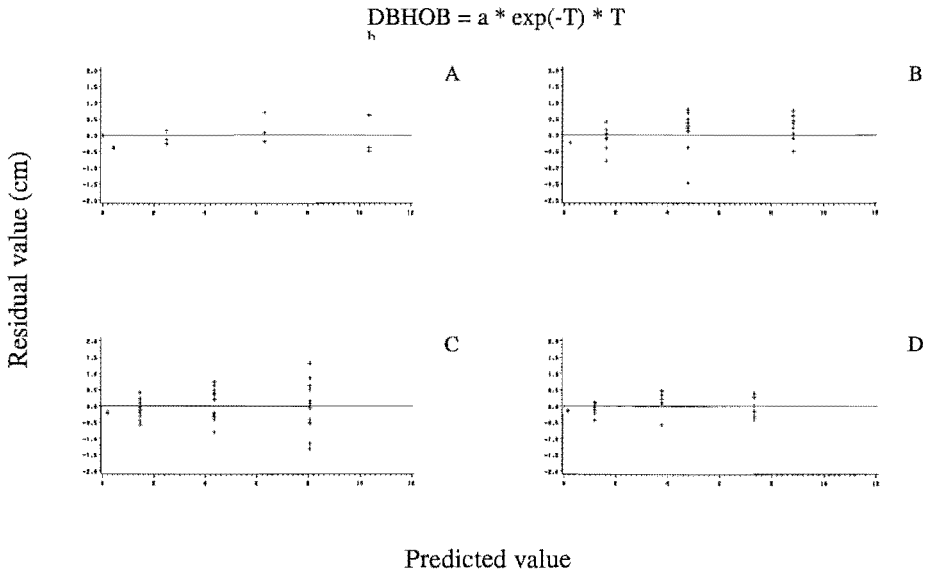

Figure 3.3. Residual (cm) vs predicted values for mean DBHOB model fitted for four group data of growth different clones. A = clone 9. B = clone 4, 5 and 2. C = clone 6, 7, 8 and 1. D = clone 10 and 3.

Table 3.2 : The results of fitting function DBHOB = a * exp (-T) * T^b with four groups of different clones.

Clone group	Parameter	Parameter estimate	Asymptotic	95 % Confidence Interval	
			Std. Error	Lower	Upper
Group A	a	0.031524	0.006341	0.017825	0.045224
	b	6.70826	0.130974	6.425308	6.991213
Group B	a	0.011645	0.002622	0.006356	0.016933
	b	7.227512	0.145178	6.934735	7.52029
Group C	a	0.010105	0.001797	0.006507	0.013703
	b	7.258911	0.114605	7.029503	7.488318
Group D	a	0.006539	0.001072	0.004344	0.008735
	b	7.470189	0.105266	7.254563	7.685814

groups for fitting equation 3.2. Figure 3.3 shows the distribution of residuals about the mean DBHOB models for the four different growth groups of clones. All the residuals about the mean DBHOB model were within ± 2 cm of the predictions. For estimating mean DBHOB, using the mean DBHOB models to predict and compare the growth difference among clones, Figure 3.4 shows the same trends as height growth. Group A had the highest growth rate in mean DBHOB, then group B, Group C, and group D. The range of mean DBHOB was from 7.3 to 10.4 cm for the four groups at age 5.

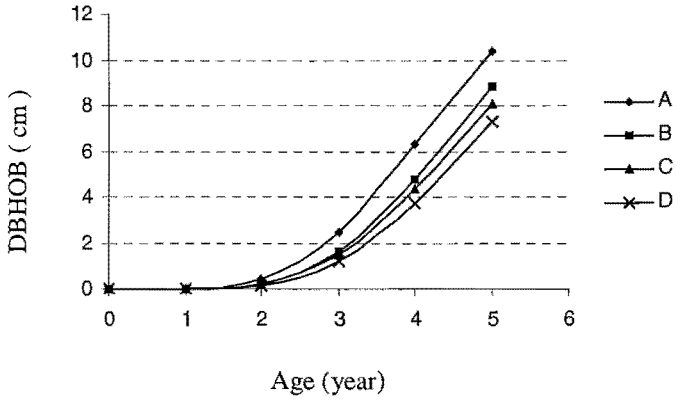

Figure 3.4. Using developed diameter function DBHOB = a * exp(-T) * T^b to predict DBHOB according to ages for four growth difference group of radiata pine clones. A = clone 9. B = clone 4, 5 and 2. C = clone 6, 7, 8 and 1. D = clone 10 and 3.

3.4.3 Groundline diameters (GLD)

For estimating GLD, the four groups' data were used to fit mean GLD equations. Table 3.3 lists the estimated parameters for fitting the mean GLD function.

Table 3.3 : The results of fitting ground level diameter function $GLDt = GLD_0 + a * T^b$ with four groups of different clones.

Clone group	GLD_0 (cm)	Parameter	Parameter estimate	Asymptotic Std. Error	95 % Confidence Interval Lower	Upper
Group A	0.71	a	0.704751	0.114368	0.434312	0.97519
		b	2.083044	0.155846	1.714524	2.451564
Group B	0.69	a	0.700114	0.086766	0.521417	0.87881
		b	1.935608	0.119853	1.688768	2.182448
Group C	0.69	a	0.702869	0.086558	0.519374	0.886363
		b	1.906519	0.119276	1.653666	2.159372
Group D	0.73	a	0.734942	0.068557	0.595618	0.874266
		b	1.883583	0.090458	1.699753	2.067414

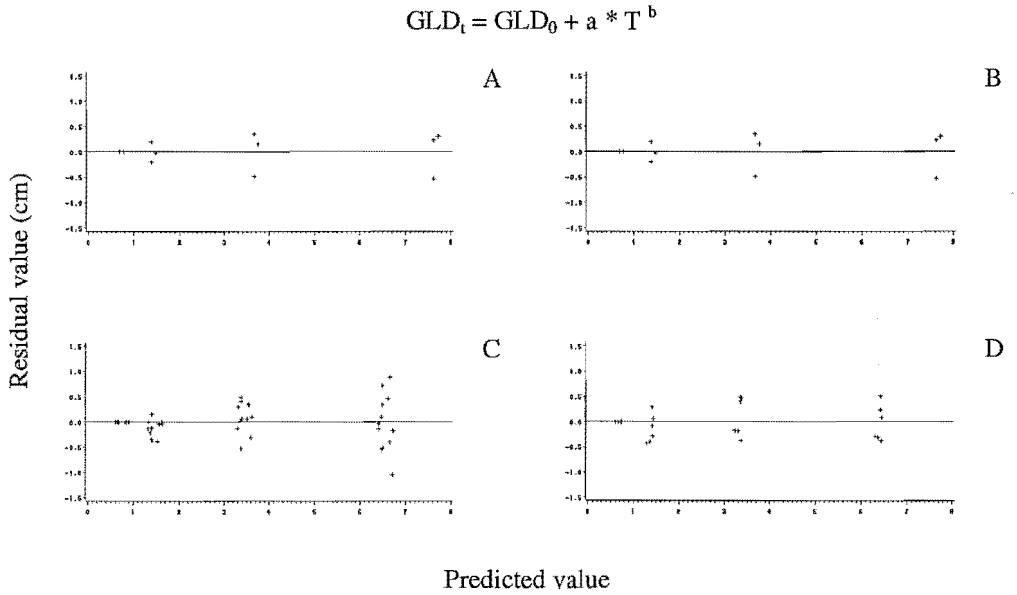

Figure 3.5. Residual (cm) vs predicted values for mean GLD model fitted for four group data of growth different clones. A = clone 9. B = clone 4, 5 and 2. C = clone 6, 7, 8 and 1. D = clone 10 and 3.

Figure 3.5 shows the residuals against predicted values (cm) for mean GLD model (3.3). All residuals distributed within ± 1.5 cm.

Mean GLD variance between the groups is illustrated in Figure 3.6. Group A was still higher than other groups for the mean GLD, but there were no significant differences among other groups for mean GLD. The range of mean GLD was from 6.5 to 7.8 cm at age 3.

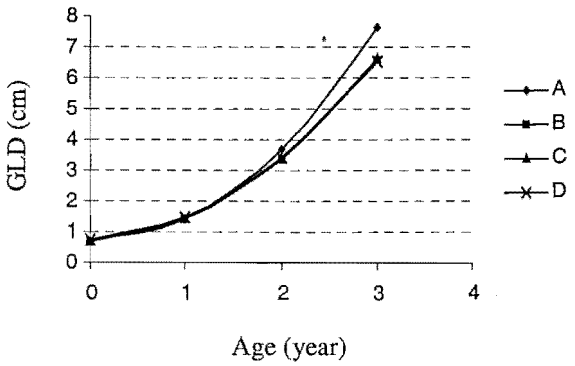

Figure 3.6. Using developed ground level diameter function $GLD_t = GLD_0 + a * T^b$ to predict GLD according to ages for four different groups of radiata pine clones. A = clone 9. B = clone 4, 5 and 2. C = clone 6, 7, 8 and 1. D = clone 10 and 3.

3.5 Discussion

There were many models that could be used to describe radiata pine growth (Mason 1997; Zhao 1999). One objective of this study was presenting the growth differences among the ten clones. So, some simple functions, such as $Ht = H_0 + a * T^b$ for estimating mean height, were used and were fitted effectively with the data measured in the clonal experiment.

Different clones have different genus. Genetic variability may cause growth differences. In forest production, the yields could be increased by genetic selection (Evans 1975). The results in this study showed that different clones grew at different rates in height and DBHOB. The question arises, did this growth difference result from different rates of CO_2 fixation, was it caused by differences in dry matter allocation or was it from some other cause? Is total tree dry matter production related to crown shape, crown volume, and foliage mass, and if so, can these relationships be expressed qualitatively? The following Chapters will address these questions.

3.6 Conclusions

— Clones varied significantly in growth rate in height and DBHOB at the same site and with same field treatment. The ten clones could be separated to four different growth groups according to the variance of height and DBHOB. Variation in mean height ranged from 3.5 to 4.8 m, and mean DBHOB ranged from 7.3 to 10.4 cm at age 5.

— There were no significant differences in GLD growth among groups B, C, and D, however, group A showed a significantly higher growth rate in GLD than other groups. The range between group A and other groups was from 6.5 to 7.8 cm at age 3.

— The model described in this study could predict initial growth in mean height, DBHOB, and GLD for the ten clones on this site. Residuals lay within ± 70 cm about the estimated mean height; distributed within ± 2 cm for the estimated mean DBHOB; and scattered ± 1.5 cm for the estimated mean GLD.

CHAPTER 4

SEASONAL NEEDLE PHOTOSYNTHESIS RESPONSES TO LIGHT AND TEMPERATURE IN 3 NEEDLE AGE—CLASSES OF 5 -YEAR-OLD RADIATA PINE (*PINUS RADIATA*) CLONES

4.1 Abstract

Seasonal photosynthetic responses to light and temperature curves of 1-, 2- and 3-year-old needles of 5-year-old radiata pine (*Pinus radiata* D. Don) clones were measured under controlled environmental conditions in the field. Needle net photosynthetic rates did not show statistically significant differences between two radiata pine clones with different rates of growth in any season. However, both showed the following trends: 1-year-old needles had the highest rates of net photosynthesis 3.46–5.28 (μmol $m^{-2}s^{-1}$) in winter, 7.6–11.18 (μmol $m^{-2}s^{-1}$) in spring, 1.04–2.75 (μmol $m^{-2}s^{-1}$) in summer and 5.89–8.63 (μmol $m^{-2}s^{-1}$) in autumn (the range was affected by temperature). Net photosynthesis decreased with leaf age but increased with temperature (5°C - 20°C). Comparing the maximum photosynthetic rates under the same measurement conditions, there were no statistically significant differences among the ten clones or according to crown position (crown level and aspect i.e. north-, south-, east-, and west-facing). A simple model of needle photosynthesis was developed with needle age-class, vapor pressure deficit and temperature as independent variables in four seasons. The model is useful for describing needle photosynthesis according to needle age-class and temperature in a given season, and can be used to further simulate whole tree photosynthetic CO_2 fixation when this is combined with research on crown shape, needled surface area and light interception.

4.2 Introduction

In general, tree growth depends on net photosynthesis rate (***A***), total leaf area and leaf retention on the tree (Samsuddin, 1979). The photosynthetic capacity of leaves varies greatly during their development. Differences occur in rate of photosynthesis of juvenile and adult leaves and in adult leaves of different ages (Hom and Oechel 1983). Coniferous species normally carry several needle age-classes that behave differently both physiologically and phenologically and thus may exhibit wide differences in response to photosynthesis and temperature (Kaiyun, W. 1995). Radiata pine, as a conifer species, carries needles for many years (Rook, D. A., 1976; Wood, G. B., 1974). Periods of leaf retention on the species are longer than in deciduous trees, so it is more important to study photosynthetic capacity according to needle age-class in response to light, temperatures and season.

Clonal experiments of radiata pine showed great differences (Chapter 3) in height and DBHOB (diameter of breast height). The growth differences among clones may be the result of differences in net photosynthesis rate (***A***), total leaf area, crown shape, needle distribution within crown, and difference in biomass allocation, underground roots distribution etc. This study addressed needle photosynthetic factors that may have caused differences in photosynthetic rates among the different radiata pine clones.

Photosynthesis of evergreens in a given season varies with climatic regions. In Mediterranean regions, the photosynthetic capacity of evergreens was reduced only slightly during the winter (Kozlowski, T. T. and Pallarardy, S. G. 1997). However, in Vermont, Schaberg *et al.* (1995) reported that photosynthesis rates of red spruce generally were low during the winter but increased substantially during thaws, and on some days the rates of individual trees were as high as those during the growing season of spring. In Canterbury, New Zealand, winter temperatures are generally between –2 °C and 8 °C, and most daytime temperatures are above zero (McCracken, I. J. 1980). In summer, the air temperature and soil temperature are not the limiting factors for photosynthetic CO_2 fixation, but summer is very dry in the Canterbury region, and water is the limiting factor

for photosynthetic CO_2 fixation. Therefore, to evaluate whole tree photosynthetic production in each clone, it is important to study the capacity of needle photosynthesis in a given season and to compare the capacity of each clone for needle photosynthesis in each season.

The objectives of this study include the following four parts are:

(1) To compare net photosynthesis rate (***A***, μmol CO_2 $m^{-2}s^{-1}$) in response to light between clone 9 (rapidly growing) and clone 10 (slowly growing) for different temperatures and leaf ages, and to evaluate whether net photosynthesis rate (***A***, μmol CO_2 $m^{-2}s^{-1}$) was significantly different between the two clones in a given season; (2) to investigate the effect of leaf age and temperature on net photosynthesis rate in four seasons; (3) to understand whether crown position affected needle photosynthesis rate of juvenile clonal radiata pine with an uncovered crown; (4) to develop a simple needle photosynthetic model for evaluating needle photosynthesis and for simulating whole tree CO_2 fixation.

4.3 Materials and methods

4.3.1 Study area and field environmental conditions

The study site was located at Dalethorpe (Altitude 520m, 42°45'E, 171°55'S) about 70 km west of Christchurch, New Zealand. The sample trees used were from a five-year-old radiata pine (*Pinus radiata* D. Don) clones experiment established by the School of Forestry, University of Canterbury. The site was planted with one year-old trees in September 1993. All of the clones were provided by the Fletcher Challenge Ltd. Centre for Advanced Biotechnology. Two experiments were established and each contained three blocks. A completely randomized block design was used for each of the three clone experimental blocks. Each block had 11 plots and the size of each plot was 20 x 16 m. The planting spacing was 2 x 4 m.

The climate at Craigieburn (Altitude 910m, 43°10'S, 171°45'E), was reported by McCracken (1980) as follows: winter temperatures are generally between –2 °C and 8 °C, and daytime temperatures mostly above zero (mean temperature 2 °C). The maximum winter temperatures can reach 13.5°C in July and 16.2 °C in August. The mean temperatures in spring are between 1.7°C and 13.2°C, and the maximum temperature reached is 25.2°C in October. The warmest month (February) has mean temperatures of 13.9°C and 9.7°C, and the coldest month (July) has means of 2.0°C and –1.4°C respectively. Soils seldom freeze and mean soil temperatures do not fall below 2.0°C. Mean annual precipitation is 1447 mm. Distribution of precipitation is fairly even throughout the year although a marked dry period can occur in low-altitude areas during February and March. Mean daily radiation is at a maximum in December and a minimum in June. Annual mean radiation is 4745 MJ/ m^2 at the Craigieburn Forest climate station.

4.3.2 Field measurement of photosynthetic response curves

A sample tree was selected with average height and DBHOB from each of the two clones. Clone 9 was a rapidly-growing clone with a mean height of 4.2 m and DBHOB of 7.3 cm, and clone 10 was a slowly-growing clone with a mean height of 2.8 m and DBHOB of 4.1 cm (in the winter of 1997). For each sample tree, the photosynthetic response curves were measured with a Li-Cor 6400 portable photosynthesis system (Li-Cor, Inc., Lincoln, NE, 1994) for a north-facing branch at 2/3 of tree height. On each of the sample branches, net photosynthesis rate (***A***) was measured for 3 leaf age classes: 1-, 2- and 3-year-old, at temperatures of 5°C, 10°C and 15°C in winter, 10°C, 15°C and 20°C in spring, 25°C, 30°C and 35°C in summer, and 10°C, 15°C and 20°C in autumn. The sample needles and branches were all maintained in their natural orientations during measurement. For each measurement, two fascicles were selected randomly to put in the Li-Cor 6400 leaf chamber, and the measurement was repeated, using another two fascicles. For all the measurements, CO_2 concentration was kept constant at 350 μmol mol^{-1} in the leaf chamber (2x3cm curette). Also vapor pressure deficits (VPD) were kept constant at 1.2 kPa in winter and spring, 3.5 kPa in summer and 1.5 kPa in autumn. VPD could be adjusted in the leaf chamber with Li-6400, but only over a limited range and so it was used only for

keeping VPD at a constant level. An LED light attachment as light source was used on the leaf chamber to set light at 0, 100, 250, 500, 1000 and 2000 μmol $m^{-2}s^{-1}$ levels.

The measurement periods were in winter from 25 July to 25 August 1997, in spring from 5 to 25 October 1997, in summer from 1 to 24 January 1998 and in autumn from 2 to 25 April 1998. Measurement days were chosen depending on the weather: measurements were made on days when air temperatures were near our design levels, with no precipitation, and no strong wind. For example, when the field temperature was near 5°C, we adjusted and controlled the measurement temperature in the leaf chamber to 5°C, in order to keep the temperatures of collected data closer to field temperatures (The Li-Cor 6400 can adjust leaf chamber temperature).

4.3.3 Measurement of the photosynthetic rate for comparing the effects of crown position on photosynthetic rate

For comparing the effects of crown position (level and aspect) on photosynthetic rate, the photosynthetic rates were measured for 4 aspects and 3 levels (upper, middle and lower, and the distance between levels was 1 m) of the crown in 3 sample trees in all four seasons. To compare the effect of crown aspect on photosynthetic capacity, three sample trees were selected randomly from clone 10. In each sample tree, 4 aspects (east-, south-, west- and north-facing) of the crown were measured. For each aspect, 2 samples were measured (each sample containing two fascicle needles) using 1-year-old needles from the middle of the crown. To evaluate the effect of crown level on photosynthetic capacity, three sample trees were selected randomly from clone 10. In each sample tree, 3 levels (upper, middle and lower) of the crown were measured. For each level, 2 samples were measured (each sample containing two fascicle needles) using 1-year-old needles from the north-facing part of the crown. All the measurements for level and aspect were repeated in each season and the conditions of measurement were kept constant within each season (VPD = 1.5, and temperature =20 in spring; VPD =3.5, and temperature =30 in summer; VPD =1.5 and temperature =17 in autumn ; VPD =1.5 and temperature =10 in winter).

4.3.4 Measurement of the maximum photosynthetic rate for comparing photosynthetic capacity differences among the ten clones

For further comparing the photosynthetic capacity among all ten radiata pine clones, the maximum photosynthetic rates were measured under the same conditions in autumn (keeping CO_2 constant at 350 μmol mol^{-1}, VPD at 1.8 kPa, temperature at 23°C and light at the 2000 μmol $m^{-2}s^{-1}$). Three sample trees were selected randomly from each of the ten clones. In each sample tree, 3 samples were measured (each sample containing two fascicle needles) and 4 records were collected for each measurement at the same aspect and position in the crown.

All the photosynthetic measurement and measurement conditions are briefly listed in Table 4.1.

Table 4.1—List of measurements and measurement factors.

Factors	Measurements		
	Photosynthetic response curves	Comparing Maximum photosynthetic rates among 10 clones	Comparing photosynthetic rates in different crown position
Clone	2	10	1
Tree	1	3	3
Age	3	1	1
Temperature	3	1	1
Season	4	1	4
Samples	2	3	2
Light	6	1	4
Crown level	1	1	3
Crown aspect	1	1	4
Fascicles	2	2	2

4.3.5 Foliage nutrient analyses

A total of 30 fascicles of 1-year-old needles were randomly collected from each of the ten clones in winter, 1997. In each of the thirty samples, 10 fascicles were randomly collected from a sample tree, and total three sample trees were selected from each clone. All the sampled needles were put in plastic bags separately, and the fresh weight obtained immediately in laboratory. After that, foliage analysis was made using the method outlined by Ballard & Will (1981).

4.3.6 Statistical analysis

Four nonlinear equations were selected to fit all the light response curve data by using the SAS software package (SAS Institute, Cary, NC, 1990). A nonlinear equation (4.1) was described by Thornley (1976) and used by Grace (1987); equation (4.2) was developed by Hanson *et al.* (1988) and Groninger *et al.* (1996); equation (4.3) was described by Angela Crowe and Alan Crowe (1969) and used by Witowski (1997), and equation (4.4) was used to fit the relationship between photosynthesis and irradiation by Kubiske and Pregitzer (1996). The forms of the four equations tried were:

$$\boldsymbol{A} = M*B * (Q / (M + B * Q)) - K \quad \ldots\ldots\ldots\ldots\ldots\ldots \quad (4.1)$$

$$\boldsymbol{A} = M \left(1-(1+K / M)^{(1-Q/B)} \right) \quad \ldots\ldots\ldots\ldots\ldots\ldots \quad (4.2)$$

$$\boldsymbol{A} = M - (M + K) \exp(-B * Q) \quad \ldots\ldots\ldots\ldots\ldots\ldots \quad (4.3)$$

$$\boldsymbol{A} = M * (Q / (B + Q)) - K \quad \ldots\ldots\ldots\ldots\ldots\ldots \quad (4.4)$$

Where $\boldsymbol{A}$ = instantaneous photosynthesis, Q = photosynthetic active radiation (PAR) reaching the needles, and M, B and K are function parameters. The fitting was done on all data from the recorded values of photosynthesis and PAR that were measured at different levels of leaf temperature and for different leaf age classes of the two clones.

The parameters of light-saturated rate of net photosynthesis ($\boldsymbol{A}_{(max)}$, μmol CO_2 $m^{-2}s^{-1}$), dark respiration rate (Rd; μmol CO_2 $m^{-2}s^{-1}$) and light compensation point (Qc; μmol $m^{-2}s^{-1}$)

were determined from the fitted equation. Light saturation point (Qs; μmol $m^{-2}s^{-1}$) can be calculated if we set ***A*** (μmol CO_2 $m^{-2}s^{-1}$) to 95% of $\boldsymbol{A}_{(max)}$ (Man and Lieffers 1997).

Analyses of variance were used to test for differences of the parameters at different temperatures, needle-age-classes, seasons and in different clones. The GLM procedure and Tukey-Kramer HSD test of SAS were used to test and determine differences.

4.4 Results

4.4.1 Selection of equation for estimating needle photosynthesis

Results of fitting the four equations (4.1, 4.2, 4.3 and 4.4) are shown in Figure 4.1. Comparing the values of residual against predicted for the rate of photosynthesis, equation (4.4) had less residual bias. Most of the residuals about the model were within ±1 (μmol CO_2 $m^{-2}s^{-1}$) of the predictions (Figure 4.1, d), and all were within ±2 (μmol CO_2 $m^{-2}s^{-1}$). So equation (4.4) was selected to fit the measurement data and to predict needle photosynthetic response to PAR.

4.4.2 Comparing the parameters of light response curves between rapidly-growing clone 9 and slowly-growing clone 10

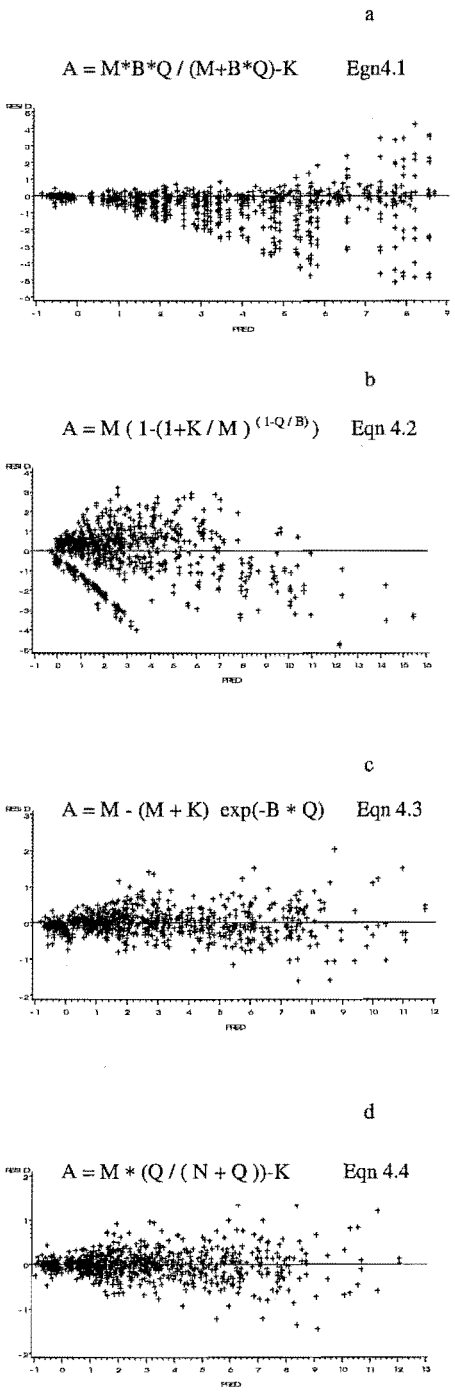

Figure 4.1. Comparing the results of residuals of fitting equations 4.1, 4.2, 4.3 and 4.4 for all data from light curve measurement.

Table 4.2 Analysis of variance of Amax for radiata pine clones at age 5 at Dalethorpe

Source	d.f.	Sum of squares	Mean square	F	P>F
Clone	1	0.43	0.43	0.53	0.4692
Season	3	874.80	291.60	358.77	0.0001
Clone x season	3	0.73	0.24	0.30	0.8255
Temperature	1	19.66	19.66	24.19	0.0001
Clone x temperature	1	0.58	0.58	0.72	0.3990
Age	3	274.31	91.44	112.50	0.0001
Clone x age	3	0.98	0.33	0.40	0.7506
Age x season	7	46.05	6.58	8.09	0.0001
Residual	145	117.85	0.81		
Total	167	1519.29			

Table 4.3 Analysis of variance of Rd for radiata pine clones at age 5 at Dalethorpe

Source	d.f.	Sum of squares	Mean square	F	P>F
Clone	1	0.00	0.00	0.12	0.7337
Season	3	2.13	0.71	26.32	0.0001
Clone x season	3	0.06	0.02	0.69	0.5590
Temperature	1	1.05	1.05	39.10	0.0001
Clone x temperature	1	0.02	0.02	0.89	0.3461
Age	3	0.09	0.03	1.09	0.3567
Clone x age	3	0.15	0.05	1.84	0.1420
Age x season	7	0.46	0.07	2.46	0.0206
Residual	145	3.91	0.03		
Total	167	7.48			

Table 4.4 Analysis of variance of Qs for radiata pine clones at age 5 at Dalethorpe

Source	d.f.	Sum of squares	Mean square	F	P>F
Clone	1	15367.79	15367.79	0.53	0.4676
Season	3	4632523.05	1544174.35	53.29	0.0001
Clone x season	3	62165.45	20721.82	0.72	0.5445
Temperature	1	54284.72	54284.72	1.87	0.1732
Clone x temperature	1	5810.36	5810.36	0.20	0.6550
Age	3	3418143.05	1139381.02	39.32	0.0001
Clone x age	3	6872.39	2290.80	0.08	0.9713
Age x season	7	398703.45	56957.64	1.97	0.0636
Residual	145	4201598.30	28976.54		
Total	167	15324012.73			

Table 4.5 Analysis of variance of Qc for radiata pine clones at age 5 at Dalethorpe

Source	d.f.	Sum of squares	Mean square	F	P>F
Clone	1	0.16	0.16	0.00	0.9703
Season	3	5840.57	1946.86	16.47	0.0001
Clone x season	3	213.55	71.18	0.60	0.6147
Temperature	1	1875.95	1875.95	15.87	0.0001
Clone x temperature	1	6.52	6.52	0.06	0.8147
Age	3	107.13	35.71	0.30	0.8239
Clone x age	3	158.30	52.77	0.45	0.7203
Age x season	7	398.33	56.90	0.48	0.8470
Residual	145	17143.34	118.23		
Total	167	36610.00			

There were no statistically significant differences between the two different clones for all values of maximum photosynthesis rate (***A***max), dark respiration rate (Rd), light saturation point (Qs), and light compensation point (Qc) under the investigated leaf ages and temperatures in all four season (Table 4.2, 4.3, 4.4 and 4.5). More detailed comparisons under different temperatures and leaf ages in all four season are listed in Appendix Table A1.1-A1.4. This result indicates that there were no statistically significant differences between the two different clones in light response curves under different temperatures and needle age classes in all four seasons.

4.4.3 Changes of net photosynthetic rate with photosynthetic active radiation

Relationships between net photosynthetic rate (***A***, μmol CO_2 $m^{-2}s^{-1}$) and temperature of radiata pine in response to photosynthetic active radiation (PAR) for 3-leaf-age classes in winter and spring are shown in Figure 4.2; for 4-leaf-age classes in summer in Figure 4.3, and in autumn in Figure 4.4. From all the Figures 4.2-4.4, they showed clearly that net photosynthetic rate (***A***, μmol CO_2 $m^{-2}s^{-1}$) increased with PAR until saturation. Net photosynthetic rate (***A***, μmol CO_2 $m^{-2}s^{-1}$) changed not only with PAR, but also with leaf age, temperatures and season.

4.4.4 Effect of leaf ages on photosynthesis

The maximum photosynthetic rates (***A***max) showed significant differences with leaf age classes at all the investigated temperature levels in all four seasons (Figure 4.2, 4.3, 4.4 and Appendix Table A1.5 and A1.6). For example, the value (***A***max) ranged from 3.46–5.28 μmol $m^{-2}s^{-1}$ in 1-year-old needles; 2.22–3.79 μmol $m^{-2}s^{-1}$ in 2-year-old needles and 1.46–1.70 μmol $m^{-2}s^{-1}$ in 3-year-old needles in winter, and it increased to 7.6–11.18 μmol $m^{-2}s^{-1}$; 6.94–8.61 μmol $m^{-2}s^{-1}$ and 5.31–7.01 μmol $m^{-2}s^{-1}$ in 1-, 2- and 3-year-old needles respectively in spring. Although the value (***A***max) range changed with temperature and VPD with season, there were still significant effects of needle age on ***A***max. The maximum photosynthetic rate (***A***max) gradually declined with needle age. Current year and 1-year-old needles showed the highest (***A***max) among the needle age-classes.

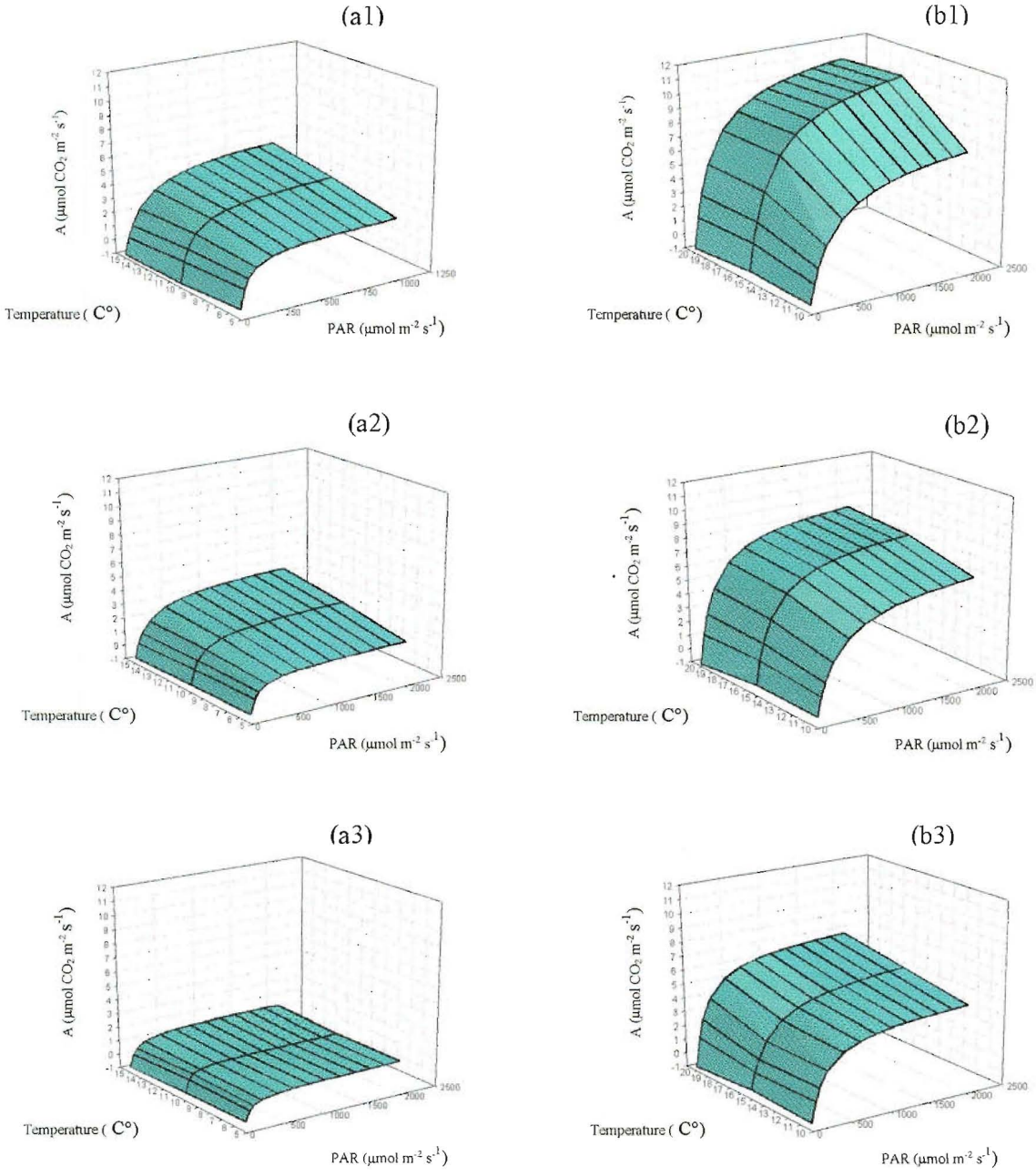

Figure 4.2. Relationships between net photosynthetic rate (***A***) and the temperature of radiata pine in response to PAR. The measurements were made for the following leaf age classes: 1-year-old (a1,b1), 2-year-old (a2,b2) and 3-year-old (a3,b3); constant vapor pressure deficit (VPD) 1.2 kPa. The data (a1,a2 and a3) were collected on 25 July to 25 August 1997 in winter and data (b1,b2 and b3) were collected on 5 to 25 October 1997 in spring.

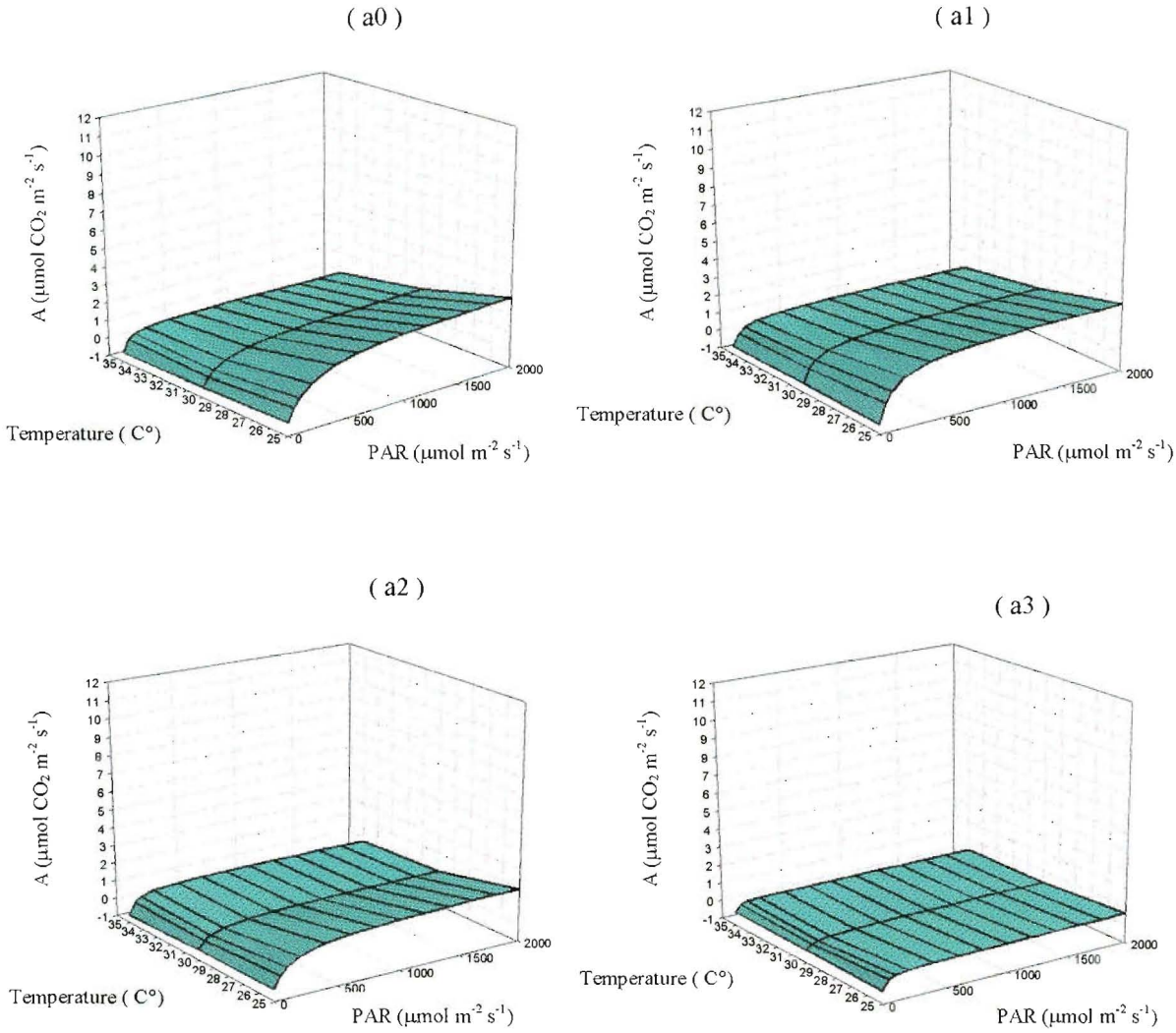

Summer

Figure 4.3. Relationships between net photosynthetic rate (***A***) and the temperature of radiata pine in response to PAR. The measurements were made for the following leaf age classes: Current-year-old (a0), 1-year-old (a1), 2-year-old (a2) and 3-year-old (a3); constant vapor pressure deficit (VPD) 3.5 kPa. The data were collected on 1 to 24 January 1998 in summer.

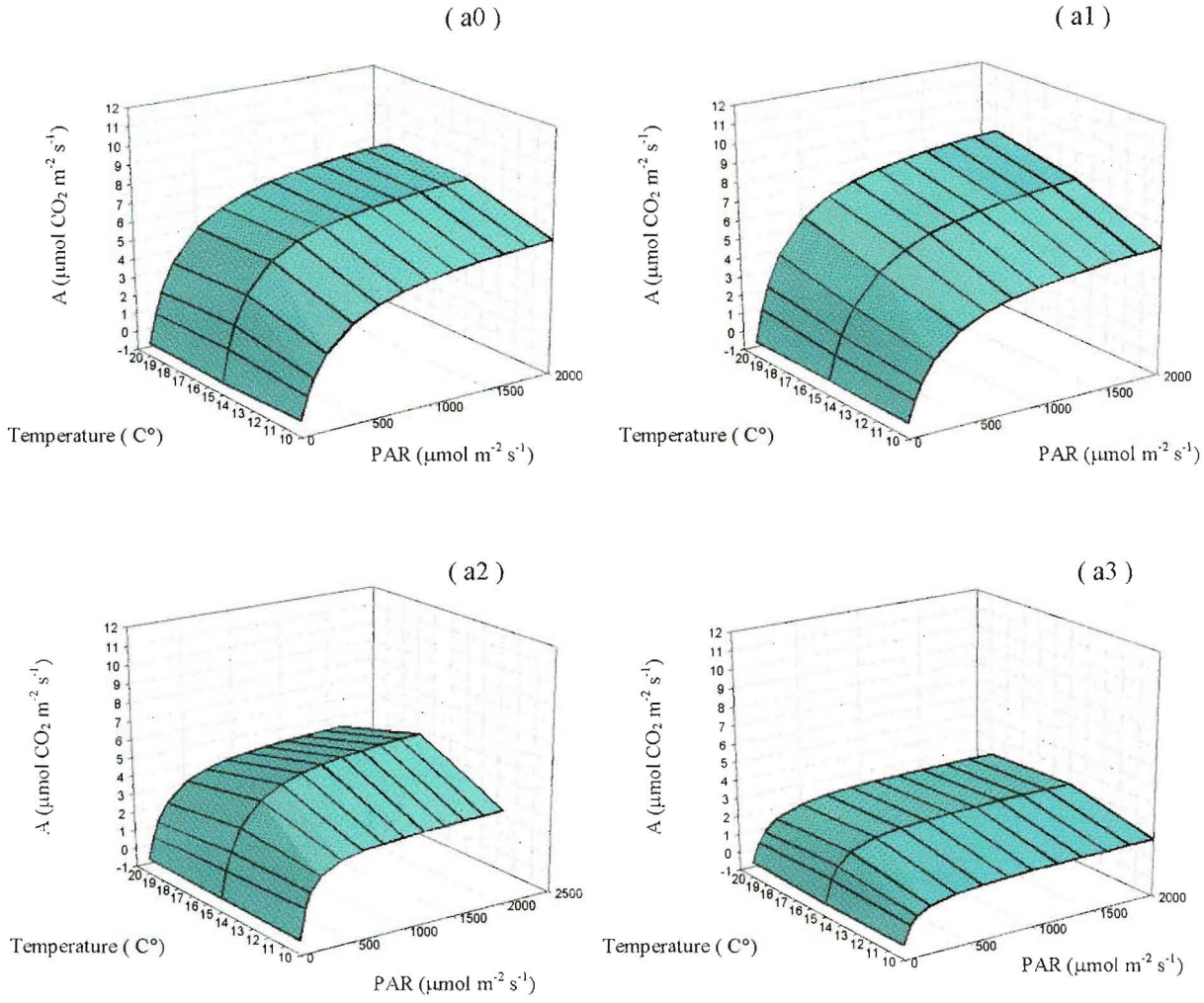

Autumn

Figure 4.4. Relationships between net photosynthetic rate (***A***) and the temperature of radiata pine in response to PAR. The measurements were made for the following leaf age classes: Current-year-old (a0), 1-year-old (a1), 2-year-old (a2) and 3-year-old (a3); constant vapor pressure deficit (VPD) 1.5 kPa. The data were collected on 2 to 25 April 1998 in autumn.

The values of dark respiration rate (Rd) had no statistically significant differences for different leaf age classes in any season (Tables 4.3 and Appendix Table A1.5 and A1.6).

Light saturation point (Qs) of 1-year-old needles and 2-year-old needles was significantly higher than for 3-year-old needles. For example, the values of Qs ranged from (the range was affected by increasing temperature) 890- 1207μmol $m^{-2}s^{-1}$ and 817- 1111μmol $m^{-2}s^{-1}$ for 1-year-old needles and 2-year-old needles to 581-759μmol $m^{-2}s^{-1}$ for 3-year-old needles in winter. In spring, all the values of Qs were higher than 1000 μmol $m^{-2}s^{-1}$. 1-year-old needles had highest Qs in all treatments, and the trends were for Qs to decrease with leaf age.

Light compensation points (Qc) showed no statistically significant differences with leaf age classes at a given temperature in all seasons (Table 4.5 and Appendix Table A1.5 and A1.6). The light compensation points (Qc) ranged from 5 to 40.77 μmol $m^{-2}s^{-1}$.

4.4.5 Effect of temperature on photosynthesis

The maximum photosynthetic rates (***A***max) showed significant differences with temperature at all the investigated leaf age-classes in a given season (Tables 4.2, Appendix Table A1.7 and A1.8, and Figures 4.2, 4.3, 4.4). The maximum photosynthetic rate (***A***max) increased with increasing temperatures for all the 3 leaf age classes in winter. However in spring and autumn, when temperatures reach 15°C, ***A***max reached a maximum then decreased slowly as temperatures increased to 20°C for some needles, such as 1-year-old needles in spring, 2-and 3-year old needles in autumn. These results indicate that under these treatment conditions, ***A***max increased with temperature and could reach its optimum temperature at 15°C for 1-year-old needles in spring, and for 2-and 3-year old needles in autumn. However, for other needles, ***A***max continued to increase with increasing temperatures to 20°C in spring and autumn. When temperature increased over 20°C, ***A***max decreased with temperature. Figure 3.3 shows clearly that ***A***max decreased when temperature increased from 25°C to 35°C.

4.4.6 Photosynthetic capacity with season

Needle photosynthetic rates changed significantly with season (Table 4.2, 4,3, 4.4 and 4.5). Needles had the highest photosynthetic rates in spring, followed by autumn, then winter and the lowest in summer. The most important factor that affected needle photosynthetic rate that changed with season was VPD, then air and soil temperature. Summer is a very dry season at Dalethorpe, and VPD is the dominant limiting factor in summer, so needle photosynthetic rates were very low (Figure 4.3). In winter, although air temperature and VPD can reach the same level as in spring, the needle photosynthetic rates were still low. Soil temperature may be the main limiting factor in winter. In spring and autumn, there were less limiting factors, so the needle photosynthetic rates were higher.

4.4.7 Comparison of the photosynthetic rates at different aspects and levels of the crown

Comparison of the photosynthetic rate at different aspects and levels of the crown showed that there were no significant differences among aspects and levels (Table 4.6).

Table 4.6 Analysis of variance of photosynthetic rates for 1-year-old needles sampled from different crown position (aspect and level) at clone 10.

Source	d.f.	Sum of squares	Mean square	F	P>F
Level	2	0.02	0.01	0.0001	0.9978
Season	3	1647.16	549.05	149.70	0.0001
Level x season	6	4.52	0.75	0.21	0.9751
Aspect	3	2.06	0.69	0.19	0.9049
Aspect x season	9	44.58	4.95	1.35	0.2071
Residual	710	2604.08	3.67		
Total	737	4528.92			

The analysis of variance indicated that the same age needles had similar photosynthetic capacities even in different positions in the crown. That means if the needles in shady positions could get enough light, they could reach the same photosynthetic rate as a same-

aged needles in open positions. This conclusion came from juvenile radiata pine with an unclosed canopy. For an isolated juvenile tree, self-shaded areas are small and temporary, unlike a closed canopy where needles are continually in shade so that these needles may gradually change, decreasing their photosynthetic capacity (Walcroft, 1998).

4.4.8 Comparison of the saturated photosynthetic rate among ten radiata pine clones

We made detailed comparisons of the light response curves between the rapidly-growing clone 9 and slowly-growing clone 10 under different temperatures and age-classes in a given season. There were no significant differences between the two clones in needle photosynthetic capacity. We know that saturated photosynthetic rate is an important pattern for estimating needle photosynthetic capacity. We measured the saturated photosynthetic rate among the ten clones under the same measurement conditions and made comparisons for all the 10 clones. The results are shown in Table 4.7. There were no significant differences among the ten clones in saturated photosynthetic rate. This result indicates that growth differences among the ten clones were not due to differences in needle photosynthetic capacity. There must have been other more important factors affecting total tree photosynthetic production, such as total foliage area, crown volume, the distribution of foliage area density in the crown, and light interception.

Table 4.7 Analysis of variance of maximum photosynthetic rates for 1-year-old needles sampled from 10 clones.

Source	d.f.	Sum of squares	Mean square	F	P>F
Clones	9	1.61	0.18	0.51	0.8640
Sample trees	2	1.21	0.60	1.74	0.1778
Clone x sample tree	18	6.96	0.39	1.11	0.3389
Residual	330	114.72	0.35		
Total	359	124.49			

4.4.9 Modeling needle photosynthesis

Since there were no statistically significant differences between the slowly- and rapidly-growing clones in light response curves under different temperature and needle age-classes in a given season, and furthermore, there were no statistically significant differences among the ten clones when we compared maximum photosynthetic rates for the same measurement conditions, we developed a model of needle photosynthesis that could be used to predict needle photosynthesis among all ten clones.

Table 4.8 —Estimated values of parameter for Equation 4.4 in four season

Parameter	Winter		Spring		Summer		Autumn	
	Estimate	±SE	Estimate	±SE	Estimate	±SE	Estimate	±SE
a0	1.000	0.000	1.000	0.000	6.800	0.564	6.925	1.218
a1	0.164	0.016	0.261	0.041	-0.089	0.025	0.107	0.033
a2	-1.602	0.081	-2.205	0.204	-0.752	0.064	-2.029	0.124
a3	3.523	0.201	7.370	0.637	-0.306	0.141	0.753	0.959
b0	1.000	0.000	1.000	0.000	-1137.735	228.301	343.142	120.204
b1	1.160	0.588	-1.217	0.943	12.870	2.964	-1.097	1.016
b2	-20.997	10.892	-27.486	16.719	-21.012	13.646	-52.065	12.751
b3	116.562	20.840	277.207	47.633	91.262	36.110	-36.538	94.809
k0	1.000	0.000	1.000	0.000	1.400	0.310	0.162	0.873
k1	0.045	0.012	0.031	0.028	-0.017	0.012	0.005	0.025
k2	-0.102	0.061	-0.070	0.138	-0.054	0.034	-0.047	0.090
k3	-0.683	0.150	-0.783	0.430	-0.184	0.082	-0.001	0.706

Note: Needle photosynthetic rate equation (4.4) in the form: $A = M * (Q / B+Q)) - K$.

Where A is the rate of net photosynthesis, Q is photosynthetic active radiation, M, B and K are function parameters. M, B and K can be estimated with following function:

M = a0 +a1 * Temp +a2 *Age +a3 * VPD.
B = b0 + b1 * ln (Temp)*Temp + b2 *Age +b3* VPD.
K = k0 + k1 * Temp + k2 * Age + k3 * VPD.

Where Temp= air temperatures, which ranged in winter 5-15°C, spring 10-20°C, summer 25-35°C and autumn 10-20°C. Age = needle ages, which include age1, 2, and 3 in winter and spring, age0 (current year), age 1, 2 and 3 in summer and autumn. VPD= vapor pressure deficit, which ranged 1-1.3 kPa in winter and spring, 3.1-3.6 kPa in summer and 1-1.5 kPa in autumn.

From the previous section, a better fitted equation was selected as Eqn 4.4 :

$$\boldsymbol{A} = M * (Q / (B + Q)) - K$$

Where ***A*** is the rate of net photosynthesis, Q is photosynthetic active radiation, and M, B and K are function parameters. When Eqn 4.4 was fitted to the data in each season, the values of M, B and K could be estimated with the following forms:

$$M = a0 + a1 * Temp + a2 * Age + a3 * VPD.$$

$$B = b0 + b1 * \ln(Temp) * Temp + b2 * Age + b3 * VPD.$$

$$K = k0 + k1 * Temp + k2 * Age + k3 * VPD.$$

Where the independent variance:

Temp = air temperatures, which ranged 5-15°C in winter, 10-20°C spring, 25-35°C summer and 10-20°C autumn.

Age = needle ages, which include age1, 2, and 3 in winter and spring, age0 (current year), age 1, 2 and 3 in summer and autumn.

VPD = vapor pressure deficit, which ranged 1-1.3 kPa in winter and spring, 3.1-3.6 kPa in summer and 1-1.5 kPa in autumn.

a0, a1, a2, a3, b0, b1, b2, b3, k0, k1, k2 and k3 are all the estimated parameters, and which are listed in Table 4.8.

Figure 4.5 shows the values of residuals against prediction from the needle photosynthetic rate model. The predicted residuals all distributed within ±2 μmol $m^{-2}s^{-1}$ of the model, and most within ± 1 μmol $m^{-2}s^{-1}$.

To simulate whole tree photosynthesis, the model could be simply written as:

$Pn = f(L_j, T_k, D_q, Age_i)$

L_j ----- Light interception.

T_k ----- Temperature.

D_q ----- VPD.

Age_i ----- Needle ages.

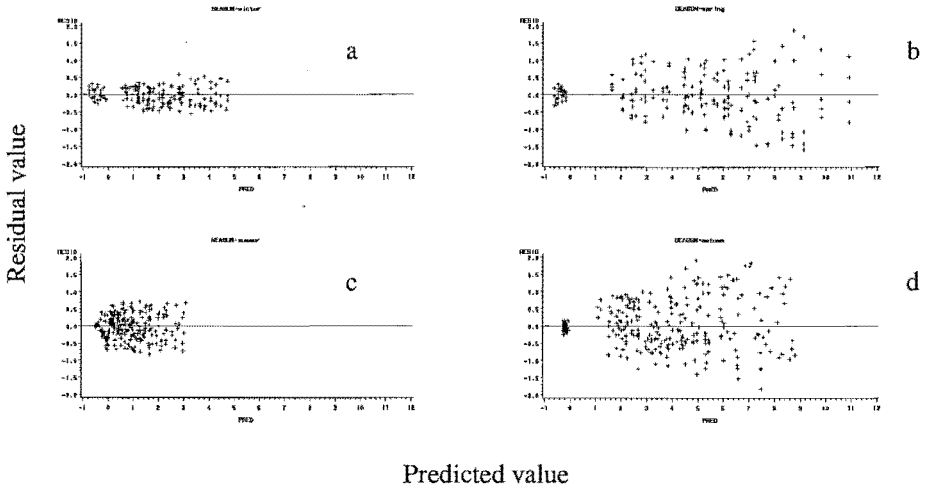

Figure 4.5- Residual vs predicted values from the needle photosynthetic rate model (4.4) in four seasons. a= winter, b= spring, c= summer, and d= autumn. All the light curve measurement data were used to fitting the model in each season.

4.4.10 Foliage nutrient concentration in 1-year-old needles of the ten clones

Comparing the results of foliage analyses, *N, K, B* and *Mn* did not show statistically significant differences among the ten clones (Appendix Table A1.9.1- A1.9.4). But *P, Ca, Mg, Zn* and *Cu* showed significant difference (Appendix Table A1.9.5-A1.9.9). Many researchers conclude that the concentration of *N* has a strong linear correlation with needle photosynthetic rate (Evens 1989, Sellers et al. 1992, Hirose and Werger 1987, Walcroft 1998). These foliage analyses results demonstrated that *N* did not differ significantly among the ten clones, and this result supports the conclusion (photosynthesis measurement results) that there were no significant differences in needle photosynthetic rate among the ten clones. For other nutrients, even though *P, Ca, Mg, Zn* and *Cu* showed significant differences among the ten clones, all of the mean valves of nutrient status (except *Mg*) were higher than critical levels for *P.radiata* (Will 1978), and most of them were higher than the satisfactory levels (Table 4.9). When the relationship between growth rate, measured as height and DBHOB, was analyzed with the foliage nutrients, there was no strong correlation between growth of different clones with the concentration of nutrients in 1-year-old foliages (Appendix Table A1.10). Consequently, the difference of the nutrients (*P, Ca, Mg, Zn* and *Cu*) among the ten clones was not a main factor contributing to the tree growth difference.

Table 4.9- Comparing foliage analysis values with critical levels of nutrient status of *P. radiata*

Nutrient	Critical level less than:	Marginal	Satisfactory more than:	The 10 clones' foliage analyses results
	----------	%	----------	
N	1.2	1.2-1.5	1.5	1.49
P	0.12	0.12-0.14	0.14	0.16
K	0.30	0.30-0.5	0.50	0.74
Ca	0.10	0.10	0.10	0.28
Mg	0.07	0.07-0.10	0.10	0.06
	----------	ppm	----------	
B	8	8-12	12	8.7
Cu	2	2-4	4	3.1
Zn	10	10-20	20	32
Mn	10	10-20	20	95

** Note: The values of the first three columns came from Will 1978.

4.5 Discussion

Generally many factors affect growth-rate differences between clones. This study showed that there were no statistically significant differences in needle photosynthesis between clone 9 and clone 10, and no statistically significant differences in saturated needle photosynthetic rate among the ten clones. These results indicate that needle photosynthetic capacity was not the main factor affecting growth differences among the ten clones.

Needle photosynthetic rate was sensitive to foliage nitrogen concentration (walcraft 1998). In this study, foliage analysis showed that there were no statistically significant differences among the ten clones for *N, K, B,* and *Mn.* (Appendix Table A1.9.1-A1.9.4). Furthermore, there were no nutrient deficiencies happened in the ten clones (except that Mg values lower than critical levels in two clones). These results indicated that nutrients other than N were not the main factors that affected tree growth different in these satisfactory nutrient levels for the ten clones.

There were no statistically significant differences among crown position (Aspect and level) in photosynthetic rate for the ten clones. These results could be used only in juvenile plantation when the trees grew individually and the canopy was not closed. For juvenile individual tree, irradiance in crown will change in the short term from brighter to darker, and there can be no fixed distribution of *N* that is proportional to absorbed irradiance (de Pury and Farquhar 1997). In the long term, when the canopy approaches closure and the incidence of self-shading and neighbor trees' shading increases, the distribution of *N* could be concentrated proportionally with irradiance in crown. Hence, this may be lead to the photosynthetic rate being different at different crown positions in a closed canopy (Walcroft 1998). These results are in agreement with Benecke's (1979) conclusion: " In older more mature stands the sun/shade differentiation of P. radiata needles within the crown can be expected to increase with increasing canopy closure." and he found there were no differences in sun/shade needles in younger trees (less than 6 years).

Needle photosynthetic rates usually increase with needle growth until near full size is attained. The net photosynthetic rates in current-year needles were slightly lower or equal to 1-year-old needles then decreased gradually with age (Kozlowski, T. T. and Pallardy, S. G., 1997). Rook (1987) reported that radiata pine needles developed from the beginning of expansion to nearly full size were in only 4 months. The needles remained on the tree for at least 3 or more years. That means studies of the photosynthetic capacity of 1-, 2- and 3-year-old needles are more important, because they have longer periods for needles to contribute their photosynthetic production to tree growth. Net photosynthetic rates are different between different species and the percentage of net photosynthetic rate decline in 1-, to 2- and to 3-year-old needles is different. Hom and Oechel (1983) studied the photosynthetic capacity of black spruce in different needle age-classes. 1-year-old needles had the highest photosynthetic rates, and older needles were found to still maintain 40% of maximum photosynthetic rates after 13 seasons. Needles with 1-4 age-classes had a photosynthetic capacity of ≥ 93% maximum photosynthetic rates, and the photosynthetic rates of older needles declined progressively with age. Teskey (1984) reported the rate of photosynthesis in 7-year-old needles of *Abies amabilis* was 48% below 1-year-old needles.

This study showed that 1-year-old needles had the highest net photosynthetic rates and the photosynthetic rate decreased with needle age. The net photosynthetic rates in current-year needles were equal to those of the 1-year-old needles. These results are similar to other researchers' conclusions. The photosynthetic capacity of 2-year-old needles was 64- 72% of the maximum for 1-year-old needles (the range was slightly increased by increasing temperature), and 3-year-old needles only had 32-42% of the maximum for 1-year-old needles in winter. However, in spring the photosynthetic capacity can reach 74-91% in 2-year-old needles and 50-70% in 3-year-old needles. These results indicate that 1- and 2-year-old needles are more important for radiata pine growth. Rook (1976) investigated the average distribution of different age classes within the tree crowns of 5-year-old and 7-year-old radiata pines at Kaingaroa, New Zealand. The distribution of foliage by age classes were 75-77% of the total foliage for 1-2 year-old needles and 20-21% for 2-3 year-old needles. 3-4 year-old needles made up only 2-5% of total foliage. Wood (1974) reported the distribution of differently aged needles within the crown of a 5.3 m tall radiata pine growing near Canberra, Australia, as follows: 1-2 year-old and 2-3 year-old needles were 44% and 38% of total crown foliage respectively. Rook said the crown he studied had not closed, but Wood's crowns were closed. That means the distribution of leaf ages within crown maybe changed with crown closure. So if we wish to model whole tree photosynthetic production, we should not only understand the photosynthetic capacity of different leaf ages under temperatures and season, but also know the distribution of leaf ages within crown. For juvenile radiata pine (1-5 year-old before crown closure), the solar radiation distributed in the crown is not same as that with in closed canopy (Grace 1990).

Temperature is very important in regulating net photosynthesis. This study showed the following trends: net photosynthesis rates increased with increasing temperature from 5 °C to 15°C for all leaf age classes in winter. In spring and autumn, net photosynthetic rates still increased with increasing temperature from 10°C to 20 °C for most of needles, but for some needles, such as 1-year-old needles in spring, 2- and 3-year-old needles in autumn, the optimum temperature for photosynthesis was 15°C. When temperature was over 20°C, net photosynthetic rates decreased with increasing temperature.

Although we have no direct data to explain the physiological mechanisms that cause the net photosynthesis rates of radiata pine to be so different between winter and spring at the same air temperature, there are several factors that lead to reductions of gas exchange in winter. Day (1991), DeLucia (1986) and Turner (1975) concluded that the reductions of photosynthetic capacity were associated with low root temperatures; they believed that low soil temperatures were the dominant factor limiting photosynthesis in winter. At our study site Dalethorpe, snow sometimes covered the soil and night frosts occurred frequently in winter, but in spring, soil temperatures increased and night frosts become fewer. Therefore low soil temperatures may be one of the factors that reduced photosynthetic capacity in winter. Oquist (1982) and Senser (1977) reported tissue hardening that induced changes in chloroplast structure, also a factor that decreased photosynthetic capacity in winter. Parker (1963) concluded that leaf biochemistry associated with the induction and maintenance of cold-hardiness might directly affect photosynthetic capacity in winter.

4.6 Conclusions

— The growth rate differences among radiata pine clones were not due to differences in needle photosynthetic capacity among the ten clones.

— Needle photosynthetic rates decreased with needle age, but increased with increasing temperature (5°C - 20°C).

— For juvenile radiata pine growing in the open with an unclosed canopy, the same aged needles had equal photosynthetic capacities, even when distributed at different positions (aspect and level) in the crown.

— A simple model of needle photosynthesis was developed, and it was useful for predicting needle photosynthesis in the ten radiata pine clones in four seasons. The independent variables included light, temperature, leaf ages, and vapor pressure deficit in the model to estimate needle photosynthesis in a given season. Furthermore, the

model could be used to simulate whole tree photosynthesis if the details of crown shape, needle surface area and light interception in the crown were known.

— Seasonal change affected not only the maximum photosynthetic rates but also the photosynthetic capacity in all needle age-classes. This means that photosynthetic capacity of different leaf age-classes was not constant in all seasons: 1-year-old needles had the highest photosynthetic rate; the photosynthetic rate for 2-and 3-year-old needles was 64-72% and 32-42% of the 1-year-old needles in winter. However, the percentage reached 74-91% and 50-70% in spring.

— Winter needle photosynthetic rates (A_{max}) in radiata pine clones were 47-59%, 45-46% and 27-28% of spring rate for leaf age-classes 1, 2 and 3 at temperatures of 10°C and 15°C.

— The changes of needle photosynthesis in the different seasons were caused by some dominant limiting factors, such as low temperature in winter and higher VPD in summer.

CHAPTER 5

ESTIMATION OF CROWN SHAPE AND VOLUME FOR CLONAL RADIATA PINE

5.1 Abstract

Two methods for the measurement of the tree crown shape are described. One method works at crown level using a digital camera to get crown photographs, and uses an Image Analysis System (MetaMorph software) to measure the crown shape data. This method was applied to collect the crown shape data of two 5-year-old radiata pine (*Pinus radiata* D. Don) clones over four seasons. The other method is a direct measurement from destructively sampled trees. This method was used to collect crown shape data according to age classes in four different clones of radiata pine. A model to describe crown shape was developed. The model can be used to calculate crown radii, the maximum crown radius, the base of crown radius, crown volume and vertical volume distribution of different needle age classes. The results were used for later studies of needle surface area density and distribution.

5.2 Introduction

Crown shape and size are two significant dimensions of a tree. It is important to study crown shape and size, because many biological and physiological processes, such as foliage mass,

foliage distribution, solar radiance interception, photosynthesis, respiration and transpiration, all take place in the tree crown. Tree crown shapes are very different in different species. Even in the same environment and with the same species, different clones could exhibit differences in crown shape and size. Many previous researchers have studied crown shapes (e.g., Baldwin and Peterson 1997; Biging and Wensel 1990; Mawson et al. 1976; Honer 1971). Most researchers collected crown shape data by direct measurement or cutting down sample trees. A new measurement method (image analysis) was used in the study described here to collect crown shape data in an experimental stand of young clonal radiata pine, which was unthinned, unpruned and unclosed.

There were three objectives for this research: One objective was to use two methods to collect crown shape data and to compare the two methods. One of the two methods is a new method for obtaining crown shape data. It uses a digital camera to collect sample tree crown photographs and a software program to measure tree crown shape. This method was applied to ten sample trees for each of the two 5-year-old radiata pine clones, and a comparison was made with the direct measurement method (cutting down the sample trees) in order to identify its applicability and discuss the limits of its application. The next objective was to develop a model that best describes the crown shapes of radiata pine clones. The third objective was to use the developed model to describe the crown volume and get the vertical distributions of volume that were useful for further studies of needle surface area density and distribution.

5.3 Materials and methods

5.3.1 Materials

All the sample trees came from a radiata pine (*Pinus radiata* D.Don) clonal experiment established by the School of Forestry, University of Canterbury. Details of the experimental design and the treatment have been described in Chapter 3.

5.3.2 Data collection

Two methods for the measurement of tree crown shapes were used. One method was using a digital camera to collect tree crown shape pictures and software to measure crown shape data from the pictures (Image analysis method). The other method was direct measurement crown shape from the felling of sample trees.

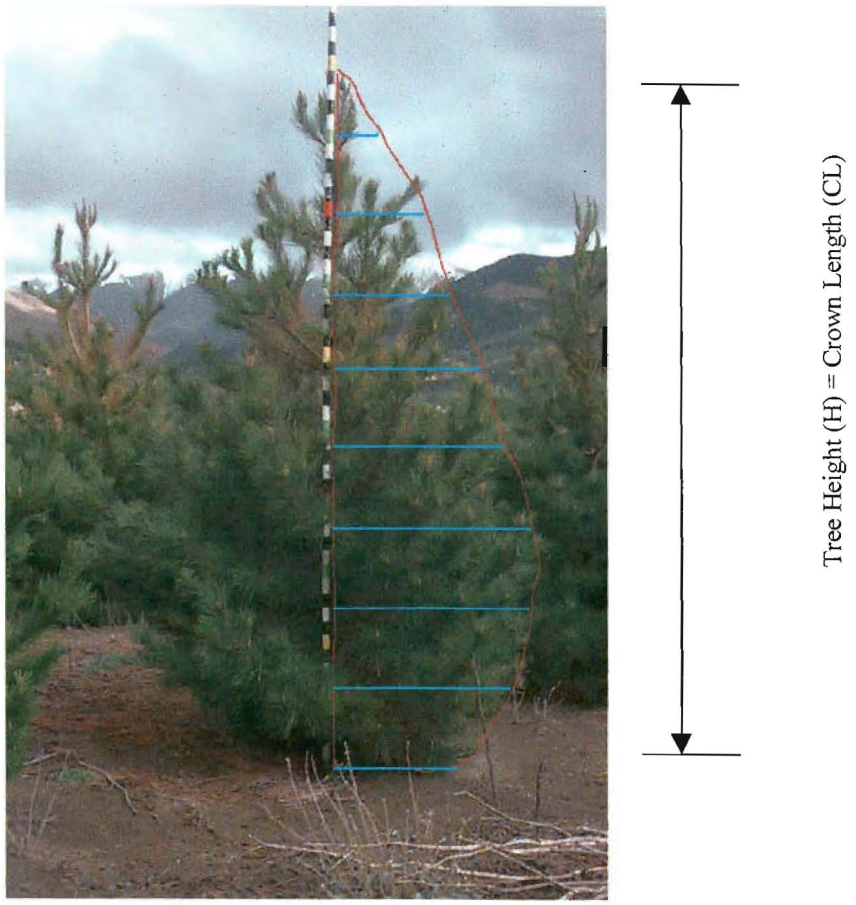

Figure 5.1. Diagram showing how to measure crown shapes on the photograph using Image Analysis System (Metamoph)

For the image analysis method, outer crown shape data were obtained in two steps: first, the collections of crown shape pictures and secondly, measurement of the pictures. Firstly, 10 sample trees were selected and photographed with a digital camera including each of the two clones (fast-growing clone, clone 9; slow-growing clone, clone 10) in the four seasons from July 1997 to April 1998. Each sample tree, together with a surveyor's pole, was photographed twice in two different directions from North to South and East to West. Secondly, crown shape was measured from crown pictures with the Image Analysis System (MetaMorph software). To start the measurement process, the pictures were calibrated. The height pole in each image (Figure 5.1) was used to calibrated pixels to actual distances. Then the diameters of the crown were measured at 0.3-m intervals from the base of the crown to total height of the tree (see Figure 5.1).

For the direct measurement method, a total of 12 trees were sampled during the winter of 1998. All sampled trees were first photographed and their images were assessed using Metamorph software. Three sample trees were cut down in each of the four clone groups (rapidly-growing clones: clone 4 and clone 9; slowly-growing clones: clone 6 and clone 10). The sample trees were selected to represent nearly the average tree height and dbhob (diameter at breast height outside bark) in each of the four radiata pine clonal experiment plantations. The growth data of dbhob and h (tree height) were measured and recorded in all the clonal plots every year.

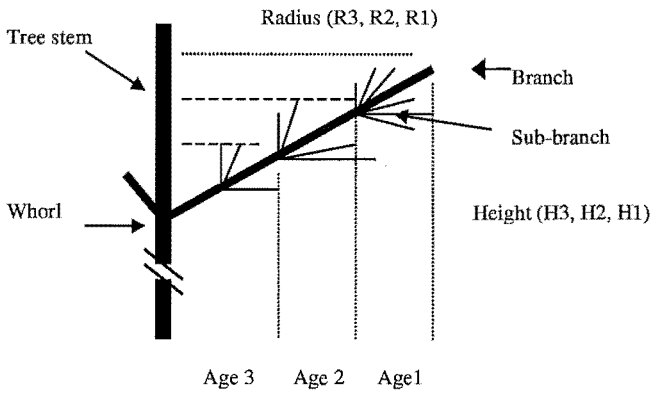

Figure 5.2 Diagram showing the measurement of branch radius and height with 3 age classes at one branch using direct measurement method

Before felling the sample trees, the following measurements were recorded for each of the sample trees for estimating crown shape and volume. First, the tree height, dbhob and crown length was measured. The crown length was the distance between the tree apex and the base of the lowest branches. As shown in Figure 5.1, the total tree height (H) equals the length of full live crown (CL) for unpruned and unthinned radiata pine at age 1-6 year-old in unclosed plantations. Next, branches were measured one by one and whorl by whorl from the base to the top of the crown. For each branch, as shown in Figure 5.2, crown radius (R1) is the horizontal distance from the branch tip to the axis of the main stem, and the vertical position (H1) of the measured crown radius is the vertical distance from the branch tip to the crown base. In the same way, crown radii (R2, R3) and their vertical positions (H2, H3) at age 2 and age 3 were measured on the internodes of the branch.

The shoot extensions of radiata pine have more than one distinct period during one growing season (Bollmann and Sweet 1976) and so the term branch node unit must be distinguished from other nodes. With the height measurement records in every year, the branch node unit in one cycle of growth could be found. The diagram in Figure 5.2 illustrates the term branch node unit.

5.3.3 Data analysis

All the collected data from the direct measurement method were sorted to different age classes and all the vertical distances (Hi) of each branch were normalized (crown vertical distance ÷ crown length) in different age classes. The data collected with the image analysis method were the relative crown lengths and radii, so the data could be directly used for analysis. The normalized data and radii were used to fit equations describing crown shapes. The NLIN procedure was used for parameter estimation in SAS (Statistical Analysis System Package, 1989).

5.4 RESULTS AND APPLICATIONS

The following sections described the results of selecting a suitable equation to fit crown shapes, applying the equation to describe crown shapes with tree growth (shapes changed with seasons and ages), using the fitted equation to calculate crown volume and vertical volume distribution, and comparing the two measurement methods.

5.4.1 The equation to describe crown forms

The following equation was selected (based on best fit crown shape data) and used to model crown shape of clonal radiata pine:

$$R = f(x) = A \cdot \frac{(x-1)}{(D \cdot x + 1)} - B \cdot (x - C) \qquad (5.1)$$

Where R is crown radius (cm), x is relative crown length ($0 \leq x \leq 1$, x = length within the crown ÷ the total crown length), and A, B, C and D are regression coefficients.

From the function 5.1, equation 5.2 can be derived:

$$X_{max} = \frac{\sqrt{\frac{A \cdot (D+1)}{B}} - 1}{D} \qquad (5.2)$$

Where X_{max} is the value of relative crown length when crown radius reaches its maximum.

Therefore, the maximum crown radius can be described with function 5.2 and 5.1. The maximum crown radius occurs at X_{max}. Using the value (X_{max}) obtained from function 5.2 and inserting it to function 5.1, we can get the maximum crown radius.

From the function 5.1, when x = 0, we can get the equation 5.3:

$$R_{base} = B * C - A \qquad (5.3)$$

Where R_{base} is crown base radius (cm). As equation 4.1 shows, A, B and C are regression coefficients. Using the equation 5.3, crown base radius can be predicted.

Equation 5.1 was fitted to data collected using the image analysis measurement methods from two different clones in four seasons, and to data collected using the destructive measurement methods of four clones at different age classes. The parameter values are presented in Tables 5.1, 5.2 and 5.3.

Table 5.1. Parameter values for fitting function 5.1 at age1, age2 and age3.

Age1

	A	B	C	D	H1
Clone 4	182.794	245.853	1.059	1.738	501
Clone 6	169.250	144.360	1.188	8.462	390
Clone 9	428	496.786	1	1	475
Clone 10	153.087	233.694	1.065	2.609	362

Age 2:

	A	B	C	D	H2
Clone 4	168.080	224.485	1.093	1	363
Clone 6	136.910	145.710	1.133	4.272	260
Clone 9	185.258	238.273	1.049	2.045	365
Clone 10	102.084	167.802	1.115	2.898	255

Age 3:

	A	B	C	D	H3
Clone 4	782.665	822.929	1.034	0.071	312
Clone 6	31.949	77.752	1.246	1	191
Clone 9	104.171	136.429	1.188	3.082	300
Clone 10	81.251	132.326	1.171	1.858	210

Table 5.2. Parameter values for fitting function 5.1 in four seasons for clone 9

	A	B	C	D	H
Winter	115.804	214.475	1.024	1.858	404
Spring	164.478	206.813	1.024	3.232	419
Summer	172.137	221.815	1.038	2.886	451
Autumn	141.508	205.387	1.020	3.915	477

Table 5.3. Parameter values for fitting function 5.1 in four seasons for clone 10

	A	B	C	D	H
Winter	139.420	177.655	1.026	2.718	269
Spring	213.386	258.249	1.026	1.813	281
Summer	164.340	213.574	1	3.280	346
Autumn	218.237	274.279	1.018	1.689	372

Note: A, B, C and D are regression coefficients. H= tree height.

Figure 5.3a illustrates the fit of equation 5.1 showing the scatter of crown radius data, and presents predicted radius curve of the crown. Figure 5.3b and Figure 5.3c illustrate predicted residuals about the crown radius with respect to the prediction curve, and relative crown

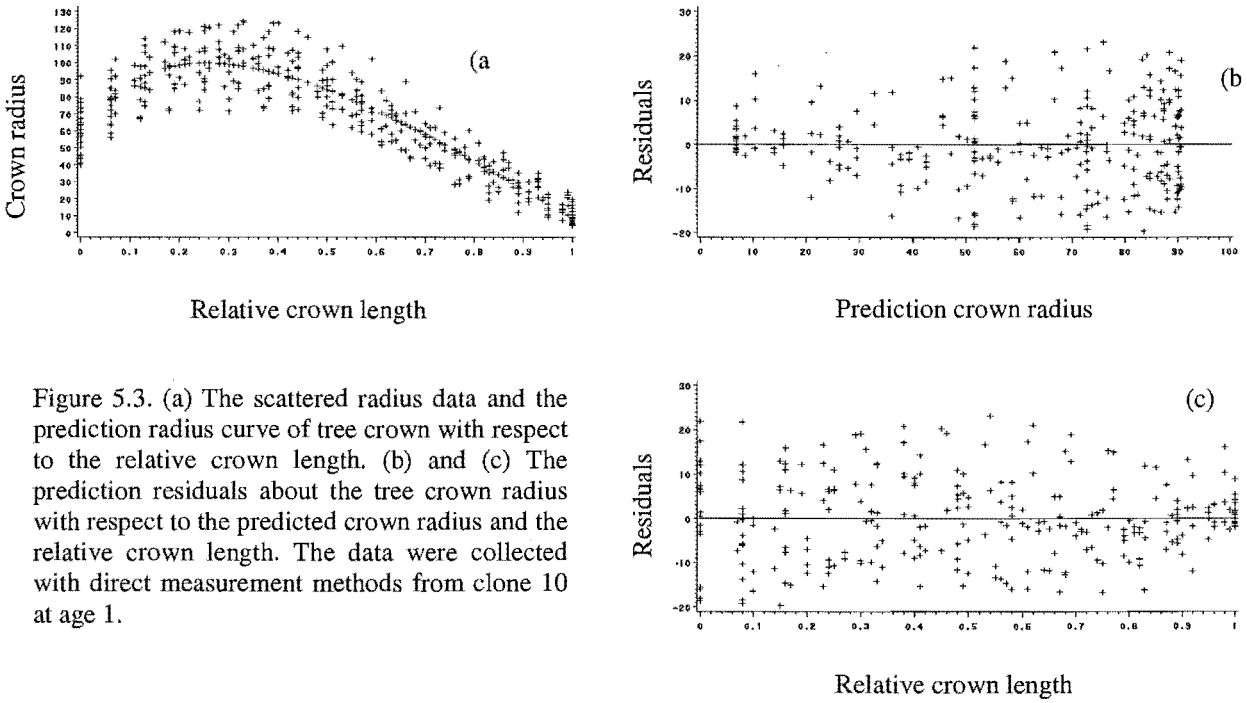

Figure 5.3. (a) The scattered radius data and the prediction radius curve of tree crown with respect to the relative crown length. (b) and (c) The prediction residuals about the tree crown radius with respect to the predicted crown radius and the relative crown length. The data were collected with direct measurement methods from clone 10 at age 1.

length. Figure 5.3 presents an example of data (collected in autumn at clone 10) fitted using equation 5.1.

5.4.2 Crown shape and season

Radiata pine grows all four seasons in New Zealand and crown shapes change with season. The crown shape changes reflect the new needle growth and its distribution patterns in the crown; it also represents changes in crown volume. In a comparison of the seasonal changes between the two clones (rapidly-growing clone 9 and slowly-growing clone 10), the following results illustrate that the fast-growing clone had some advantages for light interception. Firstly, the main difference between the two clones was that the rapidly-growing clone 9 had longer crown length, although the radius at crown base and the maximum radius were similar in both the clones. This means that clone 9 had more vertical crown space for needle distribution. Secondly, despite the fact that both clones increased their crown size (crown lengths and

crown radius) in the four seasons, the crown shape changes were all based on their original shapes (branches). This means that clone 9 had more vertical crown volumes for new needle distribution.

To illustrate the crown shape changes in the four seasons, Figure 5.4 shows that both clones increased crown radii and lengths in the four seasons. By comparison, when relative crown length (Figure 5.4b) was used, the radius increases in clone 9 was no more than those in clone 10. However, when the two clones were compared with absolute crown length (Figure 5.4a), it showed clearly that clone 9 had longer crown length, and well-distributed crown radii increases in the four seasons.

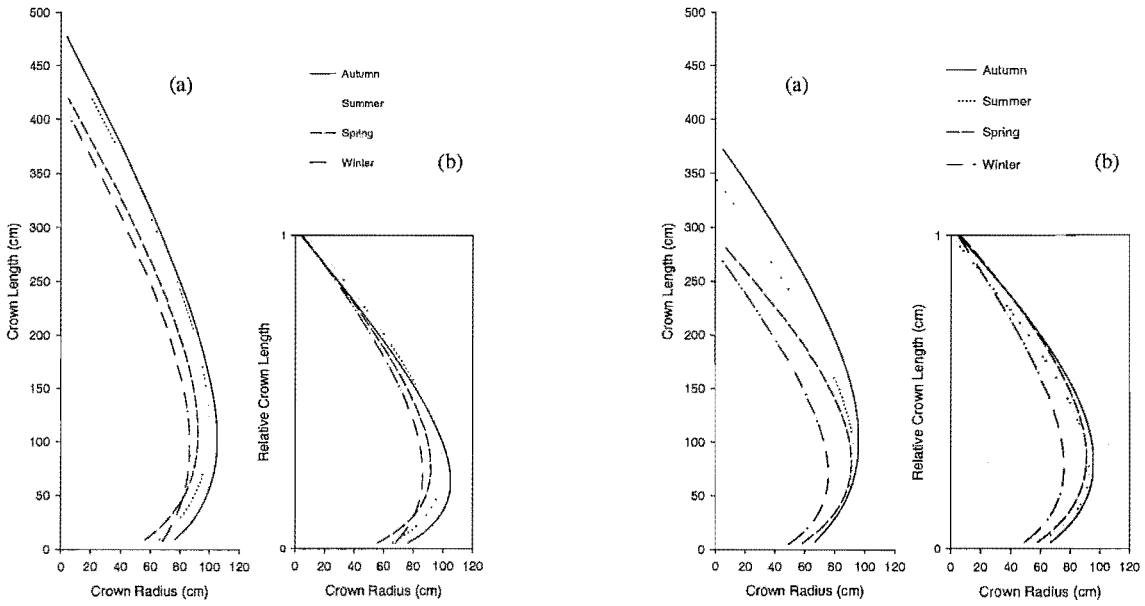

Figure 5.4. The effect of season on crown shape in clone 9 and clone 10. (a) Predicted crown radius with respect to crown length. (b) Predicted crown radius with respect to the relative crown length. The data was collected with image measurement method from winter, July 1997 to autumn, April 1998

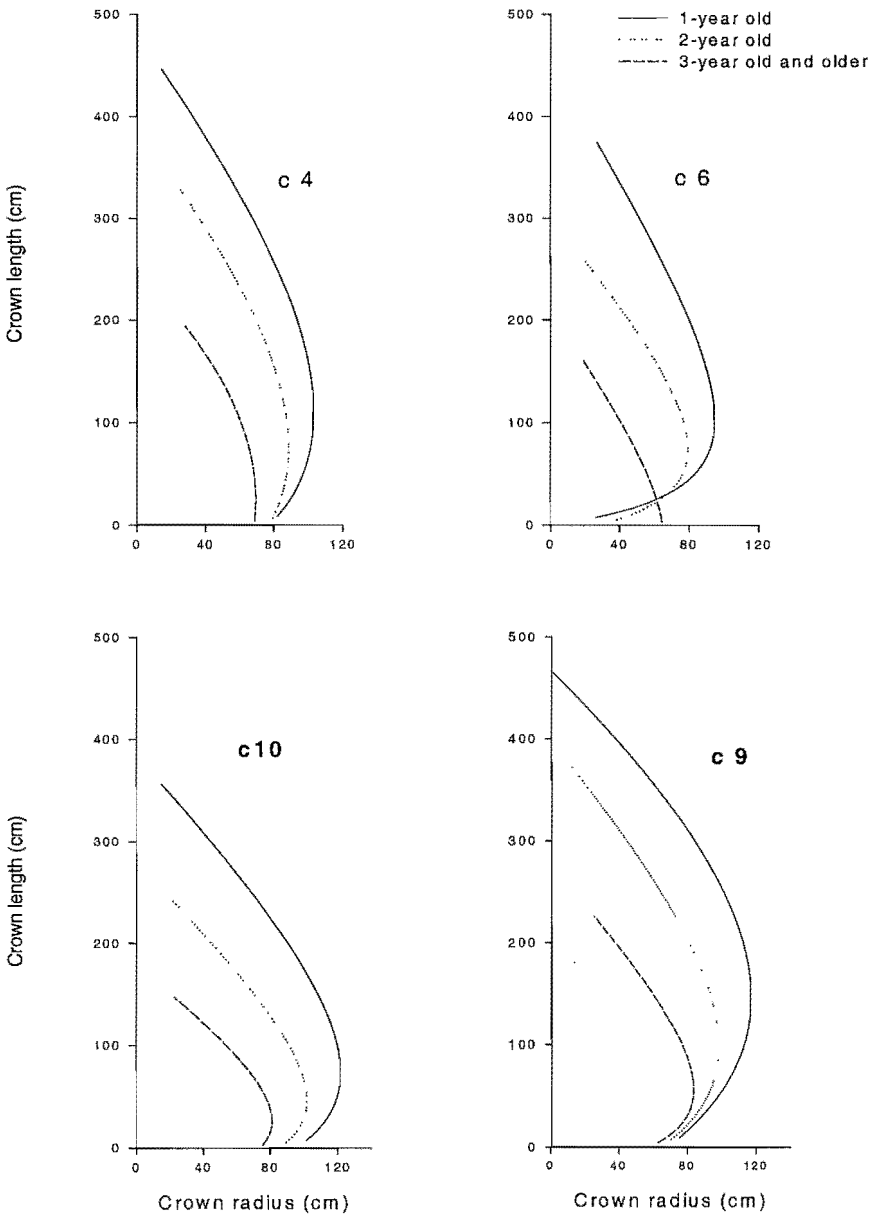

Figure. 5.5. Using fitted function to describe crown shapes in different clones and age classes. C4, 6, 9 and 10 represent clone 4, 6, 9 and 10. The data was collected with direct measurement method from 6-year-old radiata pine clonal experiment plantation. The variation in crown shapes with age means that the crown shapes were occupied by 1-, 2- and 3-year-old needles and branches from outer to inside of the crown.

5.4.3 Crown shape and age

Crown shapes changed with tree growth in different clones. Using the parameters in Table 5.2 and the equation in (5.1), it can be shown that crown shape changed according to tree age for the four clones, as described in Figure 5.5. In addition, for the crowns of coniferous trees such as radiata pine, having more than a 1-year-old needle age structure, needle age occupation in the crowns can also be described as in Figure 5.5. Current and 1-year-old needles occupied the band from the outer side edge to the middle of crown shape (age 1). 2-year-old needles

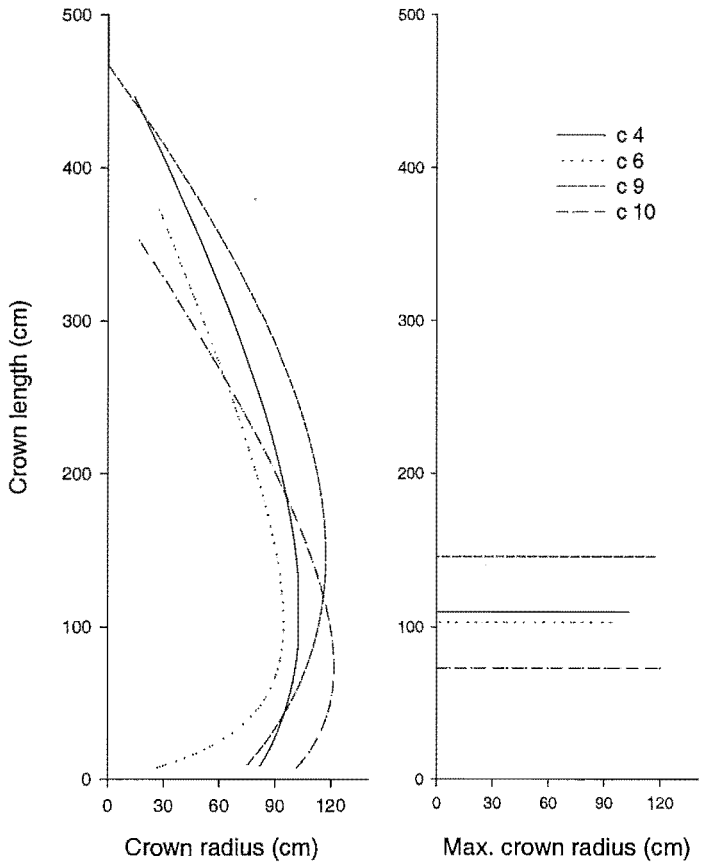

Figure 5.6. Two-dimensional illustration showing crown shapes and maximum crown radius of 6-year-old radiata pine clones. (c4, c6, c9 and c10 represent clone 4, clone 6, clone 9 and clone 10).

occupied the band from the middle to inside crown shape (age 2). The 3-year-old and older needles occupied the band on the inside crown shape (age 3). With these results, the crown volume and its vertical distribution in different ages could be characterized for the four clones.

In different clones, as Figure 5.6 shows, the outer side crown shapes were very different. Crown lengths, crown base radii, crown maximum radii and the positions of the maximum radii all changed with the different clones. For example, although clone 10 had shorter crown length than that of other clones, its maximum crown radius and crown base radius were wider than that of other clones. The results indicated that the volume or vertical distribution of volume must be different in the different clonal crowns.

5.4.4 Crown volume and vertical volume distribution with age

5.4.4.1 Crown volume with ages

Crown volume can be calculated with integration techniques and the volume equation can be described as equations 5.4 and 5.5. As figure 5.7 showed, using equation 5.4, any parts of vertical crown volume from the crown base to the crown length (Li) can be calculated. When

$$V_i = L\cdot\pi\cdot\int_0^{x_i} R^2\,dx = L\cdot\pi\cdot\int_0^{x_i}[f(x)]^2\,dx \qquad (5.4)$$

$$= L\cdot\pi\cdot\left[\int_0^{x_i} A\cdot\frac{(x-1)}{(D\cdot x+1)} - B\cdot(x-C)\right]^2 dx$$

$$= L\cdot\pi\cdot\left\{\begin{array}{l}\frac{A^2}{D^2}\cdot\left[\left(x_i+2+D+\frac{1}{D}\right)-\frac{1}{(D\cdot x_i+1)}\cdot\left(2+D+\frac{1}{D}\right)-2\cdot\left(1+\frac{1}{D}\right)\cdot\ln(D\cdot x_i+1)\right]\\ -2\cdot A\cdot B\cdot\left[\frac{1}{D^3}\cdot\left[\frac{(D\cdot x_i)^2}{2}-D\cdot x_i+\ln(D\cdot x_i+1)\right]-\frac{(C+1)}{D^2}\cdot[D\cdot x_i-\ln(D\cdot x_i+1)]+\frac{C}{D}\cdot\ln(D\cdot x_i+1)\right]\\ +\frac{B^2}{3}\cdot\left[(x_i-C)^3+C^3\right]\end{array}\right\}$$

L = Tree Crown Length

Li = Any Crown Length from the crown base.

xi = Li / L.

0 <= xi <= 1

Vi = Any vertical crown volume from crown base to the crown length Li

When xi = 1

The total tree crown volume can be calculated as below:

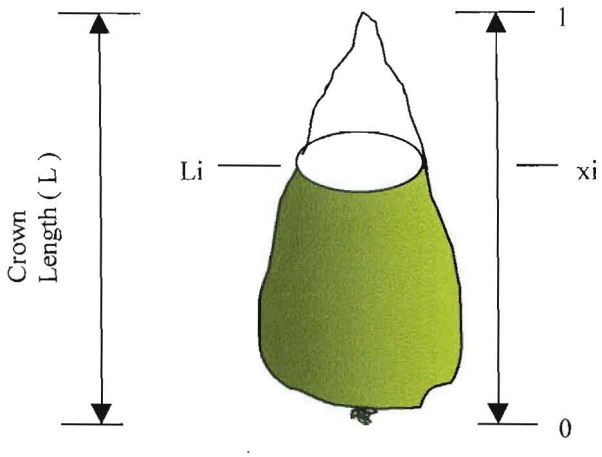

Figure 5.7. Diagram showing how to use equation (5.4) to calculate any vertical parts of a tree crown volume

the relative crown length (xi) equates to 1, the total crown volume is described as in equation 5.5.

Figure 5.8 shows the total crown volume and the volume according to age classes in the four different clones. The total of crown volume in clone 9 was larger than that in the other clones, and it was nearly twice as large as that in clone 6. The total of crown volume in clone 10 was nearly that in clone 4. The volume trend was: clone 9 > clone 4 > clone 10 > clone 6.

$$V_{Total} = L \cdot \pi \int_0^1 R^2 dx = L \cdot \pi \cdot \int_0^1 [f(x)]^2 dx \quad \text{..... .... (5.5)}$$

$$= L \cdot \pi \cdot \left[\int_0^1 A \cdot \frac{(x-1)}{(D \cdot x + 1)} - B \cdot (x - C) \right]^2 dx$$

$$= L \cdot \pi \cdot \left\{ \begin{array}{l} \frac{A^2}{D^2} \cdot \left[\left(3 + D + \frac{1}{D}\right) - \frac{1}{(D+1)} \cdot \left(2 + D + \frac{1}{D}\right) - 2 \cdot \left(1 + \frac{1}{D}\right) \cdot \ln(D+1) \right] \\ - 2 \cdot A \cdot B \cdot \left[\frac{1}{D^3} \cdot \left[\frac{D^2}{2} - D + \ln(D+1) \right] - \frac{(C+1)}{D^2} \cdot [D - \ln(D+1)] + \frac{C}{D} \cdot \ln(D+1) \right] \\ + \frac{B^2}{3} \cdot [(1-C)^3 + C^3] \end{array} \right\}$$

5.4.4.2 Crown volume vertical distribution with ages

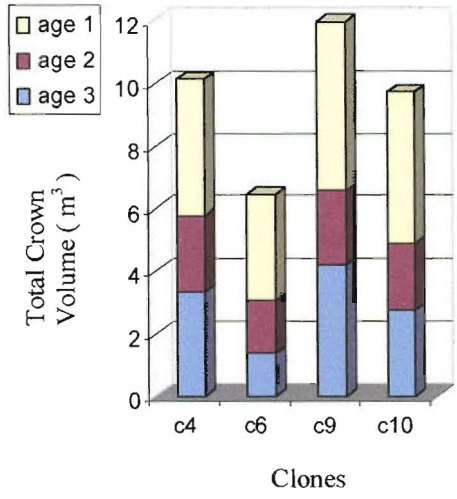

Figure 5.8 Total crown volume and the volume with age classes in clone 4, clone 6, clone 9 and clone 10.

The study of crown volume and volume distribution is important for further study of needle surface area density (NSAD) and the vertical distribution of NSAD. From Chapter 4 we know that needle photosynthetic capacity decreases with needle age. If the volume that different aged needles occupy in the crown can be isolated, it could be combined with needle biomass study to get NSAD and the distribution of NSAD with age classes. This would be more accurate than simply using average NSAD to estimate the total tree photosynthetic production, where the NSAD is usually supposed to be random or uniform within the tree crown (Charles-Edwards *et al.*, 1974; Whitfield and Conner, 1980).

Figure 5.9 shows how to use different crown equations according to ages to separate crown volume to age class and vertical volume levels.

As Figure 5.9 shows, using the different crown shape equations with age class in the four clones, the crown vertical volume distribution with age could be estimated. Figure 5.10 illustrates the results of the crown vertical volume distribution according to age in the four clones. These results are useful for further study in branch biomass density or NSAD and its distribution.

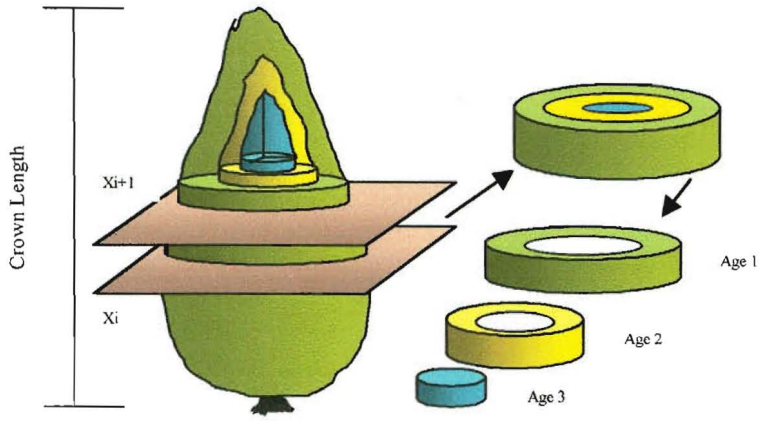

Figure 5.9. Using function (5.4) and combining with crown shape changed with ages, the crown volume can be calculated at any level (Xi to Xi+1) in different ages

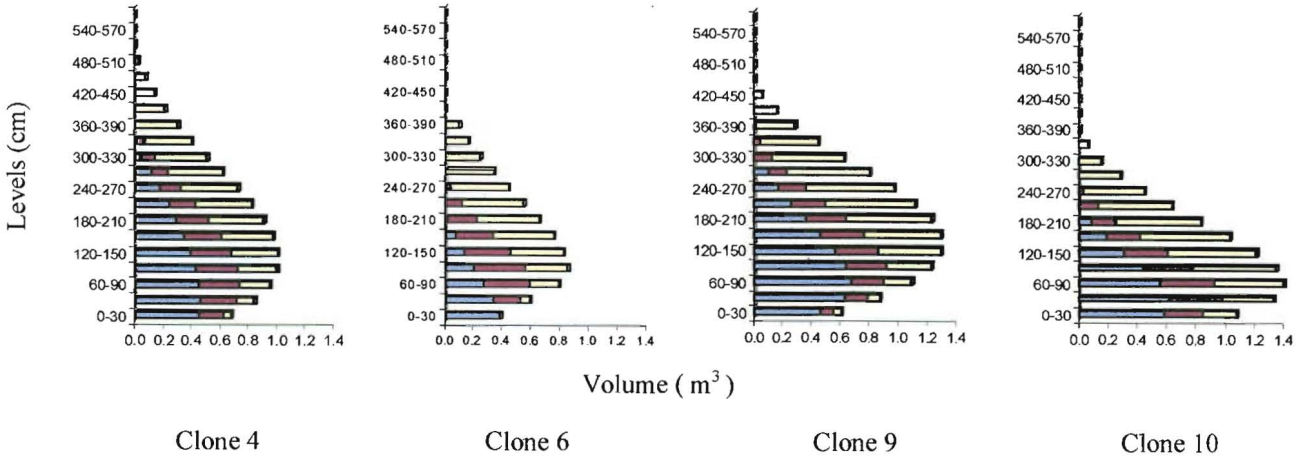

Figure 5.10. The crown vertical volume distributed with ages (from outside to inside age1, age2, age3 and older) in clone 4, clone 6, clone 9 and clone 10.

5.4.5 Comparison of the results of the two measurement methods

Regarding the two measurement methods, the sample numbers and collection time were not the same. So it is not suitable to directly compare the results of the two measurement methods. To make a comparison of the results of the two measurement methods, firstly, we used a digital camera to photograph the crown when we sampled trees in clone 10; then we used the direct measurement method to measure the sample trees. The data collected by the two methods were applied to fit equation 5.1.

To compare the prediction residuals of the two methods, SAS procedure (TTEST) was used to test whether the prediction residuals were significantly different from zero. The null hypothesis was that the difference (DIFF) between the two predictions was equal to zero. Table 5.4 shows the results that there were no significant differences between the two predictions. So both the measurement methods were applicable.

Table 5.4. The results of testing the difference between the two predictions

Variable	N	Mean	Maximum	Minimum	Std Error	T	Prob.>|T|
DIFF	20	0.3924	2.9251	-3.8807	0.5536	0.7088	0.4870

Note: DIFF = the prediction difference between the two equations developed with the two different methods

5.5 DISCUSSION AND CONCLUSIONS

Both the two measurement methods were applicable, and they both had advantages and disadvantages.

Using the direct measurement method, more information can be obtained from the sample trees (crown shape, volume, biomass, and the architecture of branches), but this required much field work and the destruction of sample trees.

Applying the image analysis method can easily collected more sample data in the field and it did not need to destroy the sample trees, but the data were limited to crown shape description and it could not get more information (such as needle, branch and stem biomass) about the sample trees. Another limitation was that this method could only be applied to young stands, where the canopy is not closed.

Although both the two measurement methods have disadvantages in application, they could be combined to use their advantages in future research. An example is using the image analysis method to collect more crown shape data in each year, to study crown shape changes with the tree growth, and at the same time using the direct measurement method but only destroying one or two sample trees to get more detailed information of biomass production.

To describe crown shapes, a simple function was developed and that is useful to characterize crown geometry (crown radius, maximum crown radius, crown volume and vertical volume distribution) for the four different clones.

By applying the developed equation, crown shape changes according to seasons and ages could be described. By comparison, crown length, maximum crown radius, base crown radius and volume with age class all showed differences between the four clones. The next step would be combine these research results with branch and needle biomass data to describe needle biomass density, branch biomass density, needle surface area density (NSAD) and distribution.

CHAPTER 6

ABOVE GROUND BIOMASS PRODUCTION, ALLOCATION AND NEEDLE SURFACE AREA OF *PINUS RADIATA* CLONES

6.1 Abstract

Above-ground biomass and needle surface area were estimated for four 5-year-old *Pinus radiata* D. Don clones in a clonal experiment. The total above-ground biomass and the biomass production allocation showed significant differences among the clones. Tree height was poorly correlated with total biomass production, but DBHOB was strongly correlated with needle, branch and total biomass. A simple model was developed to estimate branch biomass and needle biomass, where independent variables were branch base diameter (cm), branch length (cm), branch age (1-3 year), sub-branch numbers, average sub-branch base diameter (cm), and average sub-branch length (cm). The vertical distributions of needle biomass, needle surface area, and needle surface area density were studied according to age class. The results of this study are intended for later studies of light interception and simulations of whole tree photosynthetic CO_2 fixation.

6.2 Introduction

Above ground biomass has been studied by many researchers for *Pinus radiata* D. Don (Baker, *et al* 1984; Beet and Madgwick, 1988; Beets and Pollock, 1987). Different above

ground biomass production is positively related to stem growth (Madgwick 1983). However, for radiata pine clones growing on the same site, there were significant differences in growth, as measured with tree height and DBHOB (Chapter 3). The study described here contributed to the goal of determining differences between clones in above ground biomass production, and how does the relative dry matter allocation within clone trees related to their total stem production?

Foliage distributions are important in relation to radiation penetration within tree crowns (Myneni, *et al.* 1989). Needle surface area and its density distribution in the crown are important parameters for estimating radiation penetration (Norman and Jarvis 1975).

The objectives of this study were to describe and compare the above ground biomass production and its allocation into tree components among four different radiata pine clones (the four clones came from the four different growth group discussed in more detail in Chapter 3). A further objective was to estimate leaf surface area and its vertical distribution. The results were useful for a later study of light penetration and simulation of whole tree photosynthesis.

6.3 Materials and methods

6.3.1 Measurement of architectural arrangement of branches and above ground biomass

For measurement of architectural arrangement of branches and above ground biomass, the following three steps were taken: firstly, to measure the architectural arrangement of branches; secondly, to weigh above-ground fresh weight; and thirdly, to collect sample branches and needles for calculating the ratio of dry weight to fresh weight.

To start with, for the measurement of architectural arrangement of branches, like the crown shape measurement (Chapter 5), a total of twelve trees were sampled and three sample

trees were cut down in each of the four clones (clone 4, clone 6, clone 9 and clone10). For every branch complex from each whorl, the horizontal distance (width) from the center of the tree stem to the proximal end, height above ground, basal diameter and the length of each branch unit were measured (Figure 6.1a). The sub-branch numbers, average sub-branch length and base diameter were recorded and measured (Figure 6.1b) in each branch age unit (age 1,age 2, age3 and older). These processes were repeated for all the branches in each whorl. Branch numbers in each whorl were counted and recorded.

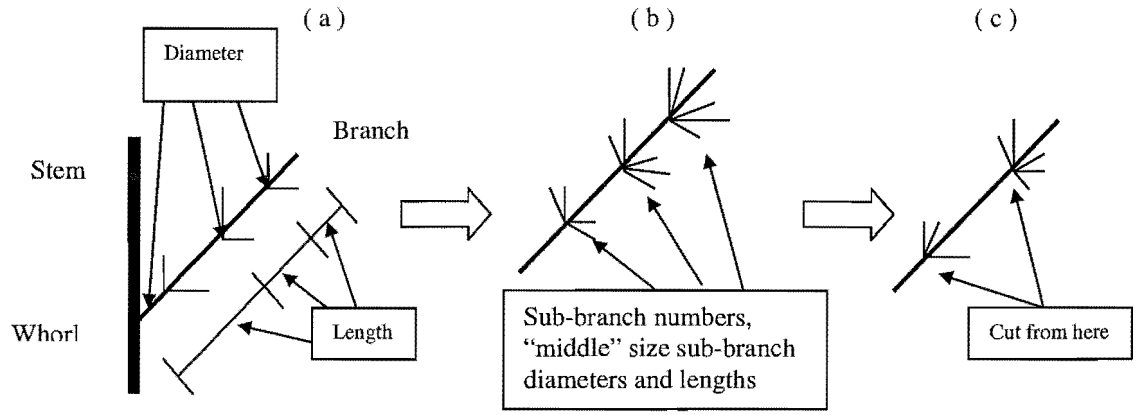

Figure 6.1- Diagram shows the measurement of architectural arrangement of branches and above ground biomass. (a) The measurement of branch diameter and length according to age classes. (b) Counting sub-branch numbers and measuring the diameter and length of 'middle' size sub-branch according to age classes. (c) Separating the branch according to age classes for weighing fresh weight.

After the measurement of the architectural arrangement of branches, the next step was to weigh the fresh weight of branches, needles and stem. For one branch, it was cut off from the whorl, and separated it into three different age classes (Figure 6.1c), i.e. 1-year-old, 2-year-old, and ≥3-year-old . Then the fresh weight of branches and needles together were weighed in each age class. In this way, branch by branch was weighed, and all branches at each whorl were weighed. At the same time, one branch was sampled from each whorl for future more detail measurement in laboratory. After cutting off all the branches, the trunk was felled and its total fresh weight was weighed. After weighing the total fresh stem weight, 2.5(cm) thick

discs was sampled from each 1-meter section of the stem for the future measurement of the ratio of dry wood to fresh wood weight in laboratory.

Finally, in the laboratory, for the measurement of the ratio of dry weight to fresh weight, each sample branch by age class and the stem discs were oven-dried. All the samples were dried at the temperature 65°C for one week in an oven. After drying the samples, the branches and needles were separated and weighed for dry weight according to age class; the stem discs were separated into wood and bark and weighed. Then we calculated the ratio of dry weight to fresh weight for branches and needles (the samples were collected from each whorl) according to age class. With the ratios and the fresh weights (which were collected in field), the branch dry weights and needle dry weights according to age class were determined for each branch in each whorl. The wood dry weights and bark dry weights of stem were determined by multiplying total stem fresh weight with the average ratios of dry weight to fresh weight for wood and bark. As a result, all the above ground biomass could be estimated by accumulating branch biomass, needle biomass, stem wood biomass and stem bark biomass.

6.3.2 Measurement of specific needle area and total needle surface area

For measurement of specific needle area, a total of 360 fascicles of needles were sampled from the four different clones according to age class. Within the total 360 sample fascicles, 10 fascicles of needles were randomly collected from different crown vertical positions for each of the 3 age classes of 3 sample trees in each of the four clones. The surface areas of the sample needles were measured and calculated by using Johnson's equation (Johnson 1984). All the sample needles were oven-dried at temperature 65°C for one week, and then weighed. Finally, the specific needle areas were calculated by using the measured surface areas divided by dry weights ($m^2\ kg^{-1}$).

Total needle surface area was determined by accumulating all the needle surface area according to age class. In each needle age class, the needle surface area was calculated by multiplying the needle dry weight by the specific needle area in the given needle age class.

6.4 Results

6.4.1 Total biomass and its allocation to tree components (stem, branches, and needles)

Total above-ground biomass production and its allocation into tree components were significantly different among the four clones.

Total above-ground biomass, the ratio of needle biomass to total biomass, the ratio of branch biomass to total biomass, and the ratio of stem biomass to total biomass all showed significant differences among the four clones (Table 6.1). Figure 6.2 shows clearly that the total tree biomass was allocated differently to needles, branches and stem among the four clones. For

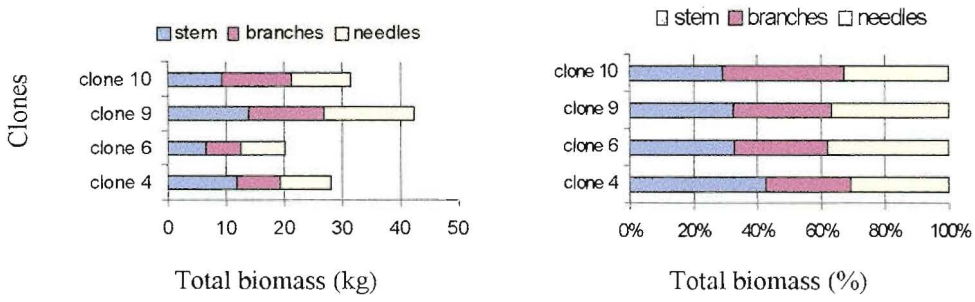

Figure 6.2- Total biomass production (a), and proportion (b) of needle, branch, and stem biomass in the four clones.

example, the total biomass was higher in clone 10 than in clone 4, however, stem biomass was reversibly lower in clone 10 than in clone 4 (Figure 6.2a). The proportions of total above ground biomass allocated to stems ranged from 29% (clone 10) to 43% (clone 4). These results indicated that the higher growth rates of height and DBHOB were not only due to

higher biomass production rates, but also due to the above ground biomass allocation into tree components.

Table 6.1 Analysis of variance of total biomass (a), the ratio of needle biomass to total biomass (b), the ratio of branch biomass to total biomass (c), and the ratio of stem biomass to total biomass (d) for radiata pine clones at age 5 at Dalethorpe

(a)

Source	d.f.	Sum of squares	Mean square	F	P>F
Clone	3	765.19	255.06	11.09	0.0073
Sample	2	49.73	24.86	1.08	0.3974
Residual	6	138.05	23.01		
Total	11	952.97			

(b)

Source	d.f.	Sum of squares	Mean square	F	P>F
Clone	3	0.0106	0.0035	9.7200	0.0102
Sample	2	0.0002	0.0001	0.2400	0.7973
Residual	6	0.0022	0.0004		
Total	11	0.0130			

(c)

Source	d.f.	Sum of squares	Mean square	F	P>F
Clone	3	0.0195	0.0065	4.7000	0.0512
Sample	2	0.0007	0.0004	0.2500	0.7837
Residual	6	0.0083	0.0014		
Total	11	0.0284			

(d)

Source	d.f.	Sum of squares	Mean square	F	P>F
Clone	3	0.0285	0.0095	7.0800	0.0213
Sample	2	0.0003	0.0001	0.1000	0.9079
Residual	6	0.0081	0.0013		
Total	11	0.0369			

6.4.2 The relationship between biomass and branch size in branch level

Determining the relationship between branch size and needle biomass was useful for later estimation of needle biomass when the sample branches still grew on trees (Bartelink 1996; Baldwin 1997). From a total of 573 sampled branches, a simple multiple linear regression equation was developed for estimating needle biomass and branch biomass. In the model (Table 6.2), the independent variables were branch base diameter (cm), branch length (cm),

branch age (1-3 year), sub-branch numbers, average sub-branch base diameter (cm), and average sub-branch length (cm). Fig 6.3 shows the values of predicted residuals against prediction of the regression equations. According to the regression equations, needle biomass appeared to be positive correlated to branch base diameter, branch length, sub-branch numbers and average sub-branch diameters. Branch biomass was strongly correlated to branch base diameter, branch length, and sub-branch numbers.

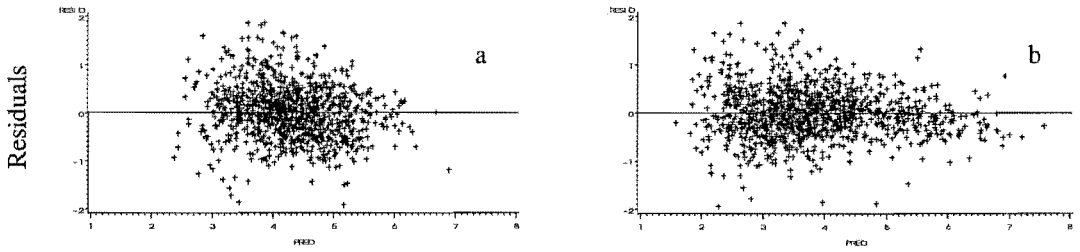

Figure 6.3- Residuals vs prediction for the equations of needle dry weight (a), and branch dry weight.

Table 6.2 - values of parameters for needle and branch dry weight equation.

Dependent Variances	Parameters (Values ±SE)							
	b0	b1	b2	b3	b4	b5	b6	t
Needle dry weight(g)	2.28	-0.33	0.35	-0.59	0.48	0.00	0.35	-0.01
	±0.0	±0.21	±0.05	±0.05	±0.05	±0.0	±0.05	±0.13
Branch dry weight(g)	1.00	0.66	0.62	0.39	0.31	0.00	0.00	1.22
	±0.17	±0.10	±0.04	±0.05	±0.04	±0.00	±0.05	±0.19

Note: the branch dry weight and needle dry weight equations are in the form:

$$\ln(ndw) = b0 + b1 * (\ln(bbd))^{t} + b2 * \ln(length) + b3 * \ln(age) + b4 * \ln(subn) + b5 * \ln(asubd) + b6 * \ln(asubl) \quad \text{Eq. 6.1}$$

$$\ln(bdw) = b0 + b1 * (\ln(bbd))^{t} + b2 * \ln(length) + b3 * \ln(age) + b4 * \ln(subn) + b5 * \ln(asubd) + b6 * \ln(asubl) \quad \text{Eq. 6.2}$$

where ndw is needle dry weight (g), bdw is branch dry weight (g), bbd is branch base diameter (cm), length is branch length (cm), age is branch age (1-3 year), subn is sub-branch numbers, asubd is average sub-branch diameter (cm), and asubl is average sub-branch length (cm)

6.4.3 The relationship between biomass and stem size at the tree level

Tree biomass generally increased with increasing DBHOB (Bartelink 1996). The relationships of total needle surface area (TNS, in m^2), stem biomass (STEMB, kg), total needle biomass (TNB, kg), total branch biomass (TBB, kg), and total biomass (TBIO, kg) respectively on DBHOB (cm) and tree height (H, cm) are shown in Table 6.3. DBHOB had strong positive liner relationship with needle biomass, branch biomass, total biomass, and total needle surface area. But, height (H) was poorly correlated with them.

Table 6.3 Regression of total needle surface area (TNS, in m^2), stem biomass (STEMB, kg), total needle biomass (TNB, kg), total branch biomass (TBB, kg), and total biomass (TBIO, kg) respectively on DBHOB (cm) and tree height (H, cm).

Regression equation	R^2
TNS = 24.575 + 29.413 * DBHOB - 0.423 * H	0.873
STEMB = -5.038 + 1.333 * DBHOB + 0.0045 * H	0.755
TNB = 1.552 + 2.135 * DBHOB - 0.029 * H	0.912
TBB = 7.511 + 2.048 * DBHOB - 0.043 * H	0.752
TBIO = 4.025+ 5.518 * DBHOB- 0.0676 * H	0.910

6.4.4 Needle biomass and its distribution

Needle biomass allocation according to age class, total needle biomass and needle biomass vertical distributions varied greatly among the four clones.

Figure 5.4 (a) shows the proportion of needle biomass according to age class for the four clones. Clone 4 and clone 9 had 40% - 41% of 1-year old needle biomass, clone 6 had 45% and clone 10 had only 32%.

Figure 5.4b shows clearly that the total needle biomass was very different among the four clones. Clone 9 had the highest amount of needle biomass among the four clones. The trend was clone 9> clone 10> clone 4> clone 6.

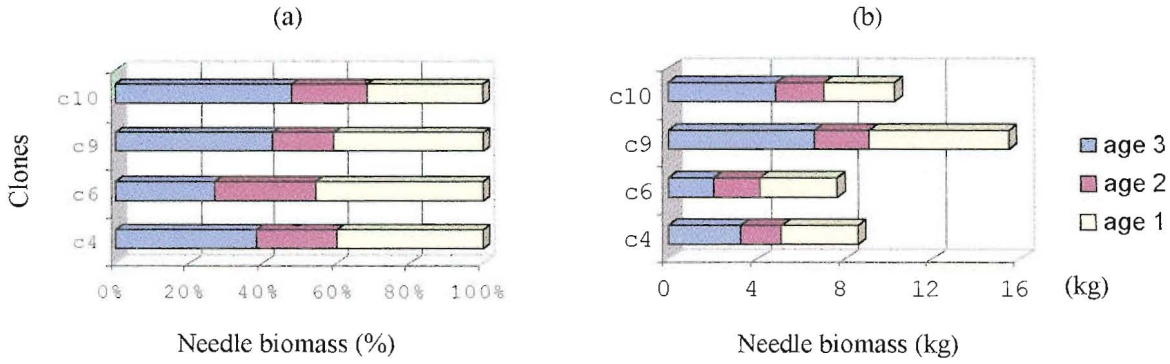

Figure 6.4 Needle biomass according to age class at the four clones. (a) Showing the proportion of needle biomass according to age class. (b) Needle biomass according to ages and accumulated all the needle age class showing the total needle biomass at the four clones (5-year old).

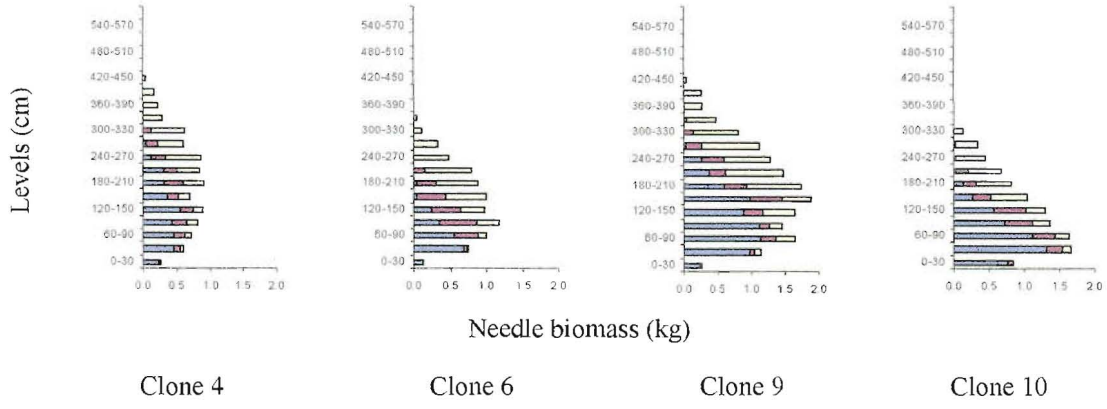

Figure 6.5- Needle biomass vertical distributed according to ages (from outside to inside: age1, age 2, age 3 and other older needles) at clone 4, clone 6, clone 9 and clone 10.

Needle biomass vertical distribution is shown in Figure 6.5. This result was useful for further studying the distribution of needle surface area and needle surface area density.

6.4.5 Specific leaf area

The calculated results of specific needle area (m^2 kg^{-1}) are shown in Table 6.4. The values of specific needle area ranged from 11 to 14 (m^2 kg^{-1}); these results are very similar to Bandara's study of specific needle area in radiata pine (Bandra, 1997).

Table 6.4-Average specific needle area (m^2 kg^{-1}) of radiata pine clones according to age class. The data were collected in winter 1998 (with standard deviation)

	1-year-old	2-year-old	3 year and older
Clone 4	12.17 (1.49)	12.04 (2.45)	11.51 (1.47)
Clone 6	13.49 (3.16)	13.16 (2.75)	14.03 (3.63)
Clone 9	14.36 (1.60)	12.83 (0.54)	11.52 (0.79)
Clone 10	13.97 (0.45)	11.30 (0.44)	11.19 (0.91)

6.4.6 Needle surface area and its vertical distribution

Needle surface areas were calculated by multiplying needle biomass by specific needle surface area. Figure 6.6 shows the needle surface area by age class and total needle surface area of the four clones. Comparing the total needle surface area among the four clones, clone 9 had the greatest surface area among the four clones and its surface area was twice that of clones 4 and 6. The surface area in clone 10 was greater than in clones 4 and 6. The interesting thing was that needle surface areas in clone 4 and clone 6 were similar, even if clone 4 and clone 6 had very different characteristics of heights, DBHOBs, crown shapes, crown volumes and total biomass.

Studying needle surface area vertical distribution was useful for a later study of the distribution of needle surface area density. The vertical distribution of needle surface area by age class was different among four clones (Figure 6.7).

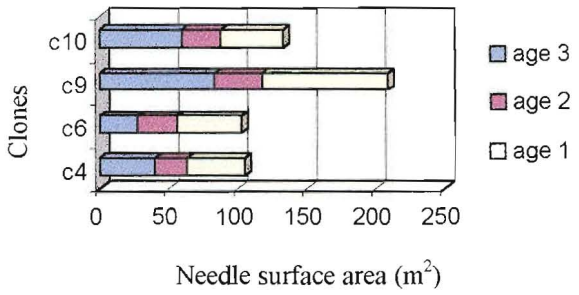

Figure 6.6- Needle surface area are presented according to age class and accumulated all the needle age class together showing the total needle surface area at the four clones (5-year).

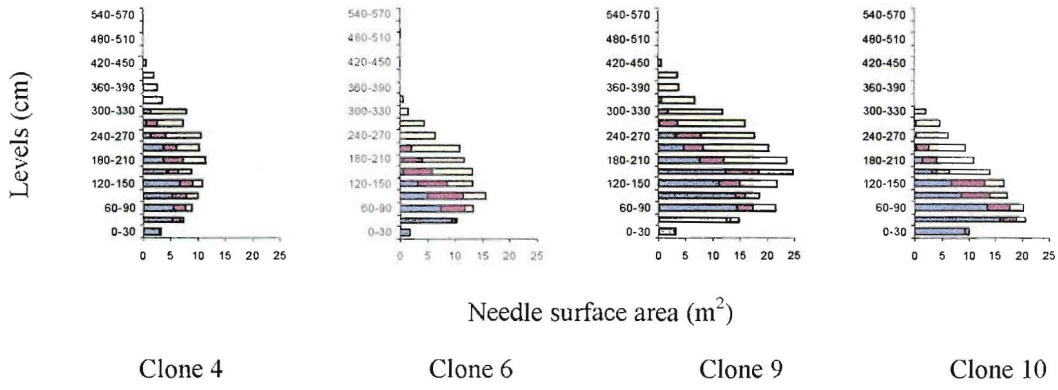

Figure 6.7- The vertical distribution of needle surface area are presented according to age-class (from outside to inside: age1, age 2, age 3 and other older needles) in clone 4, clone 6, clone 9 and clone 10.

6.4.7 Needle surface area density and its vertical distribution

To study needle surface area density (NSAD) and its vertical distribution is important, because the change of NSAD and its vertical distribution in crown affect the penetration of solar radiation; hence, affect needle photosynthetic activity.

As for the crown volume research in chapter 5 and needle surface area research above, the needles was separated to section according to age class and vertical level (0.3 m high in each level). In each age class and vertical slice, it was assumed that the foliage was randomly distributed, so needle surface area density was calculated in each part with the equation below:

$$NSAD_{ij} = NSA_{ij} / V_{ij}$$

$$i = 1, 2, 3$$

$$j = 0, 1, 2, 3, 4 \ldots L / d$$ (L is crown length, d is level distance = 0.3m)

Where NSAD is the needle surface area density, NSA is the needle surface area, V is the volume, i is the age class, and j is the vertical level.

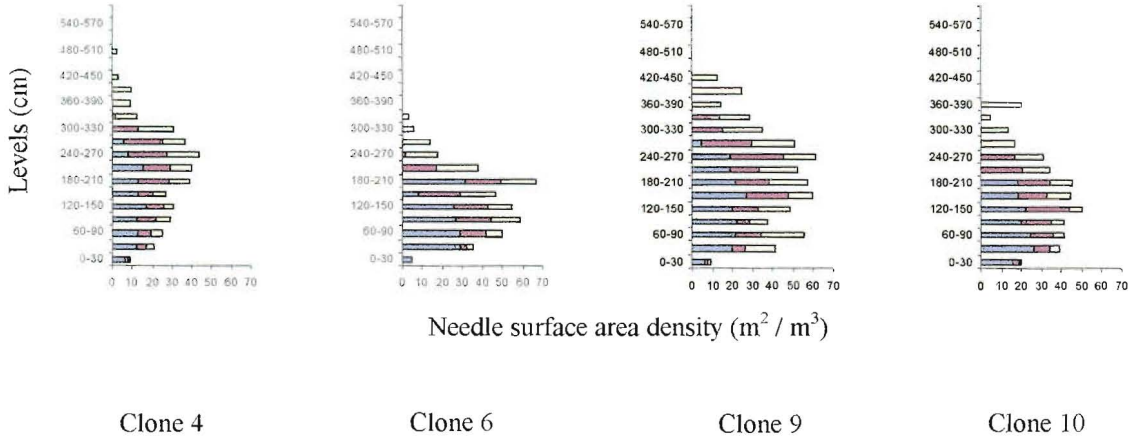

Figure 6.8- Needle surface area density vertical distributed according to age-class (from outside to inside: age1, age 2, age 3 and other older needles) in clone 4, clone 6, clone 9 and clone 10.

Figure 6.8 shows the calculated results of the NASD vertical distribution in the four clones. It is clearly that the NASD vertical distribution varies greatly among the four clones. Clone 4

had less NSAD than the other clones. The NSAD changed not only among the clones, but also according to needle age and vertical sections even within the same clone.

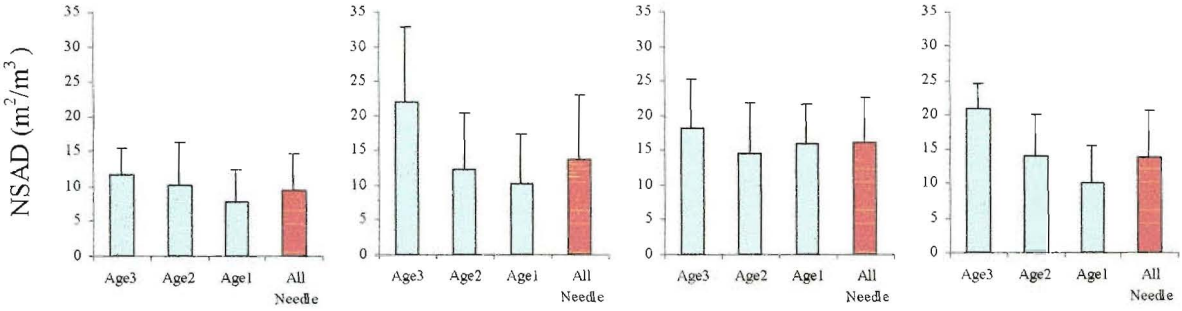

Figure 6.9- Needle surface area density distributed according to age class and all needles together at the four clones.

To calculate NSAD, the results will depend on the assumptions made on the distribution of foliage within crown. If just calculating simply NSAD with all needles together or just separating needles according to age class, it shows clearly from Figure 6.9 that the NSAD calculated by age class was different from a calculation with all needles together. Furthermore, it was known that needle photosynthetic capacity differed by age class, so using the NSAD with all needles together to estimate light interception or photosynthetic production would produce more estimating errors. Comparing Figure 6.8 with Figure 6.9, it shows that even in the same age class the NSAD vertical distributions were different in the crowns. For example, the maximum NSAD could be twice the average NSAD in age 3. The different NSAD vertical distribution would affect light penetration in each part within the crown, so separating the crown to different parts according to age class and vertical level allowed more accurate estimation of light interception than that just using all needles together or just separating them according to age class (Monsi and Saeki 1953, de Wit 1965).

6.5 Discussion and conclusion

6.5.1 Discussion

DBHOB was strongly correlated with total biomass and needle surface area. This result was in agreement with results of others (Snell and Brown 1978; St. Clair 1993; Bartelink 1996). Tree height was poorly correlated with total biomass and needle surface area.

The proportions of total above ground biomass allocated to stems ranged from 29% (clone 6) to 43% (clone 4). This result indicated that higher growth rate in height and DBHOB resulted partly from higher proportion of biomass allocation to stem. For example, a higher proportion (43%) of biomass allocated to the stem in clone 4 lead resulted in greater height (5m) and diameter (10.5cm) than that in clone 10 (proportion of biomass to stem 29%, height 3.6m, diameter 9.2 cm). However, total biomass production was reversibly higher in clone 10 (31.5 kg) than that in clone 4 (28 kg). At the very beginning of the clonal growth, the different allocation characteristics in clones may have caused some clones to have higher proportion of biomass allocated to leaves. Hence, this led to more needle surface area to catch radiation, and more leaf area to contribute to CO_2 fixation, and then gradually those clones grew faster than others.

At the branch level, branch biomass and needle biomass were positively correlated with branch base diameter, branch length, and sub-branch numbers. The relationship between branch biomass and branch size, or between needle biomass and branch size could be described with Eq. 6.1 and Eq.6.2. Branch or needle biomass was determined by the variables of branch size, which in Eq.6.1-6.2 included branch base diameter (cm), branch length (cm), branch age (1-3 year), sub-branch numbers, average sub-branch diameter (cm), and average sub-branch length (cm).

NSA and NSAD play an important role in tree growth. The different vertical distribution of NSAD in a tree crown have a great influence on radiation penetration, and hence on light interception and photosynthesis. Figure 6.8 and Figure 6.9 show clearly that the vertical distribution of NSA and NSAD were highly variable: the maximum NSAD could be twice the average NSAD.

As Chapter 4 showed that the needle photosynthetic capacity varied with needle age, current and 1-year-old needle had higher photosynthetic capacity than older needles, the photosynthetic rate and light efficiency of the crown are also dependent on the needle age distribution within tree crowns. Current and 1-year-old needles were numerically dominant in the upper and outer parts of the crown in higher radiation, and made more efficient use of light (Jarvis and Standford, 1986), whereas, older needles, distributed within inner and lower parts of the crown, used the lower light there as efficiently as the younger needles (Wang, 1988). This study not only separated needles by age, but also studied needle surface area and its vertical density distribution by age. The results were useful for subsequent study of radiation penetration in the crown, and estimating whole tree CO_2 fixation.

6.5.2 Conclusion

— Higher rates of tree height and stem diameter growth were not only due to higher biomass production rates, but also due to different above ground biomass allocation into tree components. The proportions of total above ground biomass allocated to stems ranged from 29% (clone 10) to 43% (clone 4).

— Needle biomass, branch biomass, total tree biomass, and total needle surface areas were poorly correlated with tree height (H). But they all showed strong positive liner relationship with DBHOB. A simple liner equation was developed to estimate tree above-ground biomass with DBHOB and H.

— There were significant differences among the clones in total foliage biomass allocation to differently aged foliage. The proportions of total foliage biomass allocated to foliage at age 1 were 45% for clone 6, 40-41% for clone 4 and clone 9, and 35% for clone 10%.

— NSA and NSAD vertical distribution according to age class were studied and were very different among the four clones.

— A simple model to estimate branch biomass and needle biomass was developed at the branch level with independent variables of branch base diameter (cm), branch length (cm), branch age (1-3 year), sub-branch numbers, average sub-branch base diameter (cm), and average sub-branch length (cm). Branch biomass and needle biomass were positively correlated with branch base diameter, branch length, and sub-branch numbers.

CHAPTER 7

MODELLING THE PENETRATION OF SOLAR RADIATION IN INDIVIDUAL 5-YEAR-OLD RADIATA PINE CLONES

7.1 Abstract

A simple PAR penetration program was developed for individual juvenile radiata pine clones. The program was based on data from crown architecture analysis, geometrical analysis of the PAR penetration distance within crowns and models of crown shapes. The program can be used to estimate the probability of direct PAR penetration at any given sun zenith angle and diffuse PAR penetration at any given direction with azimuth angle $\angle\theta$ and elevation angle $\angle\beta$. The probabilities of PAR penetration within clonal tree crowns were estimated and compared among clones at a given PAR level. Simulations showed that the probability of PAR (direct PAR or diffuse PAR) penetration depended not only on foliage density (penetration decreasing with increasing foliage density), but also on PAR penetration distance, which is decided by crown shape. Crown PAR extinction coefficient (k) is another important parameter for estimating PAR penetration. The probability of PAR penetration within a tree crown decreased with increasing k value. The program developed during this study was a crucial step for simulating whole tree photosynthesis.

7.2 Introduction

Tree growth depends on energy from intercepted solar radiation. PAR interception for an individual tree is dependent on the incident solar radiation arriving at the top of the canopy, the plant space, crown structure and the density of foliage area distributed within crown. Many radiative transfer models have been developed (see reviews by Lemeur and Blad, 1974; Myneni *et al.*, 1989). The main differences between those models were in how they treat the canopy architecture. For example, the canopy was sometimes assumed to be one-dimensional, and with all foliage together randomly distributed throughout the canopy space (Monis and Saeki 1953, de Wit 1965). Other models have considered the non-random distribution of foliage in vertical or horizontal directions, such as discontinues canopies with row crops or widely spaced plants with individual trees. In this situation, individual trees can be treated as geometrical objects, and the crown is made up of different, small components in a particular arrangement. Still, in each small component the foliage is assumed to be randomly distributed and is evaluated with a simple radiative transfer function (Mann *et al.*, 1979; Norman and Welles, 1983).

In the juvenile radiata pine clone plantation examined during the study reported here, the canopy was not closed. We treated the tree individually to estimate PAR interception.

The objectives of this study were: (i) to analyze the geometrical relationship between crown position and PAR penetration; (ii) to develop a simple program, by using Norman's PAR transition model combined with the geometrical analysis to estimate direct and diffuse PAR penetration within tree crowns; (iii) to estimate the effect of crown structure and the distribution of needle area on PAR penetration within tree crowns in different radiata pine clones at a given PAR level, and compare relatively at a given PAR the alteration of PAR penetration among different clones. Knowledge of the PAR distribution within a tree crown is necessary for modelling and simulating whole tree photosynthetic productivity.

7.3 Theory

7.3.1 Solar radiation interception

To estimate PAR interception by foliage within a tree crown, the following are required (i) the amount of direct and diffuse irradiance outside the crown, (ii) crown structure and foliage density distribution, and (iii) interaction between PAR and foliage distribution within the tree crown.

7.3.2 The incoming solar radiation

The variations of global radiation on a horizontal surface at the top of the canopy are approximated by Thomas and Norris (1982):

$$FG(t) = (R*\pi/ 2*H)\sin \{\pi*(t - Sunr) / H\} \qquad (7.1)$$

Where FG(t) is global irradiance (W m^{-2}) on a horizontal surface at time t, R is daily isolation (J m^{-2}), H is day length (s), Sunr is the time of sunrise (s).

The total incoming solar radiation outside the crown could is the sum of direct and diffuse photosynthetic active radiation (PAR, 400-700 nm); and diffuse and direct near-infrared radiation (NIR, 700-3000 nm). Photosynthetically active radiation (PAR) is essential for photosynthesis, and it is assumed to be 50% of global radiation.

If S_{D0} be the direct PAR intensity in the direction of sunlight propagation, and $Sd(\varphi,\theta)$ the intensity of diffuse sky PAR in the direction (φ,θ), where φ is zenith angle and θ is azimuth angle, then the total incoming photosynthetic active radiation St (PAR) can be written as:

$$St = S_D + Sd = \pi*S_{D0}*\cos\varphi + \int_0^{2\pi} d\theta \int_0^{\pi/2} Sd(\varphi,\theta)\ \cos\varphi \sin\varphi\, d\varphi \qquad (7.2)$$

where S_D represents direct solar radiation (PAR) coming vertically on the horizontal surface at the top of canopy and Sd represents diffuse radiation (PAR).

If the fraction ξ is the direct radiation of St, and it is assumed to be constant and diffuse PAR is considered to be isotropic (Myneni 1988), then

$$S_{D0} = \xi * St / (\pi * \cos\varphi) \quad (7.3)$$

$$Sd = (1 - \xi) * St \quad (7.4)$$

7.3.3 Crown shape and vertical distribution of foliage area density

Crown shapes and vertical distribution of foliage area density were discussed in Chapter 5 and 6 for the four different clones. The crowns were separated into different components according to age class and vertical levels. In each small part, the foliage was assumed to be randomly distributed with no preferred azimuth direction. The inclination angles of foliage were assumed to be distributed according to the spherical leaf angle distribution.

7.3.4 Calculating the penetration of direct and diffuse radiation within crowns

During a clear day or incompletely cloudy day, the PAR environment around tree crowns should be the irradiance, S_{D0} (PAR) and Sd (PAR), of direct solar radiation and diffuse radiation. A direct beam comes from sun, and has an identical zenith angle for all tree crown vertical levels. Diffuse radiation, unlike the direct beam, is distributed relatively uniformly over all leaves surrounding the tree crown (Campbell and Norman 1998).

For estimating direct radiation the equation of penetration probability on a horizontal plane at any level j within tree crown was approximated (Monis and Saeki 1953) as:

$$p (j, \theta) = \exp (-k* LAI / \cos\varphi) \quad (7.5)$$

where p (j, φ) is the penetration probability of direct beam, LAI is the leaf area index above j level, φ is the inclination of sun (zenith angle), k represents PAR extinction

coefficient (which can be expressed as a function of leaf angle distribution, leaf dispersion, and transmission properties (Norman and Campbell 1989)).

According to the report of Norman and Welles (1983), the term LAI / cosφ can be written as:

$$LAI / \cos\varphi = D*S \qquad (7.6)$$

where D is foliage area density and S is the distance a ray must pass through the area of crown with the density of D. So, for different components within an individual tree crown, the probability of direct radiation could be calculated as:

$$Pdir_{(i,j)} = \exp\{-k*D(i,j)*S(i,j)\} \qquad (7.7)$$

and the irradiation of a direct beam distributed at different components could be written as:

$$DIR(i,j)= S_D(i,j) * Pdir(i,j)= S_D(i,j)* \exp\{-k*D(i,j)*S(i,j)\} \qquad (7.8)$$

where i represents leaf age and j represent differents vertical levels.

In the case of a uniform overcast sky, the equation of penetration probability of diffuse PAR within tree crown was calculated as:

$$Pdif(i,j) = \exp\{-k* (Dij* \overline{Sij})\} \qquad (7.9)$$

$$DIF(i,j) = Sd * Pdif(i,j) \qquad (7.10)$$

where Pdif(i,j) is the probability of diffuse PAR penetration within crown level j according to leaf age-class i, Dij is the leaf area density above level j, $\overline{Sij}$ is the average diffuse PAR penetration distance above level j according to leaf age-class i, DIF(i,j) is the amount of diffuse radiation reaching crown components (ij), and. Sd is the amount of diffuse radiation incident around the crown.

7.3.5 Geometrical relationships between crown position and PAR penetration

Direct beams come from a single source of the sun with a zenith angle. The direct beam penetration distance to any crown level at different points was analyzed by using geometrical methods. With the geometrical analysis and crown shape model (see Chapter 5) a simple program (Appendix 2 Figure 2.1- 2.6) was developed to calculate direct PAR penetration distance for different sun zenith angles. With direct penetration distances in crown at different points, and foliage density data, the probability of direct beam penetration can be calculated using the function 7.7.

Diffuse radiation does not come from a single source as does a direct beam. It comes from all directions over the whole upper hemisphere. The penetration of diffuse radiation can be approximated by summing the penetration of direct radiation over the whole hemisphere, and then taking the mean of the summed values. For calculating diffuse radiation penetration within a crown, a simple program was developed to estimate the geometrical relationships between crown position and PAR penetration. Using a computer program (Appendix 2 Figure 2.1- 2.6), for any point in tree crown, the PAR emanating from any detailed azimuths ($\angle\theta$ = 0°-360°) and elevations ($\angle\beta$ =0°-85°) can be calculated. The maximum elevation is not 90° to avoid an excessive influence of the vertical direction in the calculation of the mean. In simulation, each point at level j according to age-class i, it was calculated 8 different azimuths ($\angle\theta$ = 0°, 45°, 90°, 135°, 180°, 225°, 270° and 315°) and 5 different elevations ($\angle\beta$ =0°, 20°, 40°, 60° and 80°). Thus, the probability of penetration of diffuse PAR to any point ij is

$$\text{Pdif(ij)} = \frac{1}{40}\sum_{\theta}\sum_{\beta} P_{dir(i,j)} \qquad (7.11)$$

Where $P_{dir\,(i,j)}$ is the probability of direct beam penetration to point ij at azimuth $\angle\theta$ and elevation $\angle\beta$.

Figure 7.1 shows the diagram of direct and diffuse PAR penetration at a given level j. The more detailed geometrical analysis of the relationship of direct and diffuse PAR

penetration within the clonal crowns is illustrated at Appendix 1 (Appendix 2 Figure A2.1-A2.6)

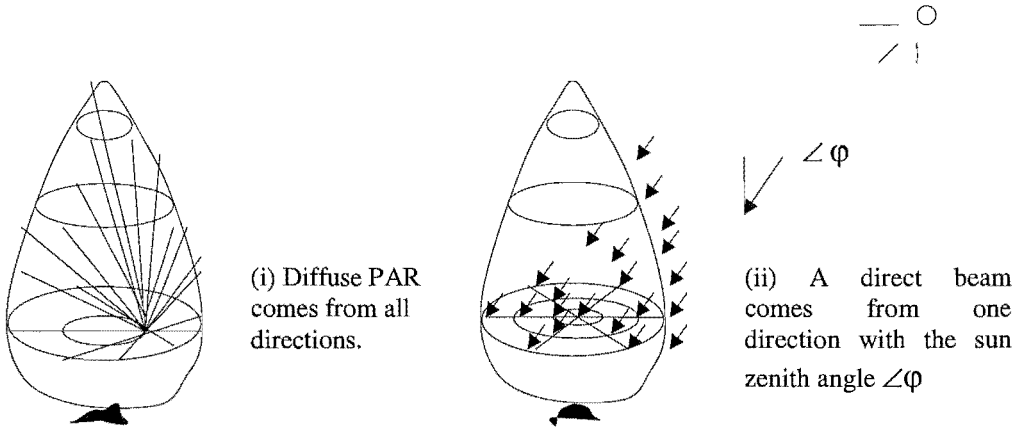

Figure 7.1. Diagrams showing diffuse PAR and direct beam penetration within a tree crown. With geometrical analysis of PAR penetration and a computer program, diffuse and direct PAR penetration distance can be calculated, and by combining Norman's PAR penetration theory the probability of diffuse and direct PAR penetration can be estimated.

7.4 Results

7.4.1 Direct beam and diffuse radiation penetration within clonal tree crowns

Generally, when the sky is not completely clouded, the PAR at the top of canopy should be both direct beam and diffuse radiation. For a given PAR St, if the fraction (ξ) of direct beam is known, we can use the equations 7.3 and 7.4 to calculate the direct beam S_D and diffuse radiation Sd, and treat them differently to calculate PAR penetration within the

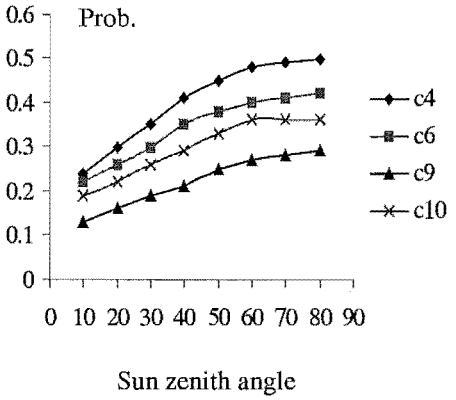

Figure 7.2 The average penetration probability of direct beam influenced by sun zenith angle. Simulation condition is k=0.2 (crown PAR extinction coefficient) in different clones. C4-C10 refer to different clones

crown by using equations 7.8 and 7.10. The PAR distributed within each small component in a tree crown should be composed of direct and diffuse PAR.

7.4.2 Direct beam penetration probability

For the individual tree, the average penetration probability of direct beam increased with sun zenith angle, and all four clones showed the same trends (Figure 7.2).

Comparing the probability of direct PAR penetration between clones, the probability of PAR penetration not only depended on foliage density (Figure 7.3), but also on PAR penetration distance, which was decided by crown shape.

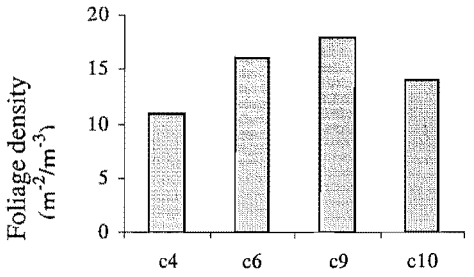

Figure 7.3 Mean tree foliage area density in the four clones (Clone 4, 6, 9 and 10 represented by c4, c6, c9 and c10).

7.4.3 Diffuse PAR penetration probability

Simulations showed that the average penetration probability of diffuse PAR within an individual tree crown mainly depended on crown PAR extinction coefficient (k), foliage density (m^2/m^3) and PAR penetration distance (m). Figure 7.4 illustrates that PAR penetration probability decreased with increasing k value.

Comparing the probability of diffuse PAR penetration between clones at the same k

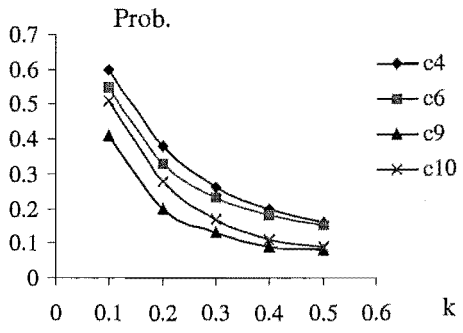

Figure 7.4. Simulation of diffuse PAR penetration probability influenced by k value (crown PAR extinction coefficient) in different clones. The simulation condition is : diffuse PAR, temperature = 15 °C, VPD = 1 kPa, PAR =1000 (μmol $m^{-2}s^{-1}$)and season = spring.

value, PAR penetration probability decreased with increasing foliage density (m^2/m^3) and penetration distance (m).

7.5 Discussion and conclusions

7.5.1 Discussion

Due to the crucial role of solar radiation in tree growth, the analysis of PAR penetration within tree crowns is an important research objective in studies of plant physiology (Kronenberg, 1986; Myneni and Ross, 1991). Because of the variability of crown structure and foliage distribution for different tree species, the main difficulty for estimating PAR penetration within a tree crown is the interaction between incoming PAR and crown characteristics.

In using a PAR transfer model to estimate PAR penetration, most researchers assumed that PAR penetration within tree canopies followed the Beer-Lampbert Law: PAR penetration probability can be expressed as Prob = exp(-k*LAI), which could be written as Prob = exp(-k*D*S) (Norman and Welles, 1983). According to Norman's equation, PAR penetration probability within a canopy will be decided by foliage density D, PAR penetration distance S and canopy PAR extinction coefficient k.

Simulations showed that PAR penetration in individual trees depended not only on foliage density distribution in crown and PAR penetration distance, but also on the crown PAR extinction coefficient k. Using a reasonable k-value to estimate PAR penetration is important, because the results of PAR penetration within crown will influence estimation of total photosynthesis. Many researchers (Brunner 1998; Chen 1994; Grace 1987a; Whitehead 1990) reported estimations of PAR penetration with assumed k-value = 0.5. However, the k value should be treated differently according to different canopies or different species individual tree crowns (Sampson 1993). For example, if we assumed canopies are unlikely to intercept more than 95% of incoming radiation, according to the Beer-Lampbert Law, we have a form like:

$0.95 = 1\text{-}\exp(k*LAI)$ or $0.95 = 1\text{-}\exp(-k*D*S)$

Then $0.05 = \exp(-k*LAI)$

$\therefore k * LAI = 3$

Thus, for broad-leaved canopies, using k values between 0.5 and 0.8 seems reasonable when LAI = 3.75-6 (Cannell 1993), but for needled canopies it is known that many conifer canopies have leaf area indices exceeding 15 (e.g., Gholz 1982), and so the effective k-values should be 0.2 or less (Cannell 1993). For individual tree crowns, such as the radiata pine clones in this study, the values D*S were higher than 12, and hence the effective k-values should be less than 0.25. Weiss and Norman (1985) used k = 0.185 in their model. Recent reports suggest that canopy PAR extinction coefficients vary with several tree species (Gholz 1991; McIntyre 1990; Smith 1991; Sampson 1993). McCrady (1998) reported that k ranged from 0.28 to 0.38 for loblolly pine families.

The mechanism for this variation of k has been explained by increased LAI (Kira, 1969), greater mean tree foliage area (Pukkala and Kuuluvainen, 1987), mean leaf angle (Campbell and Norman, 1989), steeply inclined foliage (Norman and Jarvis, 1974) and increased foliage aggregation (Oker-Blom et al., 1989).

Although it is difficult to know exactly what the k-value was for the four clones, we could use the developed program to simulate PAR penetration at any k-value, and compare the variability of PAR penetration between clones with any given k-value.

7.5.2 Conclusions

— The probability of direct beam penetration increased with sun zenith angle within individual tree crowns at a given k value (crown PAR extinction coefficient), and all the four clones showed the same trends.

— The probability of PAR (direct and diffuse) penetration between clones, depended on foliage density (decreasing with increasing foliage density), but also on PAR penetration distance, which is decided by crown shape.

— If it is assumed that PAR penetration in a tree crown follows the Beer-Lambert Law, simulations showed that PAR (direct PAR or diffuse PAR) penetration probability depended not only on foliage density (m^2/m^3) and PAR penetration distance (m), but also on crown PAR extinction coefficient (k). The probability of PAR penetration decreased with increasing k value.

— A simple PAR penetration program was developed for individual juvenile radiata pine clones. The program can be used to estimate the probability of direct PAR penetration at any given sun zenith angle and diffuse PAR penetration at any given aspect with azimuth angle $\angle\theta$ and elevation angle $\angle\beta$. The program is based on the data from crown architecture analysis, geometrical analysis of the PAR penetration distance within crown and crown shape models. The program described here is one of the basic parts of whole tree photosynthesis model.

— The developed PAR penetration program was presented in a diskette at Appendix 4.

CHAPTER 8

MODELLING NET PHOTOSYNTHESIS IN INDIVIDUAL FIVE-YEAR OLD RADIATA PINE CLONES

8.1 Abstract

A simple process model for simulating total net photosynthesis in an individual tree for *Pinus radiata* D. Don clones at age 5 was developed from measurements of rates of needle photosynthesis, crown architecture, and calculating light penetration with a radiation transfer model. Using the process model, whole tree photosynthesis could be simulated for the four different clones at a given season (include a given temperature, VPD and PAR). The influence of foliage mass, crown shape, light penetration probability, incoming sun zenith angle, crown light extinction coefficient k-value and needle photosynthetic capacity on total tree net photosynthesis was studied. Simulation results indicated that foliage mass was an important factor influencing total tree photosynthetic rate. However, other factors, such as crown shape and needle photosynthetic capacity, all influenced the variation of total tree photosynthetic rates in different environment conditions. Comparisons of simulations among the four different clones, showed that total above-ground biomass was positively correlated with total tree photosynthesis.

8.2 Introduction

Modelling net photosynthesis can be developed at varying levels. Models can vary from empirical models (e.g., Thornley, 1976) to biochemical models (e.g., Von Caemmerer and Farquhar, 1981) and the levels can be chloroplast, foliage element, or canopy. The different models are useful to simulate net photosynthesis for differing specific aims. Modelling net photosynthesis at a foliage level has its advantages, for example, linking the foliage level model with light interception and foliage distribution could scale to crown or canopy levels (Grace 1990, Pearcy 1996, De Pury 1997).

The objectives of this study were: (i) to link studies of foliage level photosynthesis, crown shape research, foliage area and density analysis and estimates of light penetration probability within tree crowns together to develop a process model to estimate total net photosynthesis on individual tree level for radiata pine clones; (ii) to compare the simulation results of different clones to find which factors influence differential clonal tree growth.

8.3 Methods

In estimating the total net photosynthesis for an individual tree in different radiata pine clones, it is necessary to know needle photosynthetic rate, light penetration probability and foliage area distribution according to ages within tree crowns. Firstly, we know that needle photosynthetic rate is positively related to PAR. Hence, to know light distribution within a tree crown is essential for estimating whole tree net photosynthesis. Secondly, to estimate light distribution within a tree crown it is usual to use a transfer model to estimate light incident on foliage in different parts of the crown (Chapter 7). Next, the net photosynthesis in each part of the crown can be estimated by using the needle photosynthesis model (Chapter 4) that relates the light and the foliage area distribution in that part of the crown. Finally, total tree photosynthesis can be calculated by summing the net photosynthesis of all the parts in the crown.

8.3.1 Needle photosynthesis study

For a given value of incident PAR, there are differences in the rate of net photosynthesis for the needles of different ages within tree crowns (Chapter 4). Hence, to develop a whole tree photosynthesis model was necessary to know the rate of needle net photosynthesis according to different types of foliage and treat them separately in the model.

In order to account for the differences in rates of needle photosynthesis due to leaf age and position in the crown (Jarvis & Sandford 1986), needle photosynthesis was studied for different foliage ages at different positions in tree crowns (Chapter 4). The results (Chapter 4) showed that rates of needle photosynthesis decreased with increasing needle age, but needle position did not significantly affect rates of CO_2 uptake for a given leaf age. A simple sub-model was developed to represent the rates of needle photosynthesis predicted by foliage age in four seasons. With the needle photosynthetic model, needle photosynthesis rate could be predicted separately in different foliage age classes.

8.3.2 Crown shape and volume sub-model

In a previous study (Chapter 5), crown shape and volume were discussed. Crown volume and its vertical distribution is essential for estimating foliage area density and light distribution within a crown. Because the shape of a tree crown varies widely among species and clones, the crown shape must be described specifically for the four different clones in order to estimate more exactly foliage area density and light distribution within crowns. A crown shape sub-model had been developed (Chapter 5) with the relationship between crown width (Ri) and relative height (hi / H). The crown shape sub-model is important not only for estimating crown shape and volume, but also for predicting foliage density and light penetration distance within tree crowns.

8.3.3 Leaf area and density

The distribution of foliage area (m^2) and foliage area density (m^2/m^3) within tree crowns was studied according to leaf age classes and vertical levels in Chapter 6. The foliage density distribution is important in relation to radiation penetration within tree crown, and foliage area is important for simulating whole tree photosynthesis.

8.3.4 Light penetration sub-model

Light penetration within tree crowns was studied with Norman's radiant transfer model. Combining the crown shape model with foliage density analysis, a light penetration sub-model was developed in Chapter 7. It can treat direct beams and diffuse radiation separately to estimate light penetration probability within tree crowns.

8.3.5 Whole tree net photosynthesis model

A simple process model was developed to simulate whole tree photosynthesis for the four different radiata pine clones. In predicting whole tree net photosynthesis, the process model needs to link needle photosynthesis, crown shape and volume, foliage area and density, and light penetration within tree crowns. Figure 8.1. shows the structure of the whole tree net photosynthesis model. It linked each part together and treated direct light and diffuse light differently. The input variables can be selected, which are direct or diffuse radiation, sun zenith angle, light extinction coefficient k-values, season, temperature, VPD and incoming light (PAR). The output results could be needle photosynthetic rates according to leaf ages, light penetration probability and net photosynthesis for different leaf ages at different crown levels, sub-average light penetration probability and sums of the net photosynthesis by leaf ages, total whole tree photosynthesis and comparisons of whole tree net photosynthesis between clones.

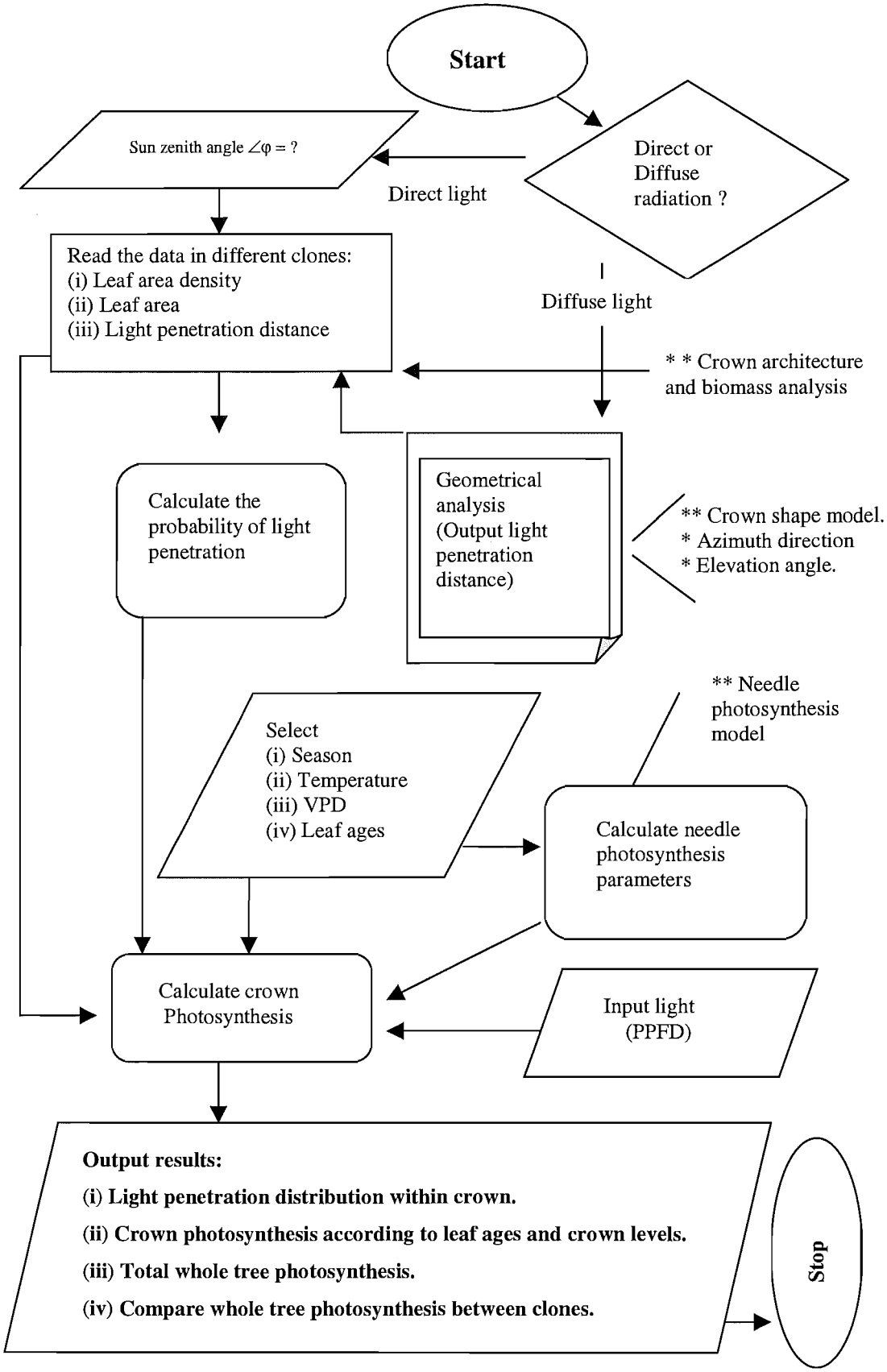

Figure 8.1 flowchart of the crown photosynthesis model. * = variables. ** models

8.4 Results of the simulation study

8.4.1 Variation of total net photosynthetic rates from direct beams with sun zenith angle for different clones

Simulations showed (Figure 8.2) that total net photosynthetic rates increased with increasing sun zenith angle (The simulation conditions are direct beam PAR = 1000 (μmol $m^{-2}s^{-1}$); k = 0.2 (crown light extinction coefficient); temperature = 15C°, VPD = 1 kPa and season = spring). These results were influenced by the increasing light penetration with sun zenith angle (Chapter 7). However, when the variation of total net photosynthetic rates were compared between clones, the increased rates of total net photosynthesis depended not only on sun zenith angle or light penetration rate, but also on foliage area. For example, when the sun zenith angle was < 20°, the total net photosynthetic rates for clone 9 were lower than other clones. This was because there was not enough light penetration within crowns with higher foliage mass for clone 9, and respiration rates were higher. Nevertheless, when the sun zenith angle was > 20°, more foliage received enough light and photosynthesis rates gradually increased. Hence, Figure 8.2 showed the more foliage area, the higher the rate of total net photosynthesis when foliage could get enough light.

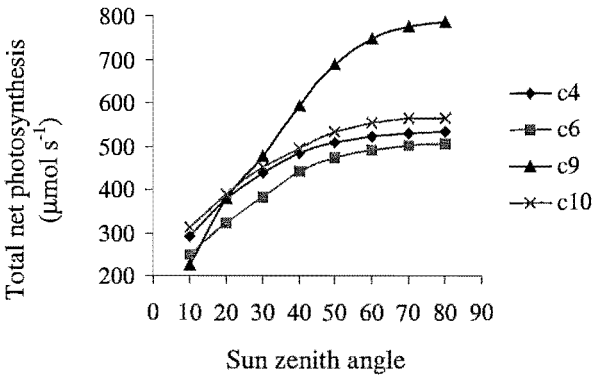

Figure 8.2 Total net photosynthesis for a tree influenced by sun zenith angle in different clones. Simulation condition is: direct beam PAR =1000(μmol $m^{-2}s^{-1}$), k=0.2 (crown light extinction coefficient), temperature =15C, VPD =1 kPa and season = spring.

8.4.2 Variation of total net photosynthetic rates in diffuse radiation with different extinction coefficient k for different clones

Simulation (Figure 8.3) showed that total net photosynthetic rates decreased with increasing k-values (The simulation conditions are diffuse radiation PAR = 1000 (μmol $m^{-2}s^{-1}$); temperature = 15C°, VPD = 1 kPa and season = spring). These results were influenced by light penetration decreasing with increasing k-values (Chapter 7). However, when we compared the variation of total net photosynthetic rates between clones, the decreased rates of total net photosynthesis depended not only on light penetration rate, but also on foliage area. For instance, if we assumed k-values <=0.25, the total net photosynthetic rates increased with increasing foliage area. However, if the k-value was > 0.25, the total net photosynthetic rates decreased with increasing foliage area. The reason was that when k-values were assumed >0.25 for the clones in this study, as the discussion in Chapter 7, there was not much (average light penetration probability <0.05) light penetration within crowns. Hence the more foliage area, the higher respiration rate would be, and that resulted in total net photosynthetic rates decreasing.

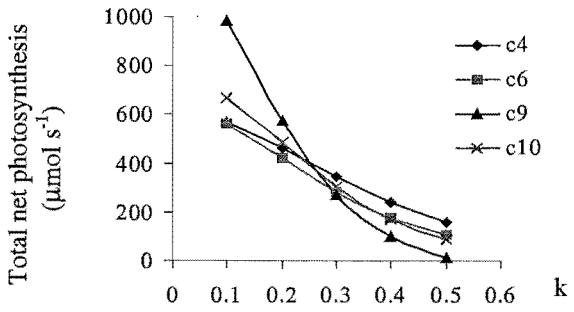

Figure 8.3 Total net photosynthesis for a tree influenced by the crown light extinction coefficient value (k) in different clones. Simulation condition is: diffuse light PAR =1000 (μmol m^{-2} s^{-1}), temperature =15C°, VPD =1 kPa and season = spring.

If two clones had similar foliage area, such as clone 4 and clone 6, the variation of total net photosynthetic rates would mainly depend on light penetration probability, which was decided by foliage area density and crown shape. For example, clone 4 had higher light penetration probability than that in clone 6, and the total net photosynthetic rates in clone 4 were higher than that in clone 6 (Figure 8.3).

8.4.3 Comparing total net photosynthetic rates in four seasons for the four different clones

Total net photosynthetic rates were compared for the four different clones in the four seasons. The simulation conditions were diffuse light, extinction coefficient k = 0.2, temperature = 15C° and VPD = 1 kPa in winter, spring and autumn; but summer's VPD and temperature were high in the field, so temperature = 25C° and VPD = 3.1 kPa were used to make a simulation for summer conditions.

Figure 8.4 shows the main trend of the variation for the total tree net photosynthesis rates in the four seasons was spring> autumn > winter > summer. However, when comparing the variation of total net photosynthetic rates between clones in a given season, the total net photosynthetic rates increased with increasing foliage area and light penetration probability, when the incoming light, PAR was > 500 (μmol $m^{-2}s^{-1}$). For instance, the total

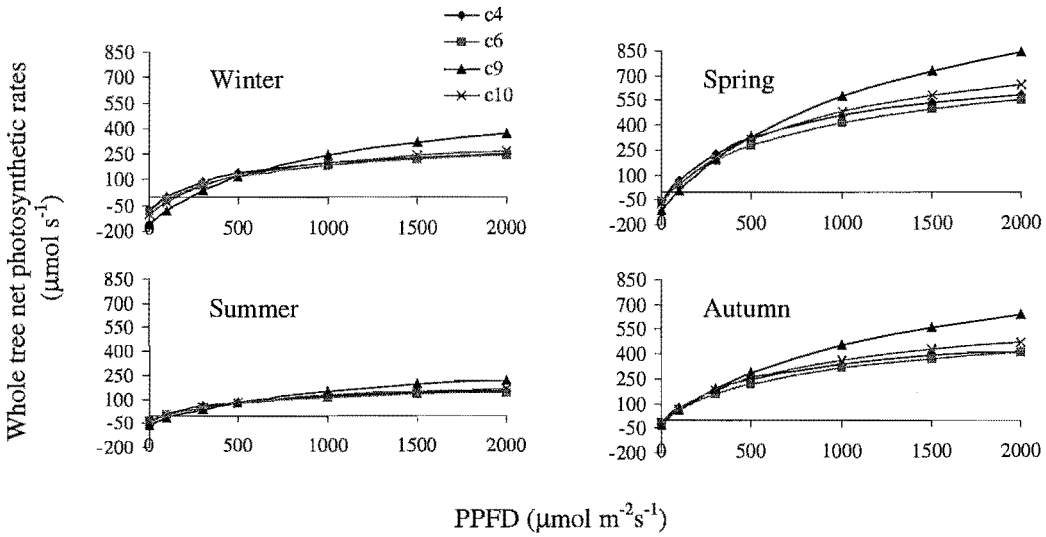

Figure 8.4. Comparing whole tree photosynthetic rates in the four seasons for the four different clones. c4, c6, c9 and c10 represent clone 4, 6, 9 and 10. The simulation conditions: extinction coefficient k = 0.2, temperature = 15C° and VPD = 1 kPa at winter, spring and autumn; k= 0.2, temperature = 25C° and VPD = 3.1 kPa in summer.

net photosynthetic rates showed a trend with total foliage area (Chapter 6): clone 9 > clone 10 > clone 4 > clone 6. Although the total foliage area was very similar for clone 4 and clone 6, it was known that clone 4 had higher probability of light penetration than clone 6. So, the total tree net photosynthetic rates showed clone 4 > clone 6 in all seasons (Figure 8.4).

When the incoming light PAR < 500 (μmol $m^{-2}s^{-1}$), as the highlighted Figure 8.5 shows, the light compensation points for whole tree photosynthesis were different for each season, which was influenced by the differences in needle compensation points for different seasons (Chapter 4). However, when comparing between the clones, the compensation points for whole tree photosynthesis increased with increasing foliage area. For example,

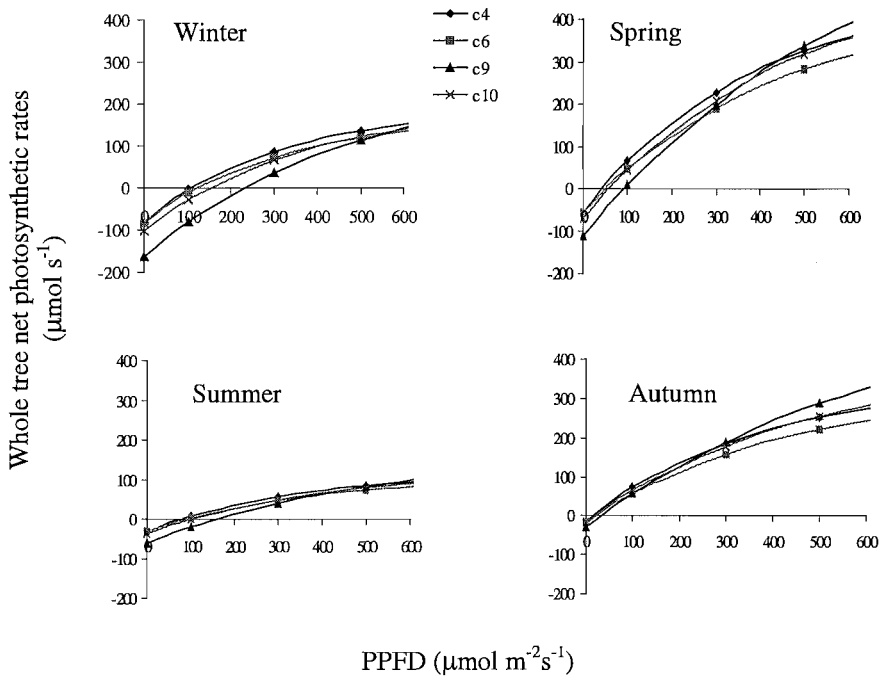

Figure 8.5. Comparing the variation of whole tree net photosynthetic rates at lower diffuse light (PPFD) in the four seasons for the four different clones. c4, c6, c9 and c10 represent clone 4, clone 6, clone 9 and clone 10. The simulation conditions: extinction coefficient k = 0.2, temperature = 15C° and VPD = 1 kPa in winter, spring and autumn; k = 0.2, temperature = 25C° and VPD = 3.1 kPa in summer.

the trend of compensation points for the four clones were clone 9 > clone 10 > clone 6 > clone 4.

If two clones had similar foliage area, such as clone 6 and clone 4, the compensation points for the whole tree photosynthesis was decided by the probability of light penetration. The compensation points decreased with increasing probability of light penetration.

8.4.4 The relationship between whole tree photosynthetic rate and total above ground biomass

Total tree above ground biomass was positively correlated with whole tree net photosynthesis. If tree crowns got enough light (for example, direct radiation with sun zenith angle >20° and PAR > 500 (μmol $m^{-2}s^{-1}$) for all light, assuming an extinction coefficient k <= 0.25), whole tree net photosynthesis in the four different clones showed the trend: clone 9 > clone 10 > clone 4 > clone 6. Comparing this result with total tree above ground biomass production in the four clones (Figure 8.6), it shows clearly that whole tree net photosynthesis increased with total tree above ground biomass. However, if the tree crown received less light (for example, direct radiation with sun zenith angle < 20°, PAR < 500 (μmol $m^{-2}s^{-1}$) for all light, or assumed extinction coefficient k >0.25 for the studied clones), then whole tree net photosynthetic rates were not positively correlated with total tree above ground biomass. Nevertheless, it is known that incoming light (PAR) generally is higher than 500 μmol $m^{-2}s^{-1}$ in the daytime (Chen and Klinka 1997), so it could be concluded that whole tree net photosynthetic rates were positively correlated with total tree above ground biomass.

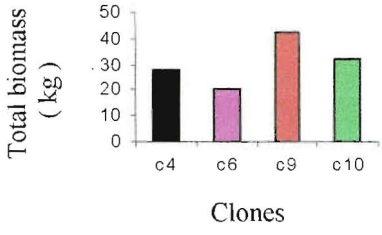

Figure 8.6 Total above-ground biomass (kg) in the four clones

8.4.5 Vertical distribution of net photosynthetic capacity in individual crowns and its application for pruning

If the crown shape and foliage area density distribution were known, the net photosynthetic capacity can be simulated at different vertical levels in an individual tree for the radiata pine clones. Figure 8.7a shows that if the vertical distribution of net photosynthetic

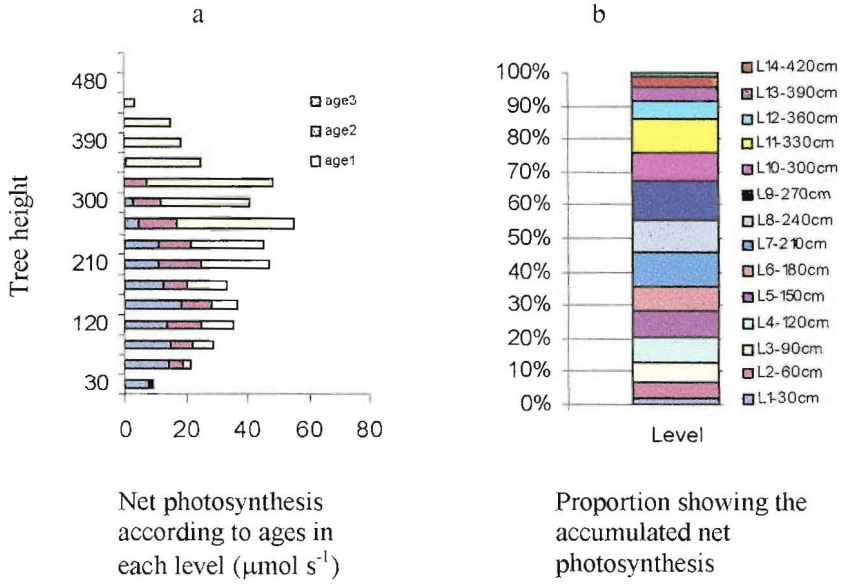

Figure 8.7 Vertical distribution of net photosynthetic capacity in crown. (a) Net photosynthesis according to ages in each level (μmol s^{-1}). (b) Proportion showing the accumulated net photosynthesis. Simulation condition are diffuse light (PPFD)=1000(μmol $m^{-2}s^{-1}$), extinction coefficient k=0.2, temperature = 15C°, VPD = 1 kPa, season = spring and clone = clone 4.

capacity was obtained in an individual crown with the developed process model, the proportion of net photosynthesis can be calculated in levels. Figure 8.7b shows the accumulating proportion of net photosynthetic capacity up a crown. If this simulated result was applied for pruning, it is easily to estimate that how much photosynthetic capacity still remained in the crown when pruning the crown to different heights.

8.5 Discussion and conclusions

8.5.1 Discussion

The developed process model linked the crown shape, foliage area and foliage density, light penetration and the tree photosynthetic performance together to simulate total net photosynthesis for an individual tree of any of the four radiata pine clones. The main difference between this model and other models (Grace, 1990) is that (i) more detailed needle photosynthetic information was collected and analyzed to use in the model for the different radiata pine clones; (ii) the model was based on detailed crown shape description and crown architecture analysis; (iii) output results could be separated according to leaf ages and crown vertical levels.

Total net photosynthesis increased with increasing sun zenith angle for individual tree. This was caused by light penetration probability increasing with increasing sun zenith angle (Chapter 7).

Total net photosynthesis increased with increasing foliage area. This conclusion is similar to other researchers' reports (Grace, 1990; De Pury, 1997). However, if the incoming light was low, then the more foliage mass is, the higher respiration would be. Hence, total net photosynthesis would be not positively correlated with foliage mass.

Light extinction coefficient k-values were important not only in estimating light penetration probability, but also in simulating whole tree photosynthesis. As Figure 8.3 showed if we assumed k-values > 0.25, the simulation results for whole tree photosynthesis will be opposite to the results from assuming k-values < 0.25, when comparing between the four different clones.

Light extinction coefficient k-values for photosynthetic radiation have been studied by several researchers (e.g. Cohen *et al.*, 1995; Jackson, 1989; Johannson, 1989; Smith *et al.*, 1991). According to the Beer Lambert law:

$$k = -\ln(I / I_0) / LAI \qquad (8.1)$$

Where k is extinction coefficient, I is irradiance below the canopy, and I_0 is irradiance above the canopy. Cohen (1995) reported that k was positively correlated with LAI for young apple trees. Johasson (1989) found the same results in young aspen and birch. However, Smith *et al.* (1991) reported the opposite results, that k decreased with increasing LAI.

For an individual tree, It is not so simple to use the Beer Lambert law to estimate k-values, as it would be for a continuous canopy, because the light environment for an individual tree is different. Therefore, further research work is clearly required. Although we don't know exact k-values for the four clones, we can use the process model with various k-values to make simulations.

With the results from the developed model, the net photosynthetic capacity distributed in vertically in a tree crown could be applied to estimate effects of pruning. This could be used to study and understand how pruning affects new foliage growth, crown shape change, light distribution after pruning, total tree biomass production and stem shape development. Such pruning studies would be useful for optioning productivity with higher quality wood production. For instance, EARLY Growth Model (West *et al.*, 1982) suggested that the effect of pruning on tree growth was closely related to the crown length remaining after pruning and tree stocking. This is generally true, however, Figure 8.8 shows that the proportion of photosynthetic capacity remaining after pruning is influenced not only by crown length remaining, but also by different crown shapes and foliage distributions, which changed with different clones. For example, when the trees were pruned to a relative crown height of 0.5, clone 10 retained only a proportion of 0.34 of the photosynthetic capacity; clone 6 retained 0.44. However, if the crown was assumed to be a cylinder, the tree retained 0.5 proportion of photosynthetic capacity. This result indicated that using the developed photosynthetic model to study the effect of pruning on tree growth could be more accurate if crown shape data were known.

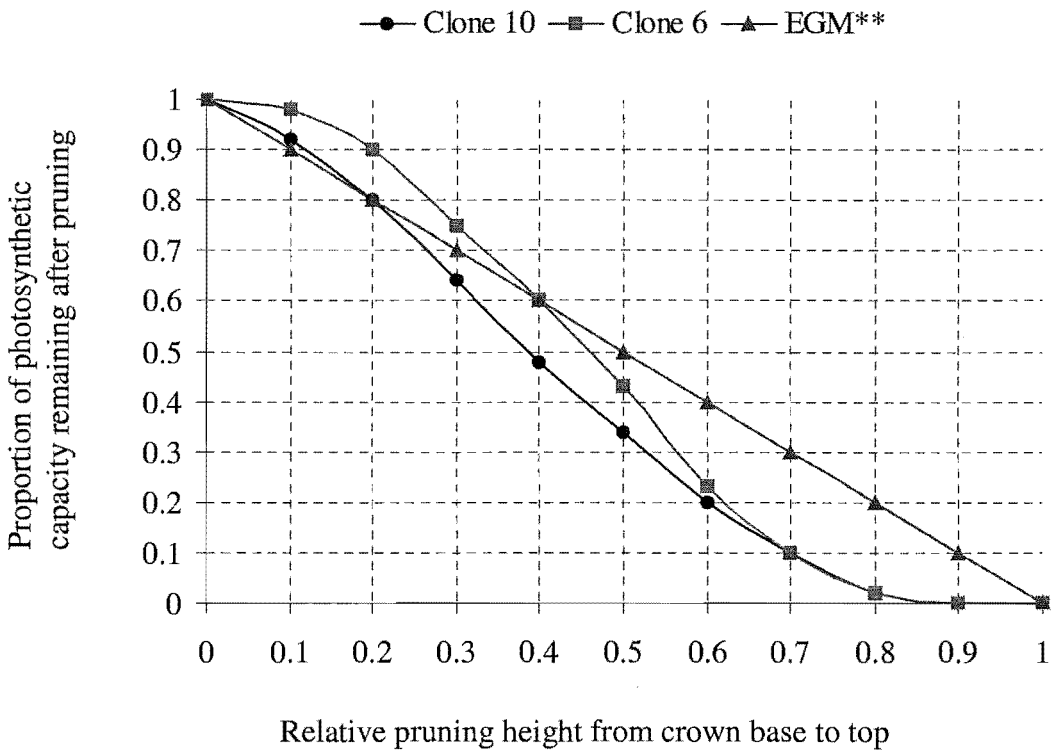

Figure 8.8 The relationship between relative pruning height and proportion of photosynthetic capacity remaining after pruning for radiata pine clones at age 5. (** EGM represents using Early Growth Model (West *et al.*, 1982) to predict proportion of photosynthetic capacity after pruning, which assumed crown as a cylinder).

Using the developed model to estimate annual yield (kg /m^2 of ground per year) in 1997, the results (in Appendix 3) showed that yield were between 2.1-3.1 (kg /m^2 of ground per year). Larcher (1980) reported that the maximal yield was 4.6 (kg /m^2 of ground per year) for *Pinus radiata* at 0.66 harvest index (harvest index = (economic yield / production yield) * 100). For juvenile clonal radiata pine stand with an open canopy, the yields could reach to 2.1-3.1 kg /m^2 of ground per year seems reasonable.

8.5.2 Conclusion

— Total net photosynthetic rates increased with increasing sun zenith angle in direct radiation.

— The increased rates of total net photosynthesis depended not only on sun zenith angle, but also on the probability of light penetration and foliage area. If the foliage received enough light, the more foliage area, the higher total net photosynthetic rates were. However, when the sun zenith angle was < 20° for the studied clones, the light penetration rate was lower, and the more foliage area, the higher respiration was.

— Total net photosynthetic rates decreased with increasing light extinction coefficient k-values. These results were mainly influenced by the light penetration probability decreased with increasing k-values.

— Decreased rates of total net photosynthesis depended not only on light penetration probability, but also on foliage area. The more foliage mass, the higher variation of total net photosynthetic rates was.

— If two clones had similar foliage area, variation of total net photosynthetic rates depended on light penetration probability, which was decided by foliage area density and crown shape.

— The trend of the variation for the total tree net photosynthesis rates in the four seasons was mainly influenced by the variation in needle photosynthetic rates with the four seasons.

— When comparing the variation of total net photosynthetic rates between clones in a given season, if the incoming light PAR was > 500 μmol $m^{-2}s^{-1}$, the total net photosynthetic rates increased with increasing foliage area and light penetration probability. However, at lower light, the compensation points for whole tree photosynthesis increased with increasing foliage area, and the more foliage mass, the less whole tree photosynthesis was.

— When two clones had similar foliage area, the compensation points for the whole tree photosynthesis were decided by the probability of light penetration, and the compensation points decreased with increasing the probability of light penetration.

— Total tree biomass was positively correlated with whole tree net photosynthesis, if tree crowns got enough light (for example, direct radiation with sun zenith angle >20°, PPFD > 500 (μmol $m^{-2}s^{-1}$) for all light, extinction coefficient $k < 0.25$).

— Having knowledge of the vertical distribution of net photosynthetic capacity in individual tree crown could be useful for evaluating pruning.

CHAPTER 9

CONCLUSIONS

The aim of this thesis was to develop a simple process model to estimate individual tree net photosynthesis for radiata pine clones at age 5 and to determine what factors mainly influenced clonal tree growth difference within the same environmental conditions.

This study concluded that there were no significant differences in needle photosynthetic capacity among the ten clones for a given needle age in similar environmental conditions, and for juvenile clonal radiata pine with an unclosed canopy. The same aged needles had equal photosynthetic capacities, even when distributed at different positions (aspect and level) in the crown. However, these results are specific to the ten radiata pine clones in this study. For other species or clones, more information of foliage photosynthetic capacity would be required for modelling individual tree photosynthesis.

Foliage nutrient analysis showed that there were no statistically significant differences among the ten clones for *N, K, B,* and *Mn.* (Appendix 1 Table 1.1-1.4). Furthermore, there were no deficiencies of N, P, K, Ca, Mg, B, Cu, Zn, and Mn. These results indicated that nutrients were not the limiting factors that caused differential tree growth among the ten clones.

The dynamic change of crown shape can be described with image analysis methods if the crown is digitally photographed over time.

Simulation showed that total net photosynthesis increased with increasing foliage area for an individual tree. This result agreed with other research (Grace, 1990; De Pury, 1997). However, if the incoming light was low, the greater the foliage mass, the greater the respiration was. Hence, total net photosynthesis was negatively correlated with foliage mass at low light levels.

The total net photosynthesis for an individual tree was determined by many factors (solar radiation (PAR), needle photosynthetic capacity, light penetration within crown and total foliage area). All the factors changed with environmental conditions. With the program developed to estimate individual tree photosynthesis, the relative importance of these factors was evaluated for given environmental conditions. Generally, if trees received enough light (PAR), the total net photosynthesis for an individual tree was positively correlated with foliage mass. Total photosynthesis was positively correlated with total biomass.

If two trees had a similar foliage mass, then total net photosynthesis for an individual tree increased with the probability of light penetration within the tree crown. For instance clone 4 and clone 6 had similar foliage mass, but clone 4 had greater crown volume (10 m^3) than clone 6 (6 m^3). Clone 4 had greater probability of light penetration than clone 6, hence, this lead to a greater photosynthesis rate at clone 4 than clone 6 in a given equivalent conditions. The probability of light penetration was determined by crown shape, foliage density, light extinction coefficient k-values and sun zenith angle.

If two clones had a similar crown shape and volume, but different foliage mass, the total biomass production would increase with foliage mass. For example, crown volume of clone 4 (10 m^3) ≅ clone 10 (9.8 m^3), but clone 10 had greater foliage mass (10 kg) than clone 4 (8 kg), simulation (Chapter 8) showed that total photosynthesis was greater for clone 10 than for clone 4 at in a given equivalent conditions.

If a tree had greater foliage mass and crown volume than other trees, the tree would grow faster than other trees. For example, clone 9 had greater foliage mass and crown volume

than other clones at the 5-year-old clonal experiments, and simulation showed that clone 9 had greater photosynthetic rates than other clones.

At the very beginning, all the planted clones had similar foliage mass and crown shape. Gradually, as time passed and the trees grew, clone 9 had a relatively greater proportion (37 %) of biomass allocation to foliage mass and more crown volume for foliage distributed within crown than other clones. The more foliage mass and greater proportion of light penetration within tree crown caused clone 9 growing gradually to over than the other clones. Comparing the proportion of foliage mass allocation, clone 6 had the greatest proportion (38%) of biomass allocation to foliage among all the studied clones. However, clone 6 had smaller crown volume for foliage distribution (higher foliage density) and lower probability of light penetration, and hence less net photosynthesis. So, the a faster growing tree should have not only greater foliage mass, but also should have greater crown volume for foliage distribution.

When the growth rate measured with DBHOB or three heights was compared, the biomass allocation proportion to different tree components needed to be considered. For example, the proportion of total above ground biomass allocated to stems was about 29% for clone 10, while it reached 43% for clone 4. The other important and unmeasured aspects affecting growth were the underground biomass and their environment conditions. Unfortunately, during this study, it was difficult to collect so much data at same time. Clearly, future research works about underground are needed.

9.1 Specific conclusions

9.1.1 Differences in growth of radiata pine clones

- Clones varied significantly in growth rate in height and DBHOB at the same site and with same field treatment. The ten clones were separated into four different growth groups according to variance of height and DBHOB. Variability in mean height ranged from 3.5 to 4.8 m, and mean DBHOB ranged from 7.3 to 10.4 cm at age 5.

- To predict initial growth in mean height, DBHOB, and GLD for the ten clones, the following equations were used:

$$H_t = H_0 + a * T^{b}$$
$$dt = a * \exp(-T) * T^{b}$$
$$GLDt = GLD_0 + a * T^{b}$$

Where H_0 = mean height after planting, T = stand age, Ht = mean height at stand age T, dt = mean diameter at breast height at stand age T, GLDt = mean groundline diameter at stand age T, GLD_0 = mean groundline diameter after planting, and a and b were estimated coefficients. Residuals lay within ± 70 cm about the estimated mean height model; distributed within ± 2 cm for the estimated mean DBHOB model; and scattered ± 1.5 cm for the estimated mean GLD model.

9.1.2 Needle photosynthesis of radiata pine clones

- Differences in growth rate among the ten radiata pine clones studied were not due to detectable differences in needle photosynthetic capacity. There were no significant differences in needle photosynthetic capacity among the ten clones for a given needle age for a given season.

- Needle photosynthetic rates decreased with needle age, but increased with increasing temperature (5°C - 20°C).

- For juvenile radiata pine with an unclosed canopy, the same aged needles had equal photosynthetic capacities, even when distributed at different positions (aspect and level) in the crown.

- Needle photosynthesis was effectively modeled with a function of the form:

$$\boldsymbol{A} = M * PPFD / (N + PPFD) - K$$

Where $\boldsymbol{A}$ = instantaneous photosynthesis, PPFD = photosynthetic photon flux density reaching the needles.

M, N, and K could be determined by the following equations in a given season:

$M = a0 + a1 * Temp + a2 * Age + a3 * VPD.$
$N = b0 + b1 * \ln (Temp) * Temp + b2 * Age + b3 * VPD.$
$K = k0 + k1 * Temp + k2 * Age + k3 * VPD.$

Where Temp = air temperatures. Age = needle ages. VPD = vapor pressure deficit. a0, a1,a2, a3, b0, b1, b2, b3, k0, k1, k2, and k3 are function parameters

Residuals about the estimated model was distributed within ±1 (μmol $m^{-2}s^{-1}$) of the model estimates.

- The proportion of photosynthetic capacity in different leaf age-classes was not constant during all seasons. One-year-old needles had the highest photosynthetic rate; the photosynthetic rate for 2-and 3-year-old needles had only 64-72% and 32-42% of that of 1-year-old needles in winter. However, the percentage reached 74-91% and 50-70% in spring.

- Winter needle photosynthetic rates (Amax) in radiata pine clones were only 47-59%, 45-46% and 27-28% of the spring rate for leaf age-classes 1, 2 and 3 respectively at temperatures of 10°C and 15°C.

9.1.3 Crown shape and volume

- A simple function was developed to characterize crown geometry (crown radius, maximum crown radius, crown volume and vertical volume distribution) for four different clones. The functions were of the forms:

— To estimate crown radii

$$R = f(x) = A \cdot \frac{(x-1)}{(D \cdot x + 1)} - B \cdot (x - C)$$

Where R is crown radius (cm), x is relative crown length ($0 \leq x \leq 1$, x = length within the crown ÷ the total crown length), and A, B, C and D are regression coefficients.

— To estimate maximum crown radius:

$$X_{max} = \frac{\sqrt{\frac{A \cdot (D+1)}{B}} - 1}{D}$$

Where X_{max} is the value of relative crown length when crown radius reaches its maximum.

— To estimate crown base radius

$$R_{base} = B * C - A$$

Where R_{base} is crown base radius (cm).

— To estimate the crown volume from crown base to any height (i)

$$V_i = L \cdot \pi \cdot \int_0^{x_i} R^2 dx = L \cdot \pi \cdot \int_0^{x_i} [f(x)]^2 dx = L \cdot \pi \cdot \left[\int_0^{x_i} A \cdot \frac{(x-1)}{(D \cdot x+1)} - B \cdot (x-C) \right]^2 dx$$

Where L = Tree Crown Length. Li = Any Crown Length from the crown base. xi = Li/ L, relative crown length (0 <= xi <= 1). Vi = Any vertical crown volume (cm^3) from crown base to the crown length Li.

— To estimate the crown total volume from crown base to top

$$V_{Total} = L \cdot \pi \int_0^1 R^2 dx = L \cdot \pi \cdot \int_0^1 [f(x)]^2 dx = L \cdot \pi \cdot \left[\int_0^1 A \cdot \frac{(x-1)}{(D \cdot x+1)} - B \cdot (x-C) \right]^2 dx$$

Where V_{total} = total tree crown volume (cm^3).

9.1.4 Above-ground biomass and its allocation

- Higher rates of tree height and stem diameter growth were not only due to higher biomass production rates, but also due to different above ground biomass allocation into tree components. The proportions of total above ground biomass allocated to stems ranged from 29% (clone 10) to 43% (clone 4).

- Needle biomass, branch biomass, total tree biomass, and total needle surface areas were poorly correlated with tree height (H). But they all showed strong positive linear relationships with DBHOB.

- There were significant differences among the clones in total foliage biomass allocation to different aged foliage. The proportions of total foliage biomass allocated to foliage at age 1 were 45% for clone 6, 40-41% for clone 4 and clone 9, and 35% for clone 10%.

- A simple model to estimate branch biomass and needle biomass was developed at branch level with independent variables including branch base diameter (cm), branch length (cm), branch age (1-3 year), sub-branch numbers, average sub-branch base diameter (cm), and average sub-branch length (cm). Branch biomass and needle biomass were positively correlated with branch base diameter, branch length, and sub-branch numbers

9.1.5 Light penetration within tree crowns

- The probability of direct beam penetration increased with sun zenith angle within individual tree crowns at a given k value (crown light extinction coefficient), and all the four clones showed the same trends.

- Comparing the probability of light (include direct light and diffuse light) penetration between clones, the probability of light penetration not only depended on foliage density (decreasing with increasing foliage density), but also on light penetration distance, which was decided by crown shape.

- If it was assumed that light penetration in tree crowns followed the Beer-Lambert Law, simulations showed that light (direct light or diffuse light) penetration probability depended not only on foliage density (m^{-2}/m^{-3}) and light penetration distance (m), but also on crown light extinction coefficient (k). The probability of light penetration decreased with increasing k value.

- A simple light penetration program was developed for individual juvenile radiata pine clones. The program can be used to estimate the probability of direct light penetration at any given sun zenith angle and diffuse light penetration at any given aspect with azimuth angle $\angle\theta$ and elevation angle $\angle\beta$. The program is based on the data from crown architecture analysis, geometrical analysis of the light penetration distance

within crown and crown shape model. The program is one of the basic parts of a whole tree photosynthesis model.

9.1.6 Simulation of whole tree photosynthesis

- Total net photosynthetic rates increased with increasing sun zenith angle in direct radiation for the individual clonal trees.

- Comparing the variation of total net photosynthetic rates between clones, the increased rates of total net photosynthesis depended not only on sun zenith angle, but also on the probability of light penetration and foliage area. If the foliage received enough light, the higher foliage area was, the higher total net photosynthetic rates were. However, when the sun zenith angle was <20° for the studied clones, the light penetration rate was lower, and more foliage meant higher respiration, and lower net photosynthetic rates with more foliage mass.

- Total net photosynthetic rates decreased with increasing light extinction coefficient k-values. These results were mainly influenced by the light penetration probability decreasing with increasing k-values.

- Comparing the variation of total net photosynthetic rates between clones, the decreased rates of total net photosynthesis depended not only on light penetration probability, but also on foliage area. The more foliage mass was, the higher total net photosynthetic rates were.

- If two clones had similar foliage areas, the variation of total net photosynthetic rates depended on light penetration probability, which was decided by foliage area density and crown shape.

- The trend of the variation for the individual tree net photosynthesis rates in the four seasons was mainly decided by changes in needle photosynthetic rates in the four seasons.

- When comparing the variation of individual tree net photosynthetic rates between clones at a given season, if the incoming light PPFD > 500 (μmol $m^{-2}s^{-1}$), then individual tree net photosynthetic rates increased with increasing foliage area and light penetration probability. However, at lower light, the compensation points for individual tree net photosynthesis increased with increasing foliage area, and the more foliage mass was, the less individual tree photosynthesis would be.

- When two clones had similar foliage area, the compensation points for individual tree photosynthesis were decided by the probability of light penetration, and the compensation points decreased with increasing probability of light penetration.

- Total tree biomass was positively correlated with whole a tree net photosynthesis if tree crowns got enough light (for example, direct radiation with sun zenith angle >20°, PPFD > 500 (μmol $m^{-2}s^{-1}$) for all light (PPFD), extinction coefficient k <= 0.25).

- Clone 9 had greater foliage mass and larger crown volume than other clones which suggests that clone 9 had a greater proportional increase in whole tree net photosynthesis rate compared with other clones at a given condition. This may help explain observed field behavior where clone 9 grows well relative to other clones. However, the higher growth rate measured with height and DBHOB were determined not only by total net photosynthetic rate, but also by biomass allocation to stem. For example, clone 4 had less foliage mass than clone 10, and the total net photosynthesis was lower than that in clone 10. Nevertheless, clone 4 had higher biomass allocation to stem (43%) than that in clone 10 (29%), hence, the observed field measurement of height and DBHOB in clone 4 was greater than that in clone 10. Consequently, total tree biomass production was decided by the total photosynthetic rates which were

influenced by foliage mass and crown shape. However, the stem height and DBHOB determined not only by total biomass, but also by biomass allocation.

9.2 Future research

The following possibilities for future research originate from this thesis:

— Light extinction coefficient k-values were assumed in the light transfer model to estimate light penetration within crowns, yet future research work is required to define the dynamic response of k-values to individual tree crown structure and incoming light.

— Crown shape is an important parameter for estimating foliage density and light (PPFD) penetration within tree crowns. Crown shape could be described by using image analysis. With rapidly developing digital image techniques, image analysis could bring us a lot of information, so using digital camera records of crown shape from planting time and collections of image data annually will be very useful for analyzing crown dynamic change with time.

— Biomass was allocated differently into tree components for different clones. Additional research is required to determine the causes or what factors were correlated with the different biomass allocations.

— Most of light penetration models developed follow the Beer-Lambert Law, and the mainly difference among the models is that foliage area density is assumed to be uniform at different levels. The more detailed the level is, the more specific crown architecture information was to be. An evaluation of effects of resolution of crown models is required.

— The development of a process-level model has many advantages. However, in this study it was based on only ten radiata pine clones. If a model is needed to be applied to a larger range or a deeper level, clearly future research is required. For example, if the

model is required to be used on other clones or species, specific detailed information is necessary, such as foliage photosynthetic rates, foliage area and foliage density, crown shape and light penetration.

— Further monitoring of the experiment will provide a validation of the relative differences in productivity between clones suggested by this study.

REFERENCE

Aber, J.D., Federer, C. A., 1992. A generalized, lumped-parameter model of photosynthesis, evapotranspiration and net primary production in temperate and boreal forest ecosystems. Oecologia 92, 463-474.

Allen, L.H., 1974. A model of light penetration in a wide row crop. Agronomy Journal 66: 41-47.

Allen, L.H., Yocum, C.S., Lemon, E.R., 1964. Photosynthetic under field conditions. VII. Radiant energy exchanges within a corn crop canopy and implications in water use efficiency. Agron. J., 56: 253-258.

Ammer, C., Krotz, G., 1997. Ecological light measurement in forests using the light degradation effect in hydrogenated amorphous silicon (a-Si:H). Annales des Sciences Forestieres. 54: 6, 539-552.

Amthor, J.S., 1994. Scaling CO2-photosynthesis relatonships from the leaf to the canopy. Photosynthesis Research. 39,321-350.

Andrienu, B., Ivanov, N., Boissard, P., 1995. Simulation of light interception from a maize canopy model constructed by stereo plotting. Agric. For. Meteorol. 75, 103-119.

Aries, F., Prevot, L., Monestiez, P., 1993. Geometrical canopy modelling in radiation simulation studies. In: Vralet-Granche, C., Bonhomme, R., Sinoquet, H. (Eds), Crop Structure and Light Microclimate. Characterization and Applicatons. INRA edn., Science update, Paris, pp. 159-173.

Arkebauer, T.J., Weiss, A., Sinclair, T.R., Blum, A., 1994. Discussion: in defense of radiation use efficiency: a response to Demetriades-Shah et al. (1992). Agric. For. Meteorol. 68, 221-227.

Azam-Ali, S. N., Crout, N.M.J., Bradley, R.G., 1994. Perpectives in modelling resource capture by crops. In: Monteith, J.L., Scott, R.K., Unsworth, M.H.(Eds.), Resource Capture by Crops. Univ. Press, Nottingham, pp. 125-148.

Baker, T.G., Attiwill, P.M., Stewart, H. T. L., 1984. Biomass equations for *Pinus radiata* in Gippsland, Victoria. N.Z.J.For.Sci.., 14(1):89-96

Baldwin, V.C., Peterson, K. D., 1997. Predicting the crown shape of loblolly pine trees. Can. J. For. Res. 27: 102-107.

Ballard, R., Will, G.M., 1981. Accumulation of organic matter and mineral nutrients under a *Piuns radiata* stand. New Zealand Journal of forestry Science. 11(2):145-151.

Bandra, G.D., 1997. Ecophysiology of clonal and seedling trees of *Pinus radiata* D. Don in an agroforestry. Lincolin University, New Zealand. Ph.D thesis.

Barnes, B.V., Zak, D.R., Denton, S.R., Spurr, S.H., 1998. Forest ecology. New York.

Bartelink, H.H., 1996. Allometric relationships on biomass and needle area of Douglas-fir. Forest Ecology and Management 86: 193-203.

Bassow, S.L., Bazzaz, F.A.,1998. How environmental conditions affect canopy leaf-level photosynthesis in fourdeciduous tree species. Ecology. 79: 8, 2660-2675.

Beets, P., 1977. Determination of the fascicle surface area for *Pinus radiata.* N.Z. J. For. Sci. 7: 397-407.

Beets, P.N., Madgwick, H.A.I., 1988. Above-ground dry matter and nutrient content of Pinus radiata as affected by lupin, fertiliser, thinning and stand age, N.Z.J.For.Sci., 18(1):43-64.

Beets, P.N., Pollock, D.S., 1987. Accumulation and partitioning of dry matter in Pinus radiata as related to stand age and thinning. N.Z.J.For.Sci., 17(2/3):246-271.

Begue, A., Hanan, N.P., Prince, S.D., 1994. Radiative transfer in shrub savanna sites in Niger: preliminary results from HAPEX-Sahel. 2. Photosynthetically active radiation interception of the woody layer. Agricultural-and-Forest-Meteorology. 69: 3-4, 247-266.

Benecke, U., 1979. Surface area of needles in *Pinus radiata*-variation with respect to age and crown position. N. .Z. J. For. Sci. 9(3):267-271.

Benecke, U., 1980. Photosynthesis and transpiration of *Pinus radiata* D. Don under natural conditions in a forest stand. Oecologia. 44: 2, 192-198.

Biging, G.S., Dobbertin, M., 1992. A comparison of distance-dependent competition measures for light and basal area growth of individual conifer trees. For. Sci. 38, 695-720.

Biging, G.S., Wensel, L.C., 1990. Estimation of crown form for six conifer species of northern California. Can. J. For. Res. 20: 1137-1142.

Bollmann, M.P., Sweet. G.B., 1976. Bud morphogenesis of *Pinus radiata* in New Zealand. 1. The initiation and extension of the leading shoot of one clone at two sites. N.Z.J.For.Sci. 6:376-392.

Bonan, G.B., 1991a. A biophysical surface energy budget analysis of soil temperature in the boreal forest of interior Alaska. Water Resour. res. 27,767-781.

Bonan, G.B., 1991b. Atmosphere-biosphere exchange of carbon dioxide in boreal forests.J.Geophys. Res. 96,7301-7312.

Brix, H., Mitchel, A., 1983. Thinning and fertilization effects on sapwood development and relationships of foliage quantity to sapwood area and basal area in Douglas-fir. Can. J. For.Res. 13, 384-389.

Brown, P.S., Pandolfo, J.P., 1969. An equivalent-obstacle model for the computation of radiative fux in obstructed layers Agric. Meteorol. 6, 407-421.

Brown, R.D., O'Neill, S.P.T., Gillespie, T.J., 1994. An evaluation of the solar radiant environment in the shade of deciduous trees. Arboricultural Journal. 18: 2, 193-204.

Brunner, A., 1998 A light model for spatially explicit forest stand models.For. Ecol. Manage. 107: 19-46.

Burke, I.C., Yonker, C.M., Parton, W.J., Cole, C.V., Flach, K., Schimel, D.S., 1989. Texture, climate, and cultivation effects on soil organic mater content in U.S. grassland soils. Soil Sci. Soc.Am. J. 53,800-805.

Campbell, G. S., Norman, J. M., 1989. The description and measurement of plant canopy structure. In: G. Russell, B. marshall, and P. G. Jarvis (Eds), Plant canopies: their Growth, form and function. Cambridge University Press, Cambridge, pp. 1-20.

Campbell, G. S., Norman, J. M., 1998, An introduction to environmental biophysics. Second edition, New York, p 254-255.

Cannell, M. G. R., 1978. Improving per hectare forest productivity. p. 120-148 in Proc 5th N.Am. For. Biol. Works, Hollis, C.A., and A.E.Squillace (Eds).

Cannell, M.G.R., Grace, J., 1993. Competition for light: detection, measurement, and quantification. Can. J. For. Res. 23: 1969-1979.

Cannell, M.G.R., Milne, R., Sheppard, L.J., Unsworth, M.H., 1987. Radiation interception and productivity of willow. J.Appl. Ecol.24, 261-268

Carson, M.J., 1986a. Advantages of clonal forestry for *Pinus radiata*--real or Imagined? N. Z. J. For. Sci. 16, 3: 403-415.

Castro, F. de., Fetcher, N., 1998. Three dimensional model of the interception of light by a canopy. Agricultural-and-Forest-Meteorology. 90: 3, 215-233.

Cescatti, A., 1997. Modelling the radiative transfer in discontinuous canopies of asymmetric crowns. I. model structure and algorithms. Ecological Modelling. 100: 2-3, 263-274.

Cescatti, A., 1997. Modelling the radiative transfer in discontinuous canopies of asymmetric crowns. II. Model testing and application in a Norway spruce stand. Ecological-Modelling. 100: 2-3, 275-284.

Ceulemans,R., Stettler, R.F., Hinckley, T.M., Isebrands, J.G., Heilman, P.E., Dickson, R.E., 1990. Crown architecture of *Populus* clones as determined by branch orientation and branch characteristics. Tree Physiol. 7: 1-4, 157-167.

Charles-Edwards, D. A., and Thornley, J. H. M., 1974. Light interception by an isolated plant. Ann. Bot., 37: 919-928.

Chen, H.Y.H., Klinka, K., 1997. Light availability and photosynthesis of *Peudotsuga menziesii* seedlings grown in the open and in the forest understory. Tree Physiol. 17, 23-29.

Chen, S.G., Celulemans, R., Impens, I., 1994. A fractal based *Populus* canopy structure model for the calculation of light interception. For. Ecol. Manage. 69: 97-110.

Clinton, P.W., Mead, D.J., 1990. Competition between pine and pasture: An Agroforestry study. Proc.of the A.F.D.I. Biennial conference, Australia. Dept. of Conservation and Land Management, pp. 145-154.

Cown, D. J., 1992. New Zealand Radiata Pine and Douglas-Fir. FRI Bulletin 168.

Crowe, A., Alan, C., 1969. Mathematics for Biologists. Academic Press, New York, 109pp

Day, T. A., Heckathorn S. A., DeLucia, E. H., 1991. Limitations of photosynthesis in *Pinus taeda* L. (loblolly pine) at low soil temperatures. Plant Physiol. 96: 1246-1254.

De Pury, D.G.G., Farquhar, G. D., 1997. Simple scaling of photosynthesis from leaves to canopies without the errors of big-leaf models. Plant, Cell and Environment. 20, 537-557.

De Reffye, P., Houllier, F., Blaise, F., Barthelemy, D., Dauzat, J., Auclair, D., 1995. A model simulating above- and below- ground tree architecture with agroforestry applications. Agro-for. Syst. 30,175-179.

De Wit, c. T., 1965. Photosynthesis of leaf canopies. Agric. Res. Eep. No. 663. Pudoc, Wageningen.

DeLucia, E. H., 1986. Effect of low root temperature on net photosynthesis, stomatal conductance and carbohydrate concentration in Engelmann spruce (*Picea engelmannii* Parry ex Engelm.) seedlings. Tree Physoil. 2:143-154.

Demetriades-Shad, T.H., Fuchs, M., Kanemasu,e. T., Flitcroft, I.D., 1994. Discussion: further discussions on the relationship between cumulated intercepted solar radiation and crop growth. Agric. For. Meteorol. 68, 231-242.

Dewer, R. C., 1993. A root-shoot partitioning model based on carbon-nitrogen-water interaction and Munch phloem flow. Funct. Ecol. 7:356-368.

Dirr, M. A., 1990. Manual of woody landscape plants- heir identification, ornamental, characteristics, culture, propagation and uses. 4th ed. Stepes Publishing Company, Champaign, Ill.

Erbs, D.G., Klein, S.A., Duffie, J.A., 1982. Estimation of the diffuse radiation fraction for hourly, daily and monthly average global radiation. Sol. Energy, 28:293-302.

Evans, L. T., 1975. The physiological basis of crop yield. Crop Physiology. Cambrdge University Press. pp.327-355.

Evens, J., 1989. Photosynthesis and nitrogen relationships in leaves of C3 plants. Oecologia. 78, 9-19.

Farquhar, G. D., 1989. Models of integrated photosynthesis of cells and leaves Philosophical Transactions of the Royal Society of London. Series B. Biological Sciences 323, 357-367.

Farquhar, G.D., Von Caemmerer, S., 1982. Modelling of photosynthetic response to environmental conditions. In "Physiological Plant Eccology II. Water Relations and Carbon Assi,ilation" (O.L. Lange, P.S. Nobel, C.B.Osmond, and H.Ziegler, Eds.), pp. 549-588. Springer-Verlag, Berlin.

Field, C., 1983. Allocating leaf nitrogen for the maximization of carbon gain: Leaf age as a control on the allocation program. Oecologia, 56, 341-347.

Field, J. F., 1934. Experimental growing of insignias pine from slips. New Zealand Journal of Forestry. 3:185-186.

Flint, S.D., Caldwell, M. M., 1998. Solar UV-B and visible radiation in tropical forest gaps: measurements partitioning direct and diffuse radiation. Global Change Biology. 4: 8, 863-870.

Fournier, R. A., Landry, R., August, N. M., Fedosejevs, G., Gauthier, R. P., 1996. Modelling light obstruction in three conifer forests using hemispherical photography and fine architecture. Agric. For. Meteorol. 82, 47-72.

Fournier, R., Rich, P.M., Alger, Y. R., Peterson, V. L., Landry, R., August, N. M., 1995. Canopy architecture of boreal forest: links between remote sensing and ecology. Am. Soc. Photogram. Remote Sensing, Tech. Pap. 2, 225-235.

Gates, D. M., 1965. Radiant energy, its receipt and diaposal. Meteorol. Monogr., 6: 1-26.

Gendron, F., Messier, C., Comeau, P. G., 1998. Comparison of various methods for estimating the mean growing season percent photosynthetic photon flux density in forests. Agricultural and Forest Meteorology. 92: 1, 55-70.

Gholz, H. L., 1982. Environmental limits on above-ground net primary production, leaf area, and biomass in vegetation zones of the Pacific Northwest. Ecology, 63: 469-481.

Gholz, H. L., Vogel, S. A., Cropper, W. P. Jr., McKelveu. K., Ewel;. K. C., Teskey, R.O., Curran, P.G., 1991. Dynamics of canopy structure and light interception in *Pinus elliottii* stands, north Florida. Ecol. Monog. 61:33-51.

Givnish, T. J., 1986. Optimal stomatal conductance, allocation of energy between leaves and roots and the marginal cost of transpiration. In: On the Economy of Plant Form and Function. Ed. T.J. Givnish. Cambridge University Press, Cambridge, pp171-213.

Golser, M., Hasenauer, H., 1996. Height growth development of Norway spruce, fir and common beech regeneration in uneven-aged mixed species stands. In: Skovsgaard, J.P., Johannsen, V. K. (Eds.), Modelling Regeneration Success and Early Growth of Forest Stands. Proc. IUFRO Conf. Copenhagen, June 1996, Danish Forest and Landscape Research institute, pp.493-503.

Golser, M., Hasenauer, H., 1997. Predicting juvenile tree height growth in uneven-aged mined species stands in Austria. For. Ecol. Manage., 97: 2, 133-146; 43.

Goudriaan, J., 1977. Crop micrometeorology- a simulation study. Centre for Agriculture publishing and Documentation, Wageningen.

Gower, S.T., Haynes, B.E., Fassnacht, K. S., Running, S. W., Hunt, E. R., 1993a. Influence of fertilization on the allometric relations for two pines in contrasting environments. Can. J. For. Res.23, 1704-1711.

Grace, J. C., Rook, D. A., Lane, P. M., 1987. Modelling canopy photosynthesis in *Pinus radiata* stands. N. Z. J. For. Sci. 17(2/3): 210-228.

Grace, J.C., 1990. Modelling the interception of solar radiant energy and net photosynthesis. In: Dixon, R.K., Meldahl, G.A., Ruark, G.A., Warren, W.G.(Eds.), Process Modelling of Forest Growth Responses to Environmental Stress. Timber Press, Portland, OR, pp. 142-158.

Grace, J.C., Jarvis, P. G., Norman, J. M., 1987 a. Modelling the interception of solar radiant energy in intensively managed forests. N. Z. J. For. Sci. 17: 193-209.

Grace, J.C., Rook, D. A., Lane, P.M., 1987b. Modelling canopy photosynthesis in *Pinus radiata* stands. N. Z. J. For. Sci. 17: 210-228.

Grier, C. C., Lee, K.M., Archibald, R. M., 1985. Effect of urea fertilization on allometric relations in young Douglas-fir trees. Can. J. For. Res. 15,900-904.

Groninger, J. W., Seiler, J. R., Peterson, J. A., Kreh, R. E., 1996. Growth and photosynthetic responses of four Virginia Piedmont tree species to shade. Tree Physiol. 16: 773-778.

Hanson, P.J., McLaughlin, S.B., Edwards, N.T., 1988. Net CO2 exchange of *Pinus taeda* shoots exposed to variable ozone levels and rain chemistries in field and laboratory settings. Physiologia Plantarum. 74: 4, 635-642.

Harley, P.C., Baldocchi, D. D., 1995. Scaling carbon dioxide and water vapour exchange from leaf to canopy in a deciduous forest. I. Leaf model parameterization. Plant, cell and Environment. 18, 1146-1156.

Harley, P.C., Weber, J. A., Gates, D. M., 1985. Interactive effects of light, leaf temperature, CO_2 and O_2 on photosynthesis in soybean. Planta, 165, 249-263.

Haxeltine, A., Prentice, I. C., 1996. A general model for the light-use efficiency of primary production. Funct. Ecol. 10, 551-561.

Henson, I.E., 1998. Notes on oil palm productivity. II. An empirical model of canopy photosynthesis based on radiation and atmospheric vapour pressure deficit. Journal of Oil Palm Research. 10: 2, 25-28.

Hirose T., Werger M. J. A., 1987. Maximizing daily canopy photosynthesis with respect to the leaf nitrogen allocation patterns in the canopy. Oecologia. 72, 520-526.

Hollinger, D.Y., 1992. Leaf and simulated whole-canopy photosynthesis in two co-occurring tree species. Ecology. 73: 1, 1-14.

Hom, J. L., Oechel. W. C., 1983. The photosynthetic capacity, nutrient content and nutrient use efficiency of different needle age classes of black spruce (*Picea mariana*) found in interior Alaska. Can. J. For. Res. 13,834-839.

Honer, T.G., 1971. Crown shape in open- and forest-grown balsam fir and black spruce. Can. J. For. Res. 1: 203-207.

Iqbal, M., 1983. Introduction to Solar Radiation. Academin Press Toronto, 164pp.

Jack, S.B., Long, J.N., 1992. Forest production and the organization of foliage within crowns and canopies. For. Ecol. Manage.49, 233-245.

Jackson, J.E., Palmer, J.W., 1979. A simple model of light transmission and interception by discontinuous canopies. Ann. Bot. 44, 381-383.

Jackson, J.E., Palmer, J.W.,1972. Interception of light by model hedgerow orchards in relation to latitude, time of year and hedgerow configuration and orientation. J.Appl. Ecol. 9. 341-358.

Jaeger, M., De Reffye, P., 1992. Basic concepts of computer simulation of plant growth. J. Biosci. 17.275-291.

Jarvis, P. G., Standford, A. P., 1986. Temperate Forest. in :N.R. Baker and S.P. Long (Editer), Photosynthesis in contracting environments. Elsevier, Amsterdam. pp. 189-236.

Jarvis, P.G., Leverenz. J. W., 1983. Productivity of temperate, deciduous and evergreen forest. In: Lange, O. L., p.S. Nobel, C. B. Osmond, and H. Ziegler, eds. Encyclopedia of Plant Physiology, New Series, Vol. 12d. Physiological Plant Ecology. Springer-Berlag, Berlin, F.R.G. pp. 234-280

Jarvis, P.G.,Wang, Y.P., Borralho, N.M.G., Pereira, J. S., 1989. Simulation of the role of stress on radiation absorption, assimilation, transpiration and water use efficiency of stands of *Eucalyptus globulus*. In Biomass Production by Fast-Growing Trees. Eds. J.S. Pereira and Landsberg, J.J. Kluwer Academic Publishers, Dordrecht, The Netherlands, pp169-179.

Johnson, J. D., 1984. A rapid technique for estimating total surface area of pine needles. Forest Sci., Vol. 30, No. 4: 913-921.

Kaiyun,W., Kellomaki, S., Laitinen, K., 1995. Effects of needle age, long-term temperature and CO_2 treatments on the photosynthesis of Scots pine. Tree Physiol. 15: 211-218.

Karnosky, D.F., Dickson, R. E., Gagnon, Z. E., Coleman, M.D., Pechter, P., Isebrands, J. G., 1993. Genetic variability in ozone response of trees: indicators of sensitivity. Agricoltura-Ricerca. 15:146, 16-17.

Kellomaki, S., Strandman, H., 1995. A model for the structural growth of young Scots pine crowns based on light interception by shoots. Ecol. Model. 80,237-250.

Kellomaki, S., Oker-Blom, P., Kuuluvainen, T., 1985. The effect of crown and canopy structure on light absorption and distribution in a tree stand. In crop Physiology of Forest trees. Eds. P. M.A. Tigrtstedt, P. Puttonen and V. Koski. Univ. Press, Helsinki, pp 107-115.

Kerner, H., Gross, E., Koch, W., 1977. Structure of the assimilation system of a dominating spruce tree (*Picea abies* (L.) Kurst.) of closed stand: computation of needle surface area by means of a variable geometric needle model. Flora. 166: 449-459.

Kiniry, J. R., 1994. Discussion: a note of caution concerning the paper by Demetirades-Shah et al. (1992). Agric. For. Meteorol. 69, 229-230.

Kira, T., Shinozaki, K., Hozumi, K., 1969. Structure of forest canopies as related to their primary productivity. Plant Cell Physiol., 10: 129-142.

Kitajima, K., Mulkey, S. S., Wright, S. J., 1997. Decline of photosynthetic capacity with leaf age in relation to leaf longevities for five tropical canopy tree species. American Journal of Botany. 84: 5, 702-708.

Koop, H., Sterck, F. J., 1994. Light penetration through structurally complex forest canopies: an example of a lowland tropical rainforest. For. Ecol. Manage. 69, 111-122.

Kozlowski, T. T., Pallardy, S. G., 1997. Physiology of woody plants. Academic Press, New York, 128 p.

Krajicek, J. E., Brinkman, K. A., Gingrich, S. F., 1961. Crown competition- a measure of density. Forest Sci. 7(1), 35-42.

Kubiske, M. E., Pregitzer. K. S., 1996. Effects of elevated CO2 and light availability on the photosynthetic light response of contrasting shade tolerance. Tree Physiol. 16: 351-358.

Kull, O., Kruijt, B., 1998. Leaf photosynthetic light response: a mechanistic model for scaling photosynthesis to leaves and canopies. Functional-Ecology. 12: 5, 767-777.

Kull, O., Kruijt, B., 1999. Acclimation of photosynthesis to light: a mechanistic approach. Functional-Ecology. 13: 1, 24-36.

Kurth, W., 1994. Morphological models of plant growth: possibilities and ecological relevance. Ecol. Model. 75/76,299-308.

Kuuluvianen, T., Pukkala, T., 1987. Effect of crown and tree distribution on the spatial distribution of shade. Agrec. For. Meteorol. 40:215-231.

Kvet, J., Marshall, J.K., 1971. Assessment of leaf area and other assimilating plant surfaces. In Plant photosynthetic production manual of methods (Z. Sestak, H. Catsky, and P. G. Jarves, eds), p 517-555. Dr. W. Junk N. V. Publishers, The Hague.

Landsberg, J. J., Gower, S. T., 1997. Applications of physiological ecology to forest management. Academic Press,San Diego.

Larcher, W., 1980. Physiological plant ecology. Springer-Verlag Berlin pp 102

Lemeur, R., 1973. A method for simulating the direct solar radiation regime in sunflower, Jerusalem artichoke, corn and soybean canopies using actual stand structure data. Agricultural Meteorology 12: 229-247.

Lemeur, R., Blad, B. L., 1974. A critical review of light models for estimating the shortwave radiation regime of plant canopies. Agricultural Meteorology 14: 255-286.

Leuning, R., 1990. Modelling stomatal behavior and photosynthesis of *Eucalyptus grandis*. Aust. J. plant. Physiol. 17, 159-175.

Leuning, R., 1995. A critical appraisal of a combined stomatal-photosynthesis model for C_3 plants. Plant Cell Environ. 18, 339-355.

Libby, W. J., Rauter, R. M., 1984. Advantages of clonal forestry. The Forestry Chronicle 60(3):145-149.

Linder, S., 1985. Potential and actual production in Australian forest stands. In " Research for Forest Management" (J.J. Landsberg and W.Parsons, Ed.), pp. 11-35. CSIRO,Melbourne.

Linder, S., Rook, D. A., 1984. Effects of mineral nutrition on carbon dioxide and partitioning of carbon in trees. In "Nutrition of Plantation Forests" (G.D.Bowen and E.K.S.Nambiar, Eds.), pp211-236. Academic Press, London.

Lloyd, J., Grace, J., Miranda, A. C., Meir, P., Wong, S.C., Miranda, H.S., Wright, I.R., Gash, J.H.C., McIntyre, J., 1995 A simple calibrated model of Amazon rainforest productivity based on leaf biochemical properties. Plant, cell and Environment 18,1129-1145.

Luo, Y., Field, C. B., Mooney, H. A., 1994. Predicting responses of photosynthesis and root fraction to elevated CO_2 a: interactions among carbon, nitrogen and growth. Plant Cell Environ. 17:1195-1204.

Maclaren, J. P., 1993. Radiata pine growers' manual. FRI bulletin. No. 184.

Madgwick, H. A. I., 1983. Difference in growth and weight of genotypes of pine with special reference to clones of *Pinus radiata*. N. Z. J. For. Sci.,13 (2):115-124.

Madgwick, H.A.I., 1964. Estimation of surface area of pine needles with special reference to *Pinus resinosa*. J. For. 62:636.

Man R.Z., Lieffers, V. J., 1997. Seasonal photosynthetic responses to light and temperature in white spruce (*Picea glauca*) seedlings planted under an aspen (*Populus tremuloides*) canopy and in the open. Tree Physiology. 17: 437-444.

Mann, J. E., Curry, G. L., DeMichele, C. W., Baker, D. N., 1980. Light penetration in a row-crop with random plant spacing. Agron.J.72,131-139.

Mann, J. E., Curry, G. L., Sharpe, P. J. H., 1979. Light interception by isolated plants. Agric. Meteorol. 20, 205-214.

Mason, E. G., Whyte, A. G. D., 1997. Modelling Initial Survival and Growth of Radiata Pine in New Zealand. 255, ACTA FORESTALIA FENNICA.

Matsue,K., Iwagami, S., Yamamoto, T., Shibayama, Z., 1999. Modelling crown form of hinoki (Chamaecyparis obtusa) based on branch measurement. Journal of Forest Planning. 5: 1, 13-18.

Mawson, J. C., Thomas, J.W., DeGraaf, R.M., 1976. Program HTVOL. The determination of tree crown volume by layers. USDA For. Serv. Res. Pap. NE-354.

McCracken, I. J., 1980. Mountain climate in the Craigieburn range, New Zealand. Mountain environments and subalpine tree growth. p 41-60.

McGann, R.P., 1983. The Climate of Christchurch. New Zealand Meteorological service. Wellington, New Zealand.

McCrady, R. L., Jokela, E. J., 1998. Canopy dynamics, light interception, and radiation use efficiency of selected loblolly pine families. For. Sci. 44(1): 64-72.

McIntyre, B. M., School, M. A., Sigmon, J. T., 1990. A quantitative description of a deciduous forest canopy using a photographic technique. For. Sci., 36: 381-393.

McIntyre, B.D., Riha, S. J., Ong, C. K., 1996. Light interception and evapotranspiration in hedgerow agroforestry systems. Agricultural-and-Forest-Meteorology. 81: 1-2, 31-40;

Mckeabdm S., 1981. Loblolly pine tissue culture: present and future uses in southern forestry. North Carolina State University, School of Forest Resources, Technical report No.64.

McKelvey, K. S., 1990. Modelling light penetration through a slash pine (*Pinus elliottii*) canopy. Ph.D. Diss., Univ. Florida.

McMurtrie, R. E., Comins, H. N., Kirschbaum, M. U. F., Wang, Y. P., 1992a. Modifying existing forest growth models to take account of effects of elevated CO_2. Aust. J. Bot. 40, 657-677.

McMurtrie, R. E., Gholz, H. L., Linder, S., Gower, S.T., 1994. Climatic factors controlling the productivity of pine stands: a model-based analysis. Ecol. Bull. (Copenhagen) 43, 173-188.

McMurtrie, R. E., Rook, D.A., Kelliher, F. M., 1990. Modelling the yield of *Pinus radiata* on a site limited by water and nutrition. For.Ecol. Manage. 30,381-413.

McMurtrie, R. E., Wolf, L. J., 1983. Above-and below-ground growth of forest stands: A carbon budget model. Ann. Bot. 52, 437-448

McMurtrie, R.E., Wang, Y.P., 1993 Mathematical models of the photosynthetic response of plant stands to rising CO2 levels and temperatures. Plant Cell Environ, 16, 1-13.

Mebrahtu, T., Hanover, J. W., 1991. Leaf age effects on photosynthesis and stomatal conductance of black locust seedlings. Photosynthetica. 25(4): 537-544.

Monsi, M., Saeki, T., 1953. Uber den Lichtfaktor in den Pflanzengesellschaften und seine Bedeutung fur die Stoff pridyction. Jap. J.Bot. 14:22-52

Monsi, M., Uchijima, Z., Oikawa, Y., 1973. Structure of foliage canopies and photosynthesis. Annual Rev. Ecol. Systematica, 4: 301-327.

Monteith, J. L., 1973. Principles of environmental physics. Elsevier, New York, NY, 241pp.

Monteith, J. L., 1977. Climate and the efficiency of crop production in Britain. Phil. Trans. R. Soc. London, 277-294.

Monteith, J. L., 1994. Discussion: validity of the correlation between intercepted radiation and biomass. Agric. For. Meteorol. 68, 213-220.

Monthly Climate Table 1988-1992, New Zealand Meterological Service.

Morris, R. F., 1955. The development of sampling techniques for forest insect defoliators with particular reference to the spruce budworm. Can.J.Zool. 33(4), 226-309.

Murphy, G., 1983. *Pinus radiata* survival, growth, and form four years after planting off and on skidtrails. N. Z. J. For. Sci. 28 (2): 184-202.

Myneni, R. B., Ross, J., Asrar, G., 1989. A review on the theory of photon transport in leaf canopies in slab geometry. Agric. For. Meteorol., 45: 1-165.

Myneni, R.B., 1991. Modelling radiative transfer and photosynthesis in three dimensional vegetation canopies. Agric. For. Meteorol., 55:323-344.

Myneni, R.B., Gutschick, V. P., Asrar, G., Kanemasu, E. T., 1988. Photon transport in vegetation canopies with anisotropic scattering. Part IV. Discrete-ordinates / Exact-kernel technique for two-angle photon transport in slab geometry. Agric. For. Meteorol., 42: 101-120.

Myneni, R.B., Ross, J., (Eds), 1991. Photo- Vegetation Interactions. Applications in optical remote sensing and plant ecology. Springer, Berlin, 565 pp

New Zealand Forest Owners Association Inc. 1998. Forestry facts and figures 1998. Ministry of Forestry, Wellington.

New Zealand Offical Year Book. 1990-2000. Auckland, New Zealand.

Newton, J. E., Blackman, G. E., 1970. The penetration of solar radiation through leaf canopies of different structure. Ann. Bot., N.S., 34: 329-348.

Nilson, T., 1971. A theoretical analysis of the frequency of gaps in plant stands. Agric. Meteorol. 8, 25-38.

Norman, J. M. 1975. Radiative transfer in vegetation. Pp. 187-205 in de Vries, D. A.; Afgan, N. H. (Ed.)"Energy exchange in the biosphere". Scripta Book Company, Washington, D. C.

Norman, J. M. 1979. Modelling the complete crop canopy. in: Barfield , B.J., and J.F. Gerber, eds. Modification of the Aerial Environment of Plants. Monograph No. 2, American Society of Agricultural Engineers, St. Joseph, MI, U.S.A.pp.247-277.

Norman, J. M., Campbill, G.S., 1989. Canopy structure. In: R. W. Pearcy, J. Ehleringer, H.A. Mooney and P.W. Rundel (Editors), Plant Physiological Ecology. Field Methods and Instrumentation. Chapman and Hall, London, pp. 301-326.

Norman, J. M., Javis, P. G., 1975. Photosynthesis in Sitka spruce (*Picea sitchensis* (Bong.) Carr.). V. Radistion penetration theory and a test case. J. Appl. Ecol. 12:839-878.

Norman, J. M., Welles, J. M., 1983. Radiative transfer in an array of canopies. Agronomy Journal 75:481-488.

Norman. J. M., 1980 Interfacing leaf and canopy light interception models. (pp. 49-67.) In: J.D.Hesketh and J.W. Jones (Eds.), Predicting photosynthesis for ecosystem models, Vol. II, CRC Press, Boca Raton, FL, 304 pp.

Nunez, M., 1985. Modelling daily global radiation at the forest floor. bound. Layer Meteorol. 33, 379-395.

Oker-Blom, P., Kaufmann, M.R., Ryan, M. G., 1991. Performance of a canopy light interception model for conifer shoots, trees and stands. Tree Physiol. 9, 227-243.

Oker-Blom, P., Lappi, J., Smolander, H., 1991a. Radiation regime and photosynthesis of coniferous stands. In: Mynrni, R.B., Ross, J. (Eds), Photon-Vegetation Interactions. Applicatons in Optical Remote Sensing and Plant Ecology. Springer, Berlin, pp. 469-499.

Oker-Blom, P., Pukkala, T., Kuuluvainen, T., 1989. Relationship between radiation interception and photosynthesis in forest canopies: effect of stand structure and latitude. Ecol. modeling, 49: 73-87.

Oleksyn, J., Tjoelker, M.G., Lorenc, P.G., Konwinska, A., Zytkowiak, R., Karolewski, P., Reich, P.B., 1997. Needle CO_2 exchange, structure and defense traits in relation to needle age in *Pinus heldreichii Christ* - a relict of Tertiary flora. Trees: Structure and Function. 12: 2, 82-89.

Oquist, G., 1982. Seasonally induced changes in acyl lipids and fatty acids of chloroplast thylaoids of *Pinus sylvestris*. Plant Physical. 69:869-875.

Palmer, J.W., 1977. Diurnal light interception and a computer model of light interception by hedgerow apple orchards. J. Appl. Ecol. 14, 601-614.

Parker, J. 1963. Causes of the winter decline in traspiration and photosynthesis in some evergreens. For. Sci. 9:158-166.

Parton, W, J., Schimel, D. S., Cole, C. V., Ojima, D.S., 1987. Analysis of factors controlling soil organic matter levels in Great Plains grasslands. Soil. Sci. Soc. Am. J. 51, 1178-1179.

Parton, W, J., Scurlock, J. M.O., Ojima, D.S., Gilmanov, T. G., Scholes, R. J., Schimel, D. S., Kirchner, T., Menaut, J., Seastedt, T., Garcia Moya, E., Kamnalrut, A., Kinyaario, J. I., 1993. Observations and modeling of biomass and soil organic matter dynamics for the grassland biome worldwide. Global Biogeochem. Cycles 7, 785-809.

Parton, W, J., Stewart, W. B., Cole, C. V. 1988. Dynamics of C, N, P, and S in grassland soils: A model. Biogeochem. 5, 109-131.

Pastor, J., Post, W. M., 1986. Influence of climate, soil moisture, and succession on forest carbon and nitrogen cycles. Biogeochemistry 2,3-27.

Pearcy, R.W., Yang, W., 1996. A three dimensional crown architecture model for assessment of light capture and carbon gain by understory plants. Oecologia. 108 1-12.

Pearcy, R.W., Yang, W., 1998. The functional morphology of light capture and carbon gain in the Redwood forest understorey plant Adenocaulon bicolor Hook. Functional Ecology. 12: 4, 543-552.

Pereira, A.R., Machado, E.C., De Camargo, M.B.P., 1982. Solar radiation regime in three cassava (*Manihot esculenta Crantz*) canopies. Agrec. Metrorol. 26: 1-10.

Pukkala, T., Kuuluvainen, T., 1987. Effect of canopy structure on the diurnal interception of direct solar radiation and photosynthesis in a tree stand. Silva Fenn. 21: 237-250.

Radoglou, K., Teskey, R. O., 1997. Changes in rates of photosynthesis and respiration during needle development of loblolly pine. Tree Physiol. 17: 485-488.

Raison, R.J., Myers, B.J., Benson, M. L., 1992. Dynamics of *Pinus radiata* foliage in relation to water and nitrogen stress: I. Needle production and properties. For. Ecol. Manage. 52: 139-158.

Raulier, F., Bernier, P. Y., Ung,C. H., 1999. Canopy photosynthesis of sugar maple (*Acer saccharum*): comparing big-leaf and multilayer extrapolations of leaf-level measurements. Tree Physiology. 19: 7, 407-420.

Rook, D. A., Bollmann, M. P., Hong, S.O., 1987. Foliage Development within the Crowns of *Pinus Radiata* trees at two spacings. New Zealand Jounal of Forestry Science. 17(2/3): 297-314.

Rook, D. A., Whyte, A. G. D., 1976: Partial defoliation and growth of 5-year-old radiata pine. New Zealand Journal of Forestry Science. 6 (1): 40-56.

Rook, D.A., Swanson, R.H., Cranswick, A. M., 1977. Reaction of radiata pine to drought. In Proceedings of Soil and Plant Water Symposium, Palmerston North, New Zealand, 25-27 May 1976. Information Series, New Zealand Department of Science and Industrial Research. No. 126, 55-68.

Ross, J., 1981. The radiation regime and architecture of plant stands. Dr. W. Junk Publishers, Dordrecht, the Netherlands. pp391.

Running, S. W., Coughlan, J. C., 1988. A general model of forest ecosystem processes for regional applications. I. Hydrologic balance canopy gas exchange and primary production processes. Ecol. Model. 42,125-154.

Running, S. W., Gower, S.T., 1991. FOREST-BGC, a general model of forest ecosystem processes for regional applications. II Dynamic carbon allocation and nitrogen budgets. Tree Physiol. 9, 147-160.

Russell, G., 1993. Absorbed radiation and crop growth. In: Barlet-Grancher, C., Bonhomme, R., Sinoquet, H. (Eds), Crop Structure and Light Microclimate. Characterization and Applications. INRA edn., Science update, Paris, pp 459-470.

Rutter, A.J., 1957. Studies in the growth of young plants of *Pinus sylvestris* L. I. The annual cycle of assimilation and growth. Am. Bot. 83:399-426.

Ryan, M.G. 1991. A simple method for estimating gross carbon budgets for vegetation in forest ecosystems. Tree Physiology 9: 255-266.

Sampson, D.A., Smith, F.W., 1993. Influence of canopy architecture on light penetration in lodgepole pine (*Pinus contorta* var. *latifolia*) forests. Agric. For. Meteorol., 64: 63-79.

Sams, C.E., Flore, J. A., 1982. The influence of age, position, and environmental variables on net photosynthetic rate of sour cherry leaves. J. Am. Soc. Hortic. Sci. 107:339-344.

Samson, R., Follens, S., Lemeur, R., 1997. Scaling leaf photosynthesis to canopy in a mixed deciduous forest. I. Model description. Silva-Gandavensis. 62, 1-21;

Samsuddin, Z., Impens, I., 1979. The development of photosynthetic rate with leaf age in *Hevea brasiliensis* MUELL. ARG. clonal seedlings. – Photosynthetica 13:267-270.

Sanford, R. L., Parton, W.J., Ojima, D.S., Jean Lodge, D., 1991. Hurricane effects on soil organic matter dynamics and forest production in the Luquillo experimental forest Puerto Rico: Results of simulation modelling. Biotroprica 23, 364-372.

SAS Institute Inc. 1990. SAS/SAT Guide for personal computers, Version 6. SAS Institute Inc.,Cary, N.C.

Schaberg, P.G., Wilkinson, R. C., Shane, J. B., Donnelly, J. R., Cali, P. F., 1995. Winter photosynthesis of red spruce from three Vermont seed sources. Tree Physiol. 15: 5, 345-350.

Schoettle, A. W., Fahey, T. J., 1994. Foliage and fine root longevity of pines. Ecol. bull. (Copenhagen) 43, 136-153.

Schoettle, A. W., Smith, W. K., 1991 Interrelation between shoot characteristics and solar irradiance in the crown of *Pinus contorta* ssp *latifolia*. Tree Physiol. 9, 245-254.

Schoettle, A.W., Smith,W. K., 1999. Interrelationships among light, photosynthesis and nitrogen in the crown of mature *Pinus contorta ssp. latifolia*. Tree-Physiology. 19: 1, 13-22.

Schulze, E.D., Kelliher, F. M., Korner, C., Lloyd, J., Leuning, R., 1994. Relationships among maximum stomatal conductance, ecosystem surface conductance, carbon assimilation rate, and plant nitrogen nutrition: A global ecology scaling exercise. Annu. Rev. Ecol. Syst. 25, 629-669.

Schwarz, P.A., Fahey, T. J., Dawson, T. E., 1997. Seasonal air and soil temperature effects on photosynthesis in red spruce (*Picea rubens*) saplings. Tree Physiology. 17: 3, 187-194.

Sellers, P. J., Berry, J. A., Collatz, G. J., Field, C. B., Hall, F. G., 1992. Canopy reflectance, photosynthesis, and transpiration. III. A reanalysis using improved leaf models and a new canopy integration scheme. Remote sensing of environment 42, 187-216.

Senser, M. and F. Beck. 1977. On the mechanisms of frost injury and frost hardening of spruce chloroplasts. Planta 137:195-201.

Shugart, H. H., 1984. A Theory of Forest Dynamics: The Ecological Implications of Forest Succession Models, pp. 278. Springer-Cerlag, New York.

Sievainen, R., Burk, T. E., Ek, A. R., 1988. Construction of a stand growth model utilizing photosynthesis and respiration relationships in individual trees. Can. J. For.Res. 18, 1027-1035.

Smith, F. W., Sampson, D.A., Long, J. N., 1991. Comparison of leaf area index estimates from tree allometrics and measured light interception. for. Sci., 37: 1682-1688.

Smith, J., Bailey, G. R., 1964. Influence of stocking and stand density on crown widths of Douglas fir and lodgepole pine. Commonwealth Forest. Rev. 43(3), No.117, 243-246.

Smith, W.R., Somers, G. L., 1993. A system for estimating direct and diffuse photosynthetically active radiation from hemispherical photographs. Computers and Electronics in Agriculture. 8: (3): 181-193.

Snell, J. A. K., Brown, J. K., 1978. Comparison of tree biomass estimators; dbh and sapwood area. Forest Sci. 24(4):455-457.

Son, Y., Gower, S. T., 1991. Above ground nitrogen and phosphorus use by five plantation-grown tree species with different leaf longevities. Biogeochem. 14, 167-191.

St. Clair, J.B., 1993. Family differences in equations for predicting biomass and leaf area in Douglas-fir (*Pseudotsuga menziesii* var. *menziesii*). Forest Sci. 39 (4):743-755.

Stamper, J. H., Allen , J.C., 1979. A model of the daily photosynthetic rates in a tree. Agric. Meteorol. 20: 459-481.

Stenberg, P., Smolander, H., Sprugel, D., Smolander, S., 1998. Shoot structure, light interception, and distribution of nitrogen in an *Abies amabilis* canopy. Tree Physiol.18: 11, 759-767.

Stenberg, P., Kuuluvainen, T., Kellomaki, S., Grace, J. C., Jokela, E.J., Gholz, H.L., 1994. Crown structure, light interception and productivity of pine trees and stands. Ecol. Bull.(Copenhagen) 43, 20-34.

Stiell, W. M., 1962. Crown structure in plantation red pine. Can. Dep. Forest., Forest Res. Br., Tech. Note No. 122.

Sun, O. J., Sweet, G. B., 1996. Genotypic Variation in Light and Temperature Response of Photosynthesis in *Nothofagus solandri var. cliffortioides* and *N. menziesii.* Aust. J. Plant Physiol. 23: 421-8.

Szeicz, G., 1968. Measurement of radiant energy. In: R. W. Wadsworth (Editor), The measurement of environmental factors in Terrestrial ecology. Blackwell Scientific, Oxford and Edinburgh, pp.109-130.

Teskey, R. O., Grier, C. C., Hinckley, T. M., 1984. Changes in photosynthesis and water relations with age and season in *Abies amabilis.* Can. J. For.Res. 14, 77-84.

Thomas, H., Norris, I. B., 1982. Seasonal variations in frequency distribution of daily totals of short-wave solar radiation. Agric. Meteorol., 25:267-274.

Thompson, F. B., Leyton, L., 1971. Method for measuring the leaf surface area of complex shoots Nature. 229:572.

Thompson, W.A., Wheeler, A.M., 1992. photosynthesis by mature needles of field grown *Pinus radiata.* For. Ecol. Manage., 52:225-242.

Thornley, J. H. M., 1972. A model to describe the photosynthate during vegetative plant growth. Ann. Bot. 36: 419-430.

Thornley, J. H. M., 1976. Mathematical models in plant physiology. Academic press, London.

Thornley, J. H. M., Johnson, I. R., 1990. Plant and Crop Modelling. Oxford Univ. Press, Oxford.

Ticha, I., Catsky, J., Hodanova, D., Pospisilova, J., Kase, M., Sestak, Z., 1985. Gas exchange and dry matter accumulation during leaf development. In Photosynthesis during leaf development. Ed. Z. Sestak. Dr. W. Junk Publ., Dordrecht, pp 157-216.

Troeng, E., Linder, S., 1982. Gas exchange in a 20-year-old stand of Scots pin. I. Net photosynthesis of current and one-year-old shoots within and between seasons. Physiol. Plant. 54, 7-14.

Turner, N. C., Jarvis, P. G., 1975. Photosynthesis in Sitka spruce (*Picea stitchensis* (Bong.) Carr.). IV. Response to soil temperature. J. Appl. Ecol. 12:561-576.

Vandana and Bhatt, R. K., 1996. Variation in photosynthesis, transpiration and stomatal conductance in leaves of different maturity in Sesbania species. Range Management and Agroforestry. 17: 1, 41-48.

Vezina, P. E., 1962. Crown width-d.b.h. relationships for open-grown balsam fir and white spruce in Quebec. Forest. Chron. 38(4), 463-73.

Von Caemmerer, S., Farquhar. 1981. Some relationships between the biochemistry of photosynthesis and the gas exchange of leaves. Planta 153, 376-385.

Walcroft, A.S., Whitehead, D., Silvester, W.B., Kelliher, F. M., 1997. The response of photosynthetic model parameters to temperature and nitrogen concentration in *Pinus radiata* D. Don. Plant Cell and Environment. 20: 11, 1338-1348.

Walcroft, A. S., 1998. Photosynthesis and transpiration in a dry-land *Pinus radiata* forest. Ph.D thesis 1998. University of Waikato, New Zealand.

Wang, Y.P., Jarvis, P.G., 1990a. Description and validation of an array model-MAESTRO. Agric. For.Meteorol. 51257-280.

Wang, Y.P., Jarvis, P.G., 1990b. Influence of crown structural properties on PAR absorption, photosynthesis, and transpiration in Sitka spruce: application of a model (MAESTRO). Tree Phsiol. 7,297-316.

Wang, Y.P., Jarvis, P.G., Benson, M.L., 1990. Two-Dimensional needle-area density distribution within the crowns of *Pinus radiata*. Forest Ecology and Management, 32:217-237.

Wang, Y.P., Jarvis, P.G., Taylor, C. M. A., 1991. PAR absorption and its relation to above-ground dry matter production of Sitka spruce. J. Appl. Ecol. 28, 547-560.

Wang, Y.P., Jarvis. P.G., 1988. Mean leaf angle for the ellipsoidal inclination angle distribution. Agric. For. Meteorol. 43:319-321.

Wang, Y.P., Polglase, P. J., 1995. Carbon balance in the tundra, boreal forest and humid tropical forest during climate change: Scaling up from leaf physiology and soil carbon dynamics. Plant Cell Environ. 18, 1226-1244.

Waring, R. H., J.J. Landsberg, and M. Wiliams. 1998. Net primary production of forests: a constant fraction of gross primary production? Tree Physiology 18:129-134.

Weiss, A., Norman, J. M., 1985. Partitioning solar radiation into direct and diffuse, visible and near-infrared components. Agric. For. Meteorol., 34: 205-213.

West, G.G., Knowles, R.L., Koehler, A.R., 1982. Model to predict the effects of pruning and early thinning on the growth of radiata pine. New Zealand Forest Service, FRI Bulletin No. 5.

West, P. W., 1981. Comparative growth rates of several eucalypts in mixed species stands in southern tasmania. N. Z. J. For. Sci. 11 (1): 45-52.

West, P. W., Wells, K. F., 1992. Method of application of a model to predict the light environment of individual tree crowns and its use in a eucalyptus forest. Ecol. Model. 60, 199-231.

Whitehead, D., Grace, J. C., Godfrey, M. J. S., 1990. Architectural distribution of foliage in individual *Pinus radiata* D. Don. crowns and the effects of clumping on radiation. Tree Physiol. 7: 135-155

Whitfield, D. M., Connor, D. J., 1980. Architecture of individual plants in a field-grown tobacco crop. Aust. J. Plant Physiol., 7: 415-433.

Whithead, D., 1985. A review of processes in the water relations of forests. In: Research for Forest management. Eds. J.J. Landsberg and W. Parsons, CSIRO, Melbourne, pp. 94-124.

Wilkinson, D. M., 1991. Can photographic methods be used for measuring the light attenuation characteristics of trees in leaf? Landscape and Urban Planning. 20: 4, 347-349.

Will, G. M., 1978. Nutrient defficiencies in *Pinus radiata* in New Zealand. N.Z.J. For. Sci. 8(1):4-14.

Wilson, J.B., 1988. A review of evidence on the control of shot: root ratio, in relation to models. Ann. Bot. 61:433-449.

Witowski, J., 1997. Gas exchange of the lowest branches of young Scots pine: a cost-benefit analysis of seasonal branch carbon budget. Tree Physiol. 17: 757-765.

Wood, G. B., 1971. Shape of Pinus radiata fascicles and the implications for estimating needle surface area. Aust. For. Res. 5:31-36.

Wood, G. B., 1974. Age distribution of needle fascicles in the crown of a radiata pine sapling. Aust. For. Res. 6(4): 15-20.

Wood, G. B., Brittain, E.G., 1973. Photosynthesis, respiration and transpiration of Radiata pine. N.Z.J.For. Sci. 3: 2, 181-190.

Wullschleger, S. D., 1993. Biochemical limitations to carbon assimilation in C3 plants- A retrospective analysis of the A/Ci curves from 109 species. J. Exp. Bot. 44, 907-920.

Yunusa,I.A.M., Mead, D. J., Lucas, R. J., Pollock, K. M., 1995b. Process studies in a *Pinus radiata*-pasture agroforestry system in a subhumid temperate environment. II. Analysis of dry matter yield in the third year. Agroforestry Systems. 32: 185-204.

Zhao, W., 1999. Growth and yield modelling of *Pinus radiata* in Canterbury, New Zealand. Canterbury University, New Zealand. Ph.D. thesis.

APPENDIX

APPENDIX 1

Table A1.1 Comparison of light response curve parameters: maximum rate of photosynthesis (Amax,μmol m^{-2} s^{-1}); dark respiration rate (Rd,μmol m^{-2} s^{-1}); light saturation points (Qs,μmol m^{-2} s^{-1}) and light compensation points (Qc,μmol m^{-2} s^{-1}) between clone 9 (rapidly-growing) and clone 10 (slowly-growing) under different temperature and leaf age-classes. Data were collected on 25 July to 25 August 1997 (winter). Mean ± SE within rows followed by different letters indicate statistical significance ($p < 0.05$).

Temperature (°C)	Needle Ages (Year)	Parameters	Clone 9		Clone 10		Pr > F
			Mean	± SE	Mean	± SE	
5	1						
		A(max)	3.45	± 0.01a	3.47	± 0.06a	0.7758
		Rd	-0.25	± 0.09a	-0.29	± 0.04a	0.6237
		Qs	899.22	± 34.85a	882.35	± 28.14a	0.6475
		Qc	6.39	± 1.97a	7.33	± 0.58a	0.5831
	2						
		A(max)	2.18	± 0.16a	2.26	± 0.10a	0.5923
		Rd	-0.27	± 0.05a	-0.26	± 0.06a	0.9336
		Qs	776.01	± 35.11a	858.25	± 74.39a	0.2929
		Qc	8.72	± 1.87a	9.95	± 0.25a	0.4532
	3						
		A(max)	1.45	± 0.30a	1.48	± 0.18a	0.915
		Rd	-0.24	± 0.02a	-0.24	± 0.04a	0.9801
		Qs	721.89	± 183.18a	760.37	± 64.64a	0.8057
		Qc	10.73	± 1.36a	11.51	± 0.33a	0.5123
10	1						
		A(max)	4.77	± 0.18a	4.21	± 0.09a	0.0603
		Rd	-0.83	± 0.01a	-0.41	± 0.01b	0.0007
		Qs	1029.79	± 36.13a	1016.50	± 58.10a	0.8093
		Qc	23.76	± 3.03a	11.80	± 0.84b	0.0329
	2						
		A(max)	3.01	± 0.04a	3.19	± 0.08a	0.1078
		Rd	-0.63	± 0.06a	-0.18	± 0.06b	0.0178
		Qs	989.71	± 29.90a	993.22	± 0.61a	0.8834
		Qc	26.91	± 1.85a	6.19	± 1.68b	0.0072
	3						
		A(max)	1.63	± 0.31a	1.28	± 0.31a	0.3775
		Rd	-0.41	± 0.09a	-0.35	± 0.04a	0.4797
		Qs	685.42	± 114.33a	477.81	± 76.20a	0.1661
		Qc	15.81	± 5.16a	9.73	± 1.34a	0.2479
15	1						
		A(max)	4.79	± 0.18a	5.77	± 0.30a	0.0580
		Rd	-0.68	± 0.06a	-0.72	± 0.13a	0.7240
		Qs	1176.96	± 80.71a	1237.08	± 45.84a	0.4564
		Qc	26.72	± 1.65a	27.05	± 7.28a	0.9552
	2						
		A(max)	3.70	± 0.90a	3.88	± 0.01a	0.7983
		Rd	-0.72	± 0.04a	-0.39	± 0.16a	0.1015
		Qs	1086.87	± 157.08a	1136.30	± 59.43a	0.7177
		Qc	32.33	± 0.85a	15.62	± 4.92b	0.0419
	3						
		A(max)	1.54	± 0.10a	1.86	± 0.40a	0.3830
		Rd	-0.51	± 0.12a	-0.59	± 0.21a	0.6708
		Qs	780.44	± 19.64a	737.56	± 54.09a	0.4024
		Qc	27.88	± 7.64a	23.85	± 7.74a	0.6529

Table A1.2 Comparison of light response curves' parameters: maximum rate of photosynthesis (Amax,μmol m^{-2} s^{-1}); dark respiration rate (Rd,μmol m^{-2} s^{-1}); light saturation points (Qs,μmol m^{-2} s^{-1}) and light compensation points (Qc,μmol m^{-2} s^{-1}) between clone 9 (rapidly-growing) and clone 10 (slowly-growing) under different temperature and leaf age-classes. Data were collected on 5 to 25 October 1997 (spring). Mean ± SE within rows followed by different letters indicate statistical significance ($p < 0.05$).

Temperature (°C)	Needle Ages (Year)	Parameters	Clone 9		Clone 10		Pr > F
			Mean	± SE	Mean	± SE	
10	1						
		A(max)	7.88	± 0.82a	7.32	± 0.09a	0.4351
		Rd	-0.29	± 0.01a	-0.36	± 0.17a	0.6187
		Qs	1332.88	± 33.72a	1393.15	± 35.55a	0.2241
		Qc	8.40	± 0.19a	13.26	± 5.54a	0.3406
	2						
		A(max)	7.04	± 0.36a	6.85	± 0.85a	0.8033
		Rd	-0.12	± 0.05a	-0.21	± 0.13a	0.4678
		Qs	1342.07	± 96.32a	1357.52	± 64.88a	0.8681
		Qc	3.89	± 2.35a	7.29	± 4.89a	0.4689
	3						
		A(max)	5.54	± 0.74a	5.07	± 0.08a	0.4640
		Rd	-0.30	± 0.05a	-0.54	± 0.64a	0.6417
		Qs	1179.27	± 81.75a	1080.72	± 267.89a	0.6681
		Qc	8.79	± 1.32a	11.28	± 11.24a	0.7848
15	1						
		A(max)	12.07	± 0.01a	10.29	± 1.03a	0.1329
		Rd	-0.20	± 0.06a	-0.22	± 0.18a	0.8725
		Qs	1393.58	± 33.53a	1401.41	± 1.34a	0.7729
		Qc	3.99	± 1.15a	6.08	± 5.56a	0.6555
	2						
		A(max)	8.00	± 0.09a	8.46	± 0.32a	0.1885
		Rd	-0.18	± 0.12a	-0.22	± 0.06a	0.6792
		Qs	1393.77	± 37.71a	1184.42	± 8.41b	0.0166
		Qc	5.49	± 3.40a	4.10	± 1.10a	0.6388
	3						
		A(max)	6.33	± 0.47a	6.04	± 0.17a	0.5072
		Rd	-0.22	± 0.04a	-0.30	± 0.33a	0.7486
		Qs	1260.07	± 82.63a	1369.81	± 110.29a	0.3771
		Qc	6.55	± 0.42a	11.88	± 11.95a	0.5925
20	1						
		A(max)	10.57	± 0.77a	11.29	± 1.08a	0.5235
		Rd	-0.94	± 0.22a	-0.34	± 0.26a	0.1308
		Qs	1247.10	± 98.14a	1348.49	± 51.67a	0.3253
		Qc	17.91	± 1.96a	6.97	± 5.63a	0.1219
	2						
		A(max)	8.09	± 0.48a	9.13	± 2.09a	0.5647
		Rd	-0.86	± 0.15a	-0.67	± 0.04a	0.2204
		Qs	1173.20	± 49.57a	1171.00	± 6.17a	0.9560
		Qc	18.35	± 0.30a	12.33	± 2.61a	0.0833
	3						
		A(max)	6.35	± 0.59a	7.67	± 0.52a	0.1400
		Rd	-0.69	± 0.11a	-0.59	± 0.06a	0.3798
		Qs	1034.30	± 158.82a	1093.10	± 19.56a	0.6551
		Qc	14.60	± 6.43a	10.69	± 1.47a	0.4904

Table A1.3 Comparison of light response curves' parameters: maximum rate of photosynthesis (Amax,μmol m^{-2} s^{-1}); dark respiration rate (Rd,μmol m^{-2} s^{-1}); light saturation points (Qs,μmol m^{-2} s^{-1}) and light compensation points (Qc,μmol m^{-2} s^{-1}) between clone 9 (rapidly-growing) and clone 10 (slowly-growing) under different temperature and leaf age-class. Data were collected on 1 to 24 January 1998 (summer). Mean ± SE within rows followed by different letters indicate statistical significance ($p < 0.05$).

Temperature (°C)	Needle Ages (Year)	Parameters	Clone 9		Clone 10		Pr > F
			Mean	± SE	Mean	± SE	
25	1						
		A(max)	2.84	± 0.18a	2.65	± 0.03a	0.2854
		Rd	-0.51	± 0.03a	-0.42	± 0.01a	0.0565
		Qs	865.95	± 36.33a	989.59	± 160.29a	0.3989
		Qc	16.78	± 1.28a	19.95	± 6.82a	0.5846
	2						
		A(max)	1.86	± 0.07a	1.99	± 0.50a	0.7606
		Rd	-0.36	± 0.01a	-0.32	± 0.06a	0.4702
		Qs	988.22	± 1.32a	987.84	± 105.27a	0.9964
		Qc	23.89	± 0.33a	20.04	± 6.20a	0.4726
	3						
		A(max)	0.32	± 0.06a	0.91	± 0.30a	0.1100
		Rd	-0.35	± 0.02a	-0.29	± 0.23a	0.7519
		Qs	377.89	± 104.02a	439.43	± 220.55a	0.7553
		Qc	33.28	± 10.53a	12.02	± 12.73a	0.2104
30	1						
		A(max)	1.97	± 0.14a	1.42	± 0.57a	0.3148
		Rd	-0.58	± 0.21a	-0.40	± 0.09a	0.3748
		Qs	928.85	± 92.69a	757.69	± 207.71a	0.3987
		Qc	34.32	± 4.49a	22.53	± 5.23a	0.1366
	2						
		A(max)	1.21	± 0.30a	1.26	± 0.80a	0.9473
		Rd	-0.43	± 0.11a	-0.34	± 0.05a	0.1136
		Qs	861.74	± 105.87a	906.41	± 2.62a	0.6113
		Qc	39.22	± 0.95a	45.55	± 37.78a	0.8348
	3						
		A(max)	0.32	± 0.06a	0.41	± 0.16a	0.5419
		Rd	-0.24	± 0.08a	-0.30	± 0.06a	0.4929
		Qs	398.61	± 28.99a	858.88	± 53.02a	0.1024
		Qc	23.10	± 1.53a	158.84	± 89.63a	0.1655
35	1						
		A(max)	0.99	± 0.13a	1.09	± 0.17a	0.5635
		Rd	-0.68	± 0.06a	-0.41	± 0.11a	0.0837
		Qs	623.77	± 30.40a	709.42	± 262.41a	0.6916
		Qc	47.54	± 8.66a	26.04	± 5.66a	0.0989
	2						
		A(max)	0.86	± 0.11a	0.77	± 0.37a	0.7642
		Rd	-0.52	± 0.05a	-0.54	± 0.11a	0.8995
		Qs	516.31	± 188.92a	603.17	± 65.12	0.6014
		Qc	28.27	± 9.84a	53.27	± 26.76a	0.3407
	3						
		A(max)	0.32	± 0.06a	0.30	± 0.16a	0.6605
		Rd	-0.21	± 0.11a	-0.24	± 0.08a	0.6575
		Qs	398.61	± 28.99a	318.61	± 48.25a	0.3265
		Qc	21.10	± 2.41a	23.10	± 1.53a	0.8628

Table A1.4 Comparison of light response curves' parameters: maximum rate of photosynthesis (Amax,μmol m^{-2} s^{-1}); dark respiration rate (Rd,μmol m^{-2} s^{-1}); light saturation points (Qs,μmol m^{-2} s^{-1}) and light compensation points (Qc,μmol m^{-2} s^{-1}) between clone 9 (rapidly-growing) and clone 10 (slowly-growing) under different temperature and leaf age-class. Data were collected on 2 to 25 April 1998 (autumn). Mean ± SE within rows followed by different letters indicate statistical significance ($p < 0.05$).

Temperature (°C)	Needle Ages (Year)	Parameters	Clone 9		Clone 10		Pr > F
			Mean	± SE	Mean	± SE	
10	1						
		A(max)	5.97	± 1.15a	5.81	± 0.25a	0.8606
		Rd	-0.16	± 0.12a	0.02	± 0.04a	0.1950
		Qs	1304.20	± 186.42a	1412.22	± 44.72a	0.5091
		Qc	5.00	± 3.26a	-0.65	± 1.64a	0.1602
	2						
		A(max)	3.97	± 0.28a	3.99	± 0.28a	0.9501
		Rd	-0.26	± 0.11a	-0.21	± 0.01a	0.5744
		Qs	852.07	± 8.52a	899.28	± 66.48a	0.4241
		Qc	5.24	± 2.13a	4.62	± 0.91a	0.7430
	3						
		A(max)	2.12	± 0.87a	2.10	± 0.60a	0.9811
		Rd	-0.22	± 0.03a	-0.20	± 0.06a	0.6985
		Qs	851.70	± 195.42a	825.20	± 70.36a	0.8735
		Qc	10.41	± 7.10a	8.71	± 6.10a	0.8212
15	1						
		A(max)	7.77	± 0.49a	7.51	± 0.61a	0.8807
		Rd	-0.23	± 0.08a	-0.13	± 0.09a	0.2934
		Qs	1297.48	± 254.71a	1490.98	± 43.03a	0.4375
		Qc	5.91	± 0.76a	5.16	± 3.13a	0.3691
	2						
		A(max)	6.43	± 0.45a	6.17	± 0.01a	0.6853
		Rd	-0.24	± 0.04a	-0.15	± 0.03a	0.3611
		Qs	1172.94	± 17.77a	1359.99	± 5.57a	0.4005
		Qc	5.96	± 0.43a	5.76	± 0.91a	0.7743
	3						
		A(max)	3.20	± 0.10a	3.19	± 0.07a	0.4960
		Rd	-0.40	± 0.27a	-0.17	± 0.04a	0.1299
		Qs	968.43	± 149.59a	1044.66	± 252.51a	0.4049
		Qc	10.35	± 9.52a	6.63	± 2.07a	0.8091
20	1						
		A(max)	8.70	± 0.10a	8.55	± 0.21a	0.9181
		Rd	-0.17	± 0.06a	-0.14	± 0.07a	0.3544
		Qs	1308.83	± 51.72a	1341.46	± 1.37a	0.3146
		Qc	3.98	± 0.85a	3.70	± 1.87a	0.6428
	2						
		A(max)	4.96	± 0.21a	5.04	± 0.13a	0.4756
		Rd	-0.22	± 0.13a	-0.18	± 0.06a	0.0507
		Qs	1167.59	± 15.57a	1256.14	± 186.38a	0.8064
		Qc	6.86	± 4.50a	7.53	± 5.49a	0.0737
	3						
		A(max)	3.11	± 0.23a	2.97	± 0.21a	0.4605
		Rd	-0.12	± 0.03a	-0.22	± 0.13a	0.6855
		Qs	1017.53	± 118.69a	956.26	± 39.56a	0.4665
		Qc	4.62	± 2.56a	8.15	± 6.34a	0.8628

Table A1.5 Effects of leaf ages on maximum rate of photosynthesis (Amax,μmol m^{-2} s^{-1}); dark respiration rate (Rd,μmol m^{-2} s^{-1}); light saturation points (Qs,μmol m^{-2} s^{-1}) and light compensation points (Qc,μmol m^{-2} s^{-1}) in different temperature. The data (a) were collected on 25 July to 25 August 1997 in winter and data (b) were collected on 2 to 25 October 1997 in spring. Mean ± SE within rows followed by different letters indicate statistical significance ($p < 0.05$).

(a) Winter

Parameter	Leaf ages 1-year-old		2-year-old		3-year-old		Pr > F
			Temperature 5 °C				
A(max)	3.46	± 0.04a	2.22	± 0.12b	1.46	± 0.20c	0.0001
Rd	-0.27	± 0.06a	-0.26	± 0.04a	-0.24	± 0.01a	0.5843
Qs	890.79	± 27.63a	817.13	± 67.16a	741.13	± 114.33a	0.0686
Qc	6.86	± 1.30a	9.33	± 1.30b	11.12	± 0.92b	0.0023
			Temperature 10 °C				
A(max)	4.49	± 0.35a	3.10	± 0.11b	1.46	± 0.32c	0.0001
Rd	-0.62	± 0.24a	-0.40	± 0.26a	-0.38	± 0.07a	0.2501
Qs	1023.15	± 40.24a	991.47	± 17.38a	581.61	± 143.73b	0.0001
Qc	17.78	± 7.14a	16.55	± 12.05a	12.77	± 4.67a	0.6975
			Temperature 15 °C				
A(max)	5.28	± 0.60a	3.79	± 0.53b	1.70	± 0.30c	0.0001
Rd	-0.70	± 0.08a	-0.56	± 0.21a	-0.55	± 0.15a	0.3465
Qs	1207.02	± 63.85a	1111.58	± 101.07a	759.00	± 41.43b	0.0001
Qc	26.88	± 4.32a	23.98	± 10.07a	25.86	± 6.70a	0.8558

(b) Spring

Parameter	Leaf ages 1-year-old		2-year-old		3-year-old		Pr > F
			Temperature 10 °C				
A(max)	7.60	± 0.58a	6.94	± 0.54a	5.31	± 0.51b	0.0006
Rd	-0.33	± 0.11a	-0.16	± 0.10a	-0.42	± 0.39a	0.3574
Qs	1363.01	± 44.84a	1349.79	± 67.64a	1129.99	± 171.42b	0.025
Qc	10.83	± 4.26a	5.59	± 3.70a	10.03	± 6.69a	0.3317
			Temperature 15 °C				
A(max)	11.18	± 1.19a	8.23	± 0.33b	6.18	± 0.33c	0.0001
Rd	-0.21	± 0.11a	-0.20	± 0.08a	-0.26	± 0.20a	0.8100
Qs	1397.49	± 19.89a	1289.09	± 122.91a	1314.94	± 101.71a	0.2764
Qc	5.03	± 3.49a	4.79	± 2.21a	9.21	± 7.56a	0.4059
			Temperature 20 °C				
A(max)	10.93	± 0.87a	8.61	± 1.37b	7.01	± 0.89b	0.0019
Rd	-0.64	± 0.40a	-0.76	± 0.14a	-0.64	± 0.09a	0.7335
Qs	1297.79	± 86.76a	1172.10	± 28.87ab	1063.70	± 98.43b	0.0068
Qc	12.44	± 7.19a	15.34	± 3.79a	12.64	± 4.42a	0.7028

Table A1.6 Effects of leaf ages on maximum rate of photosynthesis (Amax,μmol m^{-2} s^{-1}); dark respiration rate (Rd,μmol m^{-2} s^{-1}); light saturation points (Qs,μmol m^{-2} s^{-1}) and light compensation points (Qc,μmol m^{-2} s^{-1}) in different temperature. The data (a) were collected on 1 to 24 January 1998 in summer and data (b) were collected on 2 to 25 April 1998 in autumn. Mean ± SE within rows followed by different letters indicate statistical significance ($p < 0.05$).

(a) Summer

Parameter	Leaf ages 1-year-old		2-year-old		3-year-old		Pr > F
			Temperature 25 °C				
A(max)	2.75	± 0.15a	1.92	± 0.30b	0.62	± 0.38c	0.0001
Rd	-0.47	± 0.06a	-0.34	± 0.04a	-0.32	± 0.14a	0.1697
Qs	927.77	± 118.74a	988.03	± 60.79a	408.66	± 145.20b	0.0001
Qc	18.36	± 4.41a	21.96	± 4.22a	22.65	± 15.54a	0.8666
			Temperature 30 °C				
A(max)	1.69	± 0.47a	1.23	± 0.49ab	0.36	± 0.11b	0.0005
Rd	-0.49	± 0.17a	-0.38	± 0.06a	-0.27	± 0.07a	0.0498
Qs	843.27	± 164.35a	884.08	± 66.36a	628.74	± 266.37b	0.0268
Qc	28.42	± 7.88a	42.38	± 22.12a	90.97	± 93.91a	0.3514
			Temperature 35 °C				
A(max)	1.04	± 0.14a	0.81	± 0.23a	0.32	± 0.05b	0.0002
Rd	-0.54	± 0.17a	-0.54	± 0.03a	-0.24	± 0.07b	0.0023
Qs	666.59	± 160.33a	559.74	± 125.80a	398.61	± 23.67a	0.0926
Qc	36.79	± 13.77a	40.77	± 21.89a	23.10	± 1.25a	0.3556

(b) Autumn

Parameter	Leaf ages 1-year-old		2-year-old		3-year-old		Pr > F
			Temperature 10 °C				
A(max)	5.89	± 0.68a	3.98	± 0.23b	2.11	± 0.61c	0.0001
Rd	-0.07	± 0.12a	-0.23	± 0.07a	-0.21	± 0.04a	0.0700
Qs	1358.21	± 127.04a	875.67	± 47.33b	838.45	± 120.89b	0.0001
Qc	2.17	± 3.88a	4.93	± 1.38a	9.56	± 5.49a	0.0979
			Temperature 15 °C				
A(max)	7.64	± 0.48a	6.30	± 0.30b	3.20	± 0.07c	0.0001
Rd	-0.18	± 0.09a	-0.20	± 0.06a	-0.29	± 0.21a	0.3726
Qs	1394.23	± 186.34a	1266.46	± 108.53a	906.54	± 232.70b	0.0074
Qc	5.53	± 1.91a	5.86	± 0.59a	8.49	± 6.02a	0.5643
			Temperature 20 °C				
A(max)	8.63	± 0.16a	5.00	± 0.13b	3.04	± 0.20c	0.0001
Rd	-0.16	± 0.06a	-0.20	± 0.09a	-0.17	± 0.10a	0.3623
Qs	1325.14	± 35.32a	1211.87	± 119.47a	986.89	± 80.43b	0.0001
Qc	3.84	± 1.20a	7.20	± 4.11a	6.38	± 4.44a	0.4961

Table A1.7 Effects of temperature on maximum rate of photosynthesis (Amax,μmol m^{-2} s^{-1}); dark respiration rate (Rd,μmol m^{-2} s^{-1}); light saturation points (Qs,μmol m^{-2} s^{-1}) and light compensation points (Qc,μmol m^{-2} s^{-1})in different leaf age class. The data (a) were collected on 25 July to 25 August 1997 in winter and data (b) were collected on 2 to 25 October 1997 in spring. Mean ± SE within rows followed by different letters indicate statistical significance ($p < 0.05$).

(a) Winter

Parameter	Temperature 5 °C		10 °C		15 °C		Pr > F
			1-year-old foliage				
A(max)	3.46	± 0.04a	4.49	± 0.35b	5.28	± 0.60c	0.0004
Rd	-0.27	± 0.06a	-0.62	± 0.24b	-0.70	± 0.08b	0.0063
Qs	890.79	± 27.63a	1023.15	± 40.24b	1207.02	± 63.85c	0.0001
Qc	6.86	± 1.30a	17.78	± 7.14b	26.88	± 4.32b	0.0009
			2-year-old foliage				
A(max)	2.22	± 0.12a	3.10	± 0.11b	3.79	± 0.53c	0.0002
Rd	-0.26	± 0.04a	-0.40	± 0.26a	-0.56	± 0.21a	0.1637
Qs	817.13	± 67.16a	991.47	± 17.38b	1111.58	± 101.07b	0.0008
Qc	9.33	± 1.30a	16.55	± 12.05a	23.98	± 10.07a	0.1292
			3-year-old foliage				
A(max)	1.46	± 0.20a	1.46	± 0.32a	1.70	± 0.30a	0.4071
Rd	-0.24	± 0.01a	-0.38	± 0.07b	-0.55	± 0.15b	0.0039
Qs	741.13	± 114.33a	581.61	± 143.73a	759.00	± 41.43a	0.0877
Qc	11.12	± 0.92a	12.77	± 4.67a	25.86	± 6.70b	0.0032

(b) Spring

Parameter	Temperature 10 °C		15 °C		20 °C		Pr > F
			1-year-old foliage				
A(max)	7.60	± 0.58a	11.18	± 1.19b	10.93	± 0.87b	0.0006
Rd	-0.33	± 0.11a	-0.21	± 0.11a	-0.64	± 0.40a	0.0892
Qs	1363.01	± 44.84a	1397.49	± 19.89a	1297.79	± 86.76a	0.0947
Qc	10.83	± 4.26a	5.03	± 3.49a	12.44	± 7.19a	0.1647
			2-year-old foliage				
A(max)	6.94	± 0.54a	8.23	± 0.33a	8.61	± 1.37a	0.0574
Rd	-0.16	± 0.10a	-0.20	± 0.08a	-0.76	± 0.14b	0.0001
Qs	1349.79	± 67.64a	1289.09	± 122.91a	1172.10	± 28.87b	0.0387
Qc	5.59	± 3.70a	4.79	± 2.21ab	15.34	± 3.79b	0.0025
			3-year-old foliage				
A(max)	5.31	± 0.51a	6.18	± 0.33ab	7.01	± 0.89b	0.0121
Rd	-0.42	± 0.39a	-0.26	± 0.20a	-0.64	± 0.09a	0.1684
Qs	1129.99	± 171.42a	1314.94	± 101.71a	1063.70	± 98.43a	0.0538
Qc	10.03	± 6.69a	9.21	± 7.56a	12.64	± 4.42a	0.7363

Table A1.8 Effects of temperature on maximum rate of photosynthesis (Amax,μmol m^{-2} s^{-1}); dark respiration rate (Rd,μmol m^{-2} s^{-1}); light saturation points (Qs,μmol m^{-2} s^{-1}) and light compensation points (Qc,μmol m^{-2} s^{-1}) in different leaf age class. The data (a) were collected on 1 to 24 January 1998 in summer and data (b) were collected on 2 to 25 April 1998 in autumn. Mean ± SE within rows followed by different letters indicate statistical significance ($p < 0.05$).

(a) Summer

Parameter	Temperature 25 °C		30 °C		35 °C		Pr > F
			1-year-old foliage				
A(max)	2.75	± 0.15a	1.69	± 0.47b	1.04	± 0.14c	0.0001
Rd	-0.47	± 0.06a	-0.49	± 0.17a	-0.54	± 0.17a	0.734
Qs	927.77	± 118.74a	843.27	± 164.35a	666.59	± 160.33a	0.0897
Qc	18.36	± 4.41a	28.42	± 7.88a	36.79	± 13.77a	0.0648
			2-year-old foliage				
A(max)	1.92	± 0.30a	1.23	± 0.49ab	0.81	± 0.23b	0.0056
Rd	-0.34	± 0.04a	-0.38	± 0.06a	-0.54	± 0.03b	0.0003
Qs	988.03	± 60.79a	884.08	± 66.36a	559.74	± 125.80b	0.0002
Qc	21.96	± 4.22a	42.38	± 22.12a	40.77	± 21.89a	0.2606
			3-year-old foliage				
A(max)	0.62	± 0.38a	0.36	± 0.11a	0.32	± 0.05a	0.1995
Rd	-0.32	± 0.14a	-0.27	± 0.07a	-0.24	± 0.07a	0.5742
Qs	408.66	± 145.20a	628.74	± 266.37a	398.61	± 23.67a	0.1676
Qc	22.65	± 15.54a	90.97	± 93.91a	23.10	± 1.25a	0.1851

(b) Autumn

Parameter	Temperature 10 °C		15 °C		20 °C		Pr > F
			1-year-old foliage				
A(max)	5.89	± 0.68a	7.64	± 0.48b	8.63	± 0.16c	0.0001
Rd	-0.07	± 0.12a	-0.18	± 0.09a	-0.16	± 0.06a	0.2887
Qs	1358.21	± 127.04a	1394.23	± 186.34a	1325.14	± 35.32a	0.7658
Qc	2.17	± 3.88a	5.53	± 1.91a	3.84	± 1.20a	0.2395
			2-year-old foliage				
A(max)	3.98	± 0.23a	6.30	± 0.30b	5.00	± 0.13c	0.0001
Rd	-0.23	± 0.07a	-0.20	± 0.06a	-0.20	± 0.09a	0.7445
Qs	875.67	± 47.33a	1266.46	± 108.53b	1211.87	± 119.47b	0.0006
Qc	4.93	± 1.38a	5.86	± 0.59a	7.20	± 4.11a	0.4737
			3-year-old foliage				
A(max)	2.11	± 0.61a	3.20	± 0.07b	3.04	± 0.20b	0.0051
Rd	-0.21	± 0.04a	-0.29	± 0.21a	-0.17	± 0.10a	0.4786
Qs	838.45	± 120.89a	906.54	± 232.70a	986.89	± 80.43a	0.4474
Qc	9.56	± 5.49a	8.49	± 6.02a	6.38	± 4.44a	0.7047

Table A1.9.1 Analysis of variance of *N* in 1-year-old needle for radiata pine clones at age 5 at Dalethorpe

Source	d.f.	Sum of squares	Mean square	F	P>F
Clone	9	0.0248	0.0028	0.6000	0.7814
Residual	20	0.0917	0.0046		
Total	29	0.1165			

Table A1.9.2 Analysis of variance of *K* in 1-year-old needle for radiata pine clones at age 5 at Dalethorpe

Source	d.f.	Sum of squares	Mean square	F	P>F
Clone	9	0.0716	0.0080	1.5600	0.1944
Residual	20	0.1019	0.0051		
Total	29	0.1735			

Table A1.9.3 Analysis of variance of *B* in 1-year-old needle for radiata pine clones at age 5 at Dalethorpe

Source	d.f.	Sum of squares	Mean square	F	P>F
Clone	9	62.9667	6.9963	1.3000	0.2952
Residual	20	107.3333	5.3667		
Total	29	170.3165			

Table A1.9.4 Analysis of variance of *Mn* in 1-year-old needle for radiata pine clones at age 5 at Dalethorpe

Source	d.f.	Sum of squares	Mean square	F	P>F
Clone	9	2778.0333	308.6704	0.9300	0.5225
Residual	20	6653.3333	332.6667		
Total	29	9431.3667			

Table A1.9.5 Analysis of variance of *P* in 1-year-old needle for radiata pine clones at age 5 at Dalethorpe

Source	d.f.	Sum of squares	Mean square	F	P>F
Clone	9	0.0074	0.0008	5.2300	0.0010
Residual	20	0.0031	0.0002		
Total	29	0.0105			

Table A1.9.6 Analysis of variance of *Ca* in 1-year-old needle for radiata pine clones at age 5 at Dalethorpe

Source	d.f.	Sum of squares	Mean square	F	P>F
Clone	9	0.0351	0.0039	2.7300	0.0293
Residual	20	0.0286	0.0014		
Total	29	0.0637			

Table A1.9.7 Analysis of variance of *Mg* in 1-year-old needle for radiata pine clones at age 5 at Dalethorpe

Source	d.f.	Sum of squares	Mean square	F	P>F
Clone	9	0.0020	0.0002	15.5800	0.0001
Residual	20	0.0003	0.00001		
Total	29	0.0023			

Table A1.9.8 Analysis of variance of *Zn* in 1-year-old needle for radiata pine clones at age 5 at Dalethorpe

Source	d.f.	Sum of squares	Mean square	F	P>F
Clone	9	518.3000	57.5889	3.6400	0.0077
Residual	20	316.6667	15.8333		
Total	29	834.9667			

Table A1.9.9 Analysis of variance of *Cu* in 1-year-old needle for radiata pine clones at age 5 at Dalethorpe

Source	d.f.	Sum of squares	Mean square	F	P>F
Clone	9	5.3697	0.5966	8.2900	0.0001
Residual	20	1.4400	0.0720		
Total	29	6.8097			

Table A1.10

Correlation Analysis

9 'WITH' Variables: N P K CA MG B MN ZN CU

2 'VAR' Variables: Hight (97) DBH (97)

Simple Statistics

Variable	Unit	N	Mean	Std Dev	Sum	Minimum	Maximum
N	%	30	1.48467	0.06339	44.54000	1.36000	1.58000
P	%	30	0.15870	0.01900	4.76100	0.12600	0.18900
K	%	30	0.73767	0.07734	22.13000	0.58400	0.91700
CA	%	30	0.28700	0.04685	8.61000	0.18100	0.35900
MG	%	30	0.06113	0.00883	1.83400	0.04200	0.07600
B	ppm	30	8.70000	2.42331	261.00000	5.00000	16.00000
MN	ppm	30	95.23333	18.03384	2857	56.00000	126.00000
ZN	ppm	30	32.36667	5.36581	971.00000	19.00000	44.00000
CU	ppm	30	3.10333	0.48458	93.10000	2.40000	4.20000
Hight(97)	cm	30	294.20000	38.49353	8826	246.00000	374.00000
DBH9 (97)	mm	30	46.90000	7.96263	1407	38.00000	65.00000

Pearson Correlation Coefficients / Prob > |R| under Ho: Rho=0 / N = 30

	Hight (97)	DBH (97)
N	-0.20458 0.2782	-0.19441 0.3033
P	0.11105 0.5591	0.10143 0.5938
K	0.21619 0.2512	0.25030 0.1822
CA	-0.22265 0.2370	-0.21167 0.2615
MG	0.30428 0.1021	0.34363 0.0630
B	0.03430 0.8572	-0.07488 0.6941
MN	0.35212 0.0564	0.30034 0.1068
ZN	0.05339 0.7793	0.03236 0.8652
CU	0.14490 0.4449	0.15023 0.4281

APPENDIX 2

Geometrical analysis of light penetration distance within tree crowns.

A2.1 Calculating the distance of diffuse light penetration within tree crown

A2.1.1 Diffuse light penetration at horizontal j level

The geometrical functions and diagram are showed at Appendix Figure 1.
Where Rij = f (Xij) represent the crown shape equation which was described in Chapter 5. Rij represent crown radii and Xij is the relative crown height at crown j levels with age class i.

A2.1.2 Diffuse light penetration at any given aspect with azimuth angle $\angle\theta$ and elevation angle $\angle\beta$.

Appendix Figure 2, 3 and 4 show the geometrical functions of diffuse light penetration distance at any point in j level. With the functions (beside the diagram), the distance of diffuse light penetration from any aspect (over hemisphere) with azimuth angle $\angle\theta$ and elevation angle $\angle\beta$ can be calculated.

A2.2 Calculating the distance of direct beam penetration within tree crown

A2.2.1 Direct beam penetration across crown central line

Appendix Figure 5 shows the geometrical functions and a diagram of direct beam penetration distance at crown central line in the level j. The geometrical functions (beside the diagram) can be used to calculate direct beam penetration distance at crown central line with a given sun zenith angle $\angle\lambda$.

A2.2.2 Direct beam penetration through crown beside the central line

Appendix Figure 6 shows the geometrical functions and a diagram of direct beam penetration distance beside crown central line in the level j. The geometrical functions (beside the diagram) can be used to calculate direct beam penetration distance beside crown central line with a given sun zenith angle $\angle\lambda$.

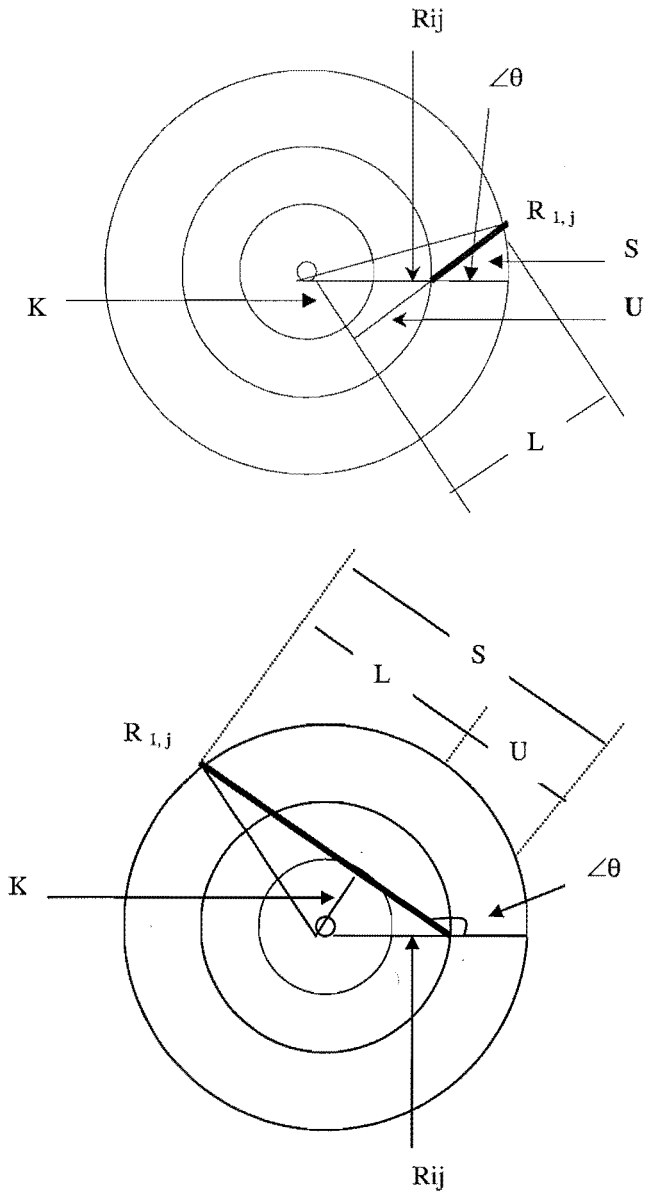

WHEN ∠θ < 90°

S = L - U

$$\mathbf{L} = \sqrt{(R_{1,j})^2 - k^2}$$

K = sin (θ) * Rij

U = cos(θ) * Rij

Rij = f(xij)

R1j= f (x1j)

WHEN ∠θ > 90°

∠φ = 180° -∠θ

S = L + U

$$\mathbf{L} = \sqrt{(R_{1,j})^2 - k^2}$$

K = sin (φ) * Rij

U = cos(φ) * Rij

Rij = f(xij)

R1j= f (x1j)

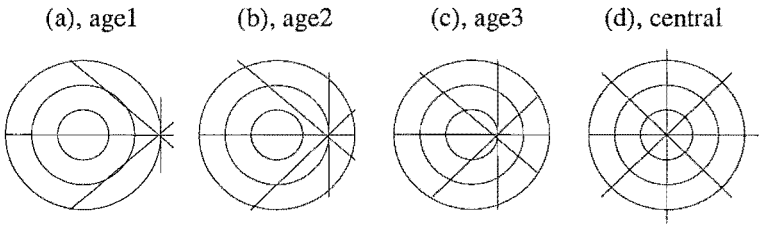

Figure A2.1 Diagram shows diffuse light penetration at a horizontal j level. Using the equations we can calculate light penetration distance at any points (a, b, c, and d) with a given azimuths ∠θ.

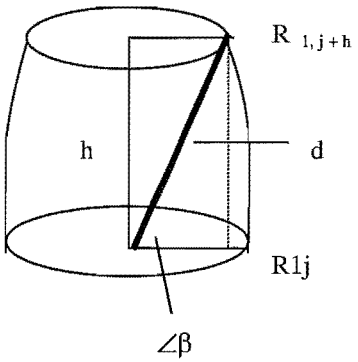

$$d = \sqrt{(R_{1,j+h})^2 + h^2}$$

$R_{1,j} = f(X_{1,j})$

$R_{1,j+h} = f(X_{1,j+h})$

$\because d = h / \sin(\beta)$

$\therefore h = \sin(\beta) * \sqrt{(R_{1,j+h})^2 + h^2}$ .....**

When we change the vertical angle ∠β, we don't know the value of h. But with equation **, increasing h value from 0 at level j, when function ** is true, then we can get the value of h and d.

Figure A2.2 Diagram showing how to calculate diffuse light penetration distance at central point in j level with a given elevation angle ∠β.

$\angle\varphi = 180 - \angle\theta$.

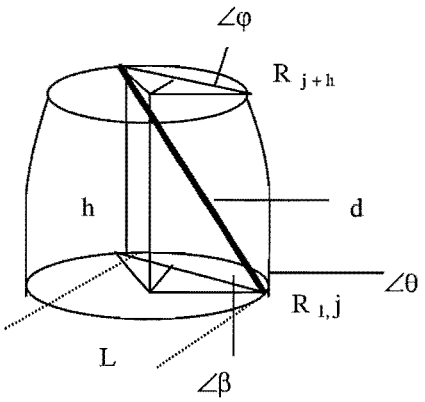

$$d = \sqrt{L^2 + h^2}$$

$L = \cos(\varphi) * (R_{1,j} + R_{1,j+h})$

$R_{1,j} = f(X_{1,j})$

$R_{1,j+h} = f(X_{1,j+h})$

$\because d = h / \sin(\beta)$

$\therefore h = \sin(\beta) * \sqrt{L^2 + h^2}$ .....**

When we change the vertical angle ∠β and horizontal angle ∠θ, we don't know the value of h. But with equation **, increasing h value from 0 at level j, when function ** is true, then we can get the values of h and d.

Figure A2.3 Diagram showing how to calculate diffuse light penetration distance at crown outside point in j level with a given elevation angle ∠β and azimuths angle ∠θ.

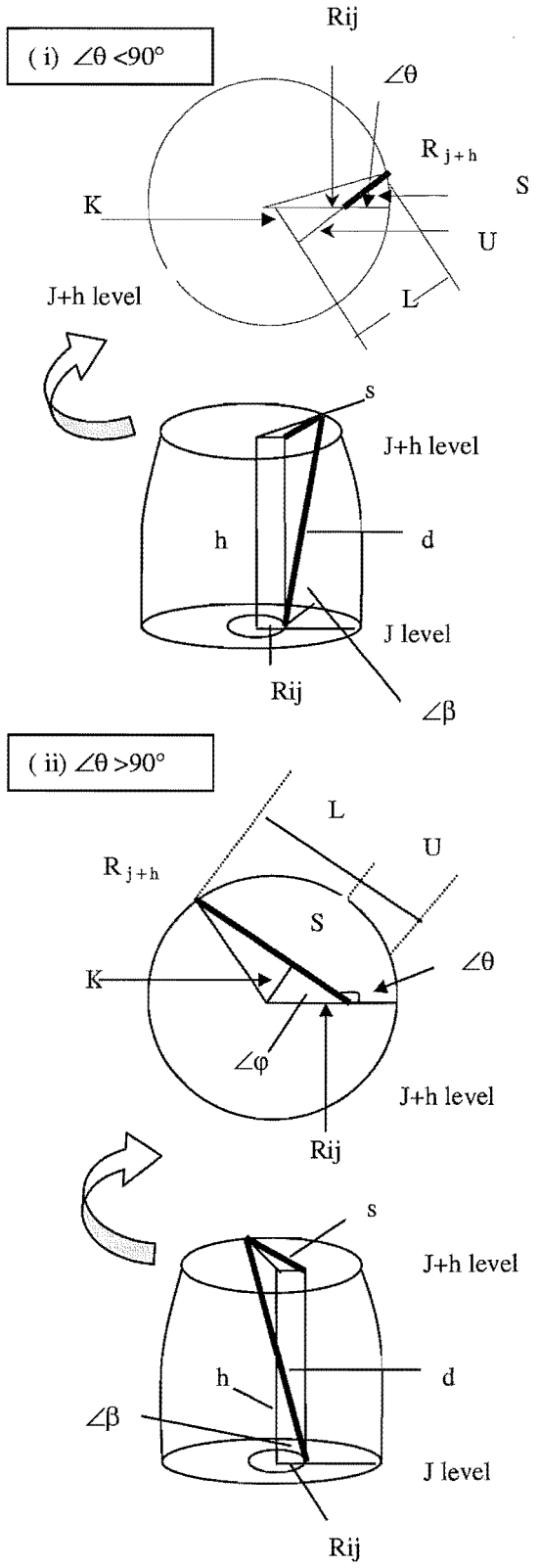

when ∠θ <90° (i)

$d = \sqrt{s^2 + h^2}$
S = L - U
$L = \sqrt{(R_{1,j+h})^2 - K^2}$
U = cos(θ)* Rij
K = sin(θ)* Rij
Rij = f (Xij)
$R_{1,j+h} = f(X_{1,j+h})$

When ∠θ > 90° (ii)

$d = \sqrt{s^2 + h^2}$
S = L + U
$L = \sqrt{(R_{1,j+h})^2 - K^2}$
U = cos (φ)* R i,j
K = sin (φ)* R i,j
R i,j = f (Xi,j)
$R_{1,j+h} = f(X_{1,j+h})$

$\because d = h / \sin(\beta) = \sqrt{s^2 + h^2}$
$\therefore h = \sin(\beta) * \sqrt{s^2 + h^2}$ .....**

Increasing h value from 0 at j level, when function ** is true, then we can get the value of h and d.

Figure A2.4. Diagram showing the diffuse light penetration within crown at ij point in j level, with a given elevation angle ∠β (0-90) and an azimuths angle ∠θ (0-180). The functions show how to calculate the diffuse light penetration distance from all directions.

(a)

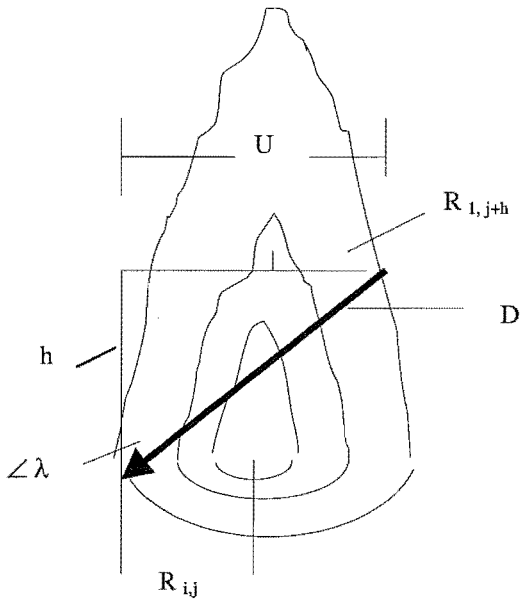

(a) Shade side

$D = \sqrt{U^2 + h^2}$

$U = R_{1, j+h} + R_{i,j}$

$Rij = f(xij)$

$R1j = f(x1j)$

$\because D = U / \sin(\lambda)$

$\therefore U = \sin(\lambda) * \sqrt{U^2 + h^2}$ .....**

(b) Sunlit side

$D = \sqrt{U^2 + h^2}$

$U = R_{1, j+h} - R_{i,j}$

$Rij = f(xij)$

$R1j = f(x1j)$

$\because D = U / \sin(\lambda)$

$\therefore U = \sin(\lambda) * \sqrt{U^2 + h^2}$ .....**

(b)

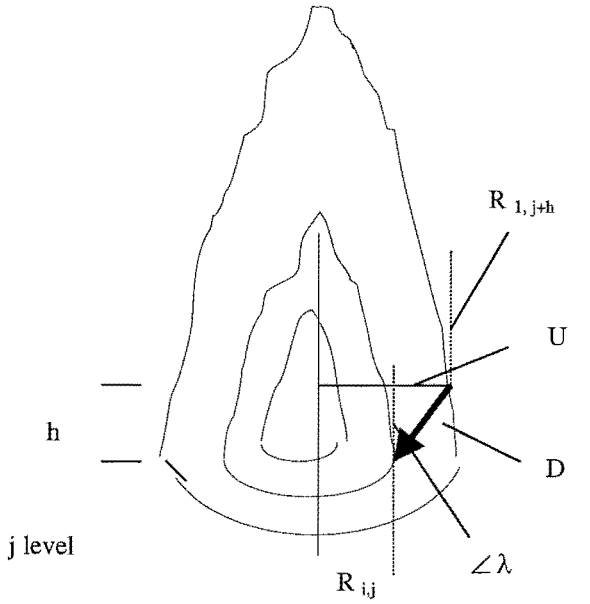

With a changed sun zenith angle ∠λ, the distance (D) of direct beam penetration to any point of central line in crown j level can be calculated. With increasing h value from 0 at j level, when equation ** is true, then we can get the values of h and D.

Figure A2.5 Diagram showing direct beam penetration through crown central line at level j with a given sun zenith angle ∠λ.

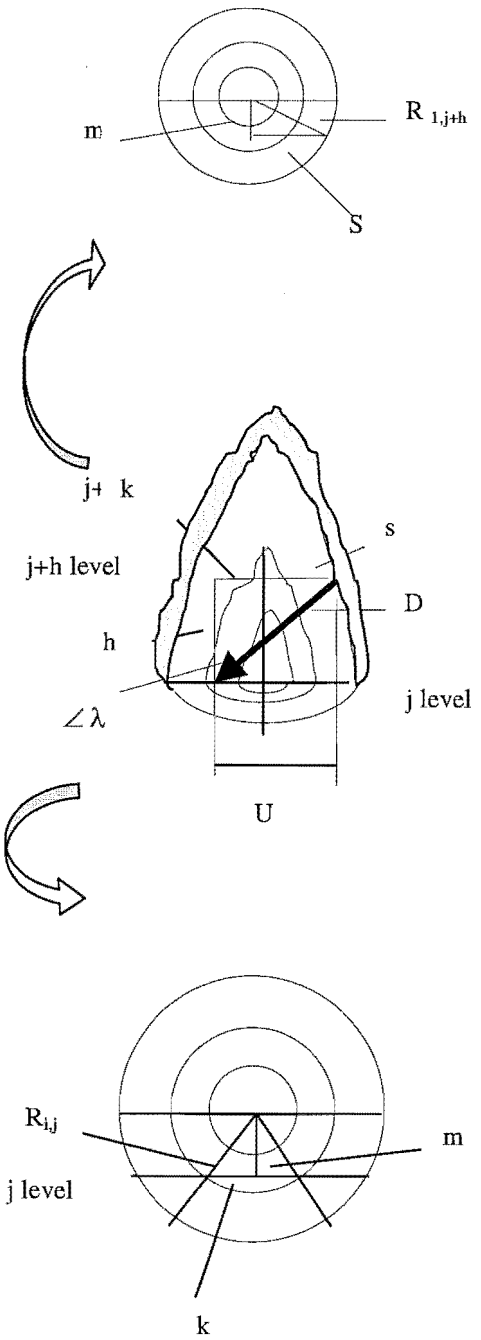

At the shade side

$D = \sqrt{U^2 + h^2}$

U = s + k

k = Rij / 2

$m = \sqrt{(R_{i,j})^2 - k^2}$

$s = \sqrt{(R_{1,j+h})^2 - m^2}$

R i,j = f(X i,j)

$R_{1,j+h} = f(X_{1,j+h})$

$\because D = U / \sin(\lambda)$

$\therefore U = \sin(\lambda) * \sqrt{U^2 + h^2}$ .....**

At sunlit side

$D = \sqrt{U^2 + h^2}$

U = s - k

R i,j = f(X i,j)

$R_{1,j+h} = f(X_{1,j+h})$

$\because D = U / \sin(\lambda)$

$\therefore U = \sin(\lambda) * \sqrt{U^2 + h^2}$ .....**

With a changed sun zenith angle ∠λ, the distance (D) of direct beam penetration to the point of beside the central line in crown j level can be calculated. With increasing h value from 0 at j level, when the equation ** is true, then we can get the values of h and D.

Figure A2.6. Diagram showing direct beam penetration through crown beside the central line at j level with a given sun zenith angle ∠λ. With the equations, direct beam penetration distance (D) beside central line of tree crown can be calculated at each level.

A3.1 "Plot annual net photosynthesis for whole tree canopies vs. stemwood growth by each clone"

Using the collected climate data list in Table A3.1.1 as parameters to estimate annual net photosynthesis with the developed model in Chapter 8, generated the results shown in Table A3.1.2, A3.1.3, Figure A3.1.4, and A3.1.6. Table A 3.1.3 and Figure A3.1.5, show clearly that there is a poor correlation between annual net photosynthesis for whole tree canopies vs. stemwood biomass for clones 4, 6, 9, and 10. This is because the biomass allocation is different for the different clones (see Chapter 6).

Larcher (1980) listed dry matter production (maximal yield) for different plant species and showed that *Pinus radiata* produced 4.6 kg / m^2.yr. Table A3.1.3 and Figure A3.1.6 show that the yields are between 2.1-3.1 kg / m^2.yr in 1997 for the clones 4, 6, 9, and 10.

Table A 3.1.1 The climate information what was used to generate parameters in the developed model (in Chapter 8) to estimate net photosynthesis. The climate data was collected from the New Zealand Meteorological Service(Monthly Climate Table(1988-1992); The Climate of Christchurch(1983));and New Zealand Official Year Book (1990-2000).

Month	J	F	M	A	M	J	J	A	S	O	N	D
Temperature C° (mean daily)	16.6	16.5	14.7	12.5	9.1	6.6	6.1	7.5	10.2	12.3	14.2	16.2
Sun Shine (hr)	207	190	170	150	130	125	126	145	165	210	215	220
Radiation 0.1MJ/ m^2 (mean daily)	230	200	150	110	70	60	65	90	130	170	220	225
PPFD (MJ/m^2)	11.5	10	7.5	5.5	3.5	3	3.3	4.5	6.5	8.5	11	11.3
VPD (kPa)	3.5	3	2.5	2	1	1	1	2	2.3	2.5	2.7	3

Table A 3.1.2 The results of estimating monthly yield (g / m^2 of ground) by using the climate data and the developed model (in Chapter 8) for clones 4, 6, 9 ,10.

Month	J	F	M	A	M	J	J	A	S	O	N	D
Clone 4	828	451	157	50	7	2	4	26	78	202	371	561
Clone 6	617	335	140	41	4	1	3	14	74	177	295	423
Clone 9	971	462	187	71	8	2	6	40	104	231	384	604
Clone 10	930	447	177	59	8	2	5	31	94	218	375	578

Table A 3.1.3 The annual results (in 1997)of estimating yield (g / $m^2$of ground per year) vs. stem biomass (kg) in 1997 for clones 4, 6, 9, and 10.

Clone	Clone 4	Clone 6	Clone 9	Clone 10
Yield (kg / m2.yr)	2.7	2.1	3.1	2.9
Stem biomass (kg)	12	6	13.5	9.5

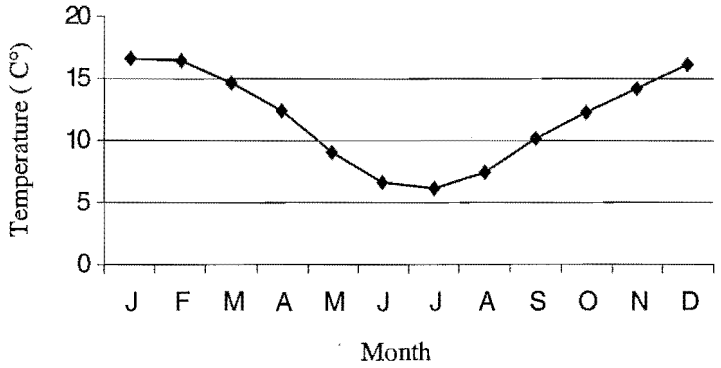

Figure A3.1.1 Mean daily temperature in each month

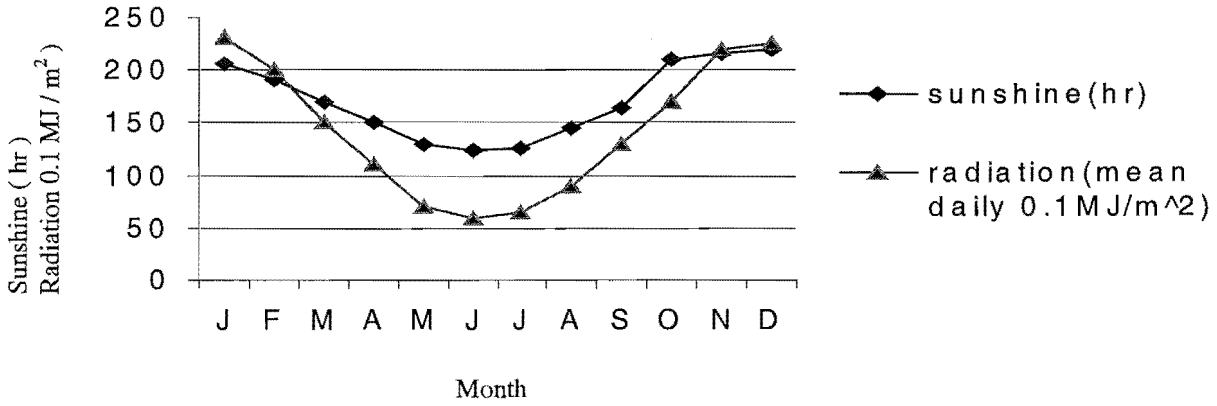

Figure A3.1.2 Mean daily radiation and sunshine in each month

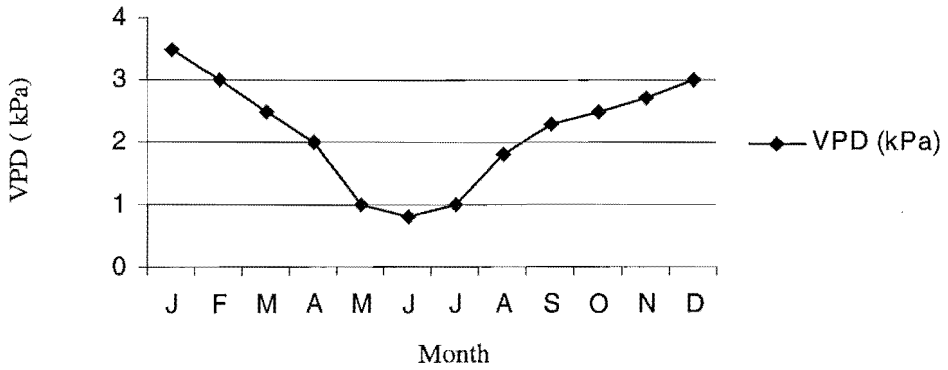

Figure A3.1.3 Mean daily VPD in each month

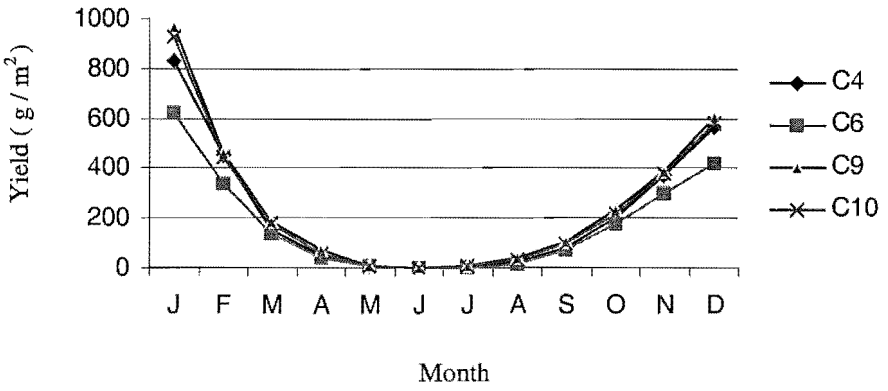

Figure A3.1.4. Showing monthly yield (g / m2 of ground) for clones 4, 6, 9, and 10.

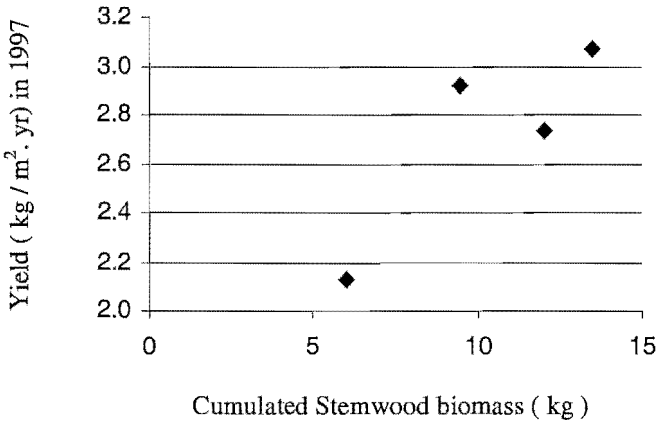

Figure A3.1.5 Plotting yields (kg / m^2 of ground per year) vs. stemwood biomass (kg). The result shows a poor correlation because allocation difference for clones 4, 6, 9, and 10. Data showing in Table A 3.3.

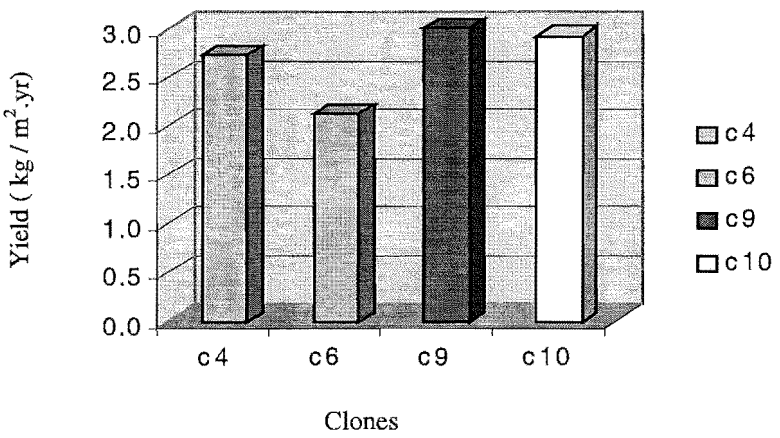

Figure A3.1.6 Annual yield (kg / m^2 of ground per year) in 1997 for clones 4, 6, 9, and 10.

A 3.2 Estimate annual gross photosynthesis and belowground biomass

Estimate NPP (Net Primary Production) using Waring's (1998) function:

$$NPP = GPP\text{-}R$$

where GPP = gross promary production. R = stand growth and maintainance respiration.

If 50% of GPP consumed for respiration, and 25% of NPP was allocated to roots, then GPP and belowground root biomass could be as shown in Table A3.2.1:

Table A3.2.1 The results of estimating GPP ($kg/m^2.yr$) and B(root) ($kg/m^2.yr$) for clones 4, 6, 9, and 10.

Clone	NPP($kg/m^2.yr$)	GPP($kg/m^2.yr$)	B(root) ($kg/m^2.yr$)
C4	2.7	5.4	0.675
C6	2.1	4.2	0.525
C9	3.1	6.2	0.775
C10	2.9	5.8	0.725

Where B(root) is belowground root biomass (kg / m^2 of ground per year). NPP is Net Primary Production come from the results of Appendix 3.1.

A3.3 Construct a total carbon balance using assumptions followed by Ryan (1991) for clones 4, 6, 9, and 10.

The assumption of **Ryan** (1991) to estimate carbon balance needs estimates of total annual litterfall L_f

The function is: $B(\text{total balance}) = a + b * L_f$

B is Biomass allocation to belowground ($g /m^2.yr$)
a and b are function parameters
Lf is litterfall ($g /m^2.yr$)

In this limited time research, litterfall data was not collected, so B can't be estimated by using Ryan's assumption. However, if the results of Appendix 3.2 was used, B was estimated first in the Appendix 3.2, then L_f could be estimated as follows:

if $B = a + b * Lf$ then $Lf = (B - a) / b$

Table A3.3.1 The results of estimating litterfall for clones 4, 6, 9, and 10.

Clone	a	b	B($g /m^2.yr$)	Lf($g /m^2.yr$)
C4	130	1.92	675	284
C6	130	1.92	525	206
C9	130	1.92	775	336
C10	130	1.92	725	310

The program diskette append here: